Presupernova Evolution of Massive Single and Binary Stars

N. Langer

Argelander-Institut für Astronomie, Universität Bonn, D-53121 Bonn, Germany;
email: nlanger@astro.uni-bonn.de

Annu. Rev. Astron. Astrophys. 2012. 50:107–64

First published online as a Review in Advance on June 6, 2012

The *Annual Review of Astronomy and Astrophysics* is online at astro.annualreviews.org

This article's doi:
10.1146/annurev-astro-081811-125534

0066-4146/12/0922-0107$20.00

Keywords

binary stars, massive stars, stellar rotation, supernovae, Wolf-Rayet stars

Abstract

Understanding massive stars is essential for a variety of branches of astronomy including galaxy and star cluster evolution, nucleosynthesis and supernovae, pulsars, and black holes. It has become evident that massive star evolution is very diverse, being sensitive to metallicity, binarity, rotation, and possibly magnetic fields. Although the problem to obtain a good statistical observational database is alleviated by current large spectroscopic surveys, it remains a challenge to model these diverse paths of massive stars toward their violent end stage.

I show that the main sequence stage offers the best opportunity to gauge the relevance of the various possible evolutionary scenarios. This also allows sketching the post-main-sequence evolution of massive stars, for which observations of Wolf-Rayet stars give essential clues. Recent supernova discoveries owing to the current boost in transient searches allow tentative mappings of progenitor models with supernova types, including pair-instability supernovae and gamma-ray bursts.

1. INTRODUCTION

Massive star: a star that is massive enough to form a collapsing core at the end of its life and, thus, avoid the white dwarf fate

Although the majority of massive stars form a collapsing iron core, the cores of the least massive ones may collapse before neon ignition, and those of the most massive stars may collapse before oxygen ignition. The minimum initial mass of massive stars at solar metallicity is likely in the range of $8\,M_\odot - 12\,M_\odot$ according to Poelarends et al. (2008), who propose a fiducial value of $9\,M_\odot$. It decreases significantly for lower metallicity (see Section 7.1). In close binaries, this limit depends on the initial system parameters. Especially for mass donors in the initially closest systems, the mass limit at solar metallicity can be as high as $15\,M_\odot$ (Wellstein, Langer & Braun 2001).

Massive stars are powerful cosmic engines. Throughout their lives, they possess high luminosities; and as they are hot stars for most of their evolution, they pour out large amounts of ionizing photons. Their high luminosities also give rise to strong stellar winds that plow supersonically through the surrounding medium. Driven by radiation pressure in spectral lines, these winds may be enhanced by pulsations or eruptions during advanced evolutionary stages, when the wind may also become enriched in elements synthesized in the stellar interior. In the violent deaths of massive stars, where most of them produce supernovae, a final splash of photons, kinetic energy, and newly synthesized chemical elements is produced.

These processes are key agents in stirring the interstellar medium of star-forming galaxies and are driving their evolution throughout the history of the Universe (Mac Low et al. 2005). Even before galaxies formed, massive stars are believed to have played an essential role in reionizing the Universe (Haiman & Loeb 1997), with important consequences for its subsequent evolution.

Beyond their active role in the Universe, massive stars are visible out to large distances owing to their high luminosities and are, thus, important probes of the conditions at their remote locations and of the conditions in the intervening space. Individual massive stars may have luminosities of up to $10^7\,L_\odot$ (Crowther et al. 2010b) and allow currently quantitative spectroscopy out to about 10 Mpc (Bresolin et al. 2001, Kudritzki 2010). As ensembles in star-forming galaxies, they can be seen at redshifts beyond $z = 5$ (Steidel et al. 1999, Douglas et al. 2010). Their explosions as supernovae or gamma-ray bursts shine through a major fraction of the Universe, probing intervening structures as well as massive star evolution, down to the lowest metallicities and up to the highest redshifts (Salvaterra et al. 2009; Savaglio, Glazebrook & Le Borgne 2009; Tanvir et al. 2009). It is anticipated that explosions of pregalactic stars will soon be discovered (Toma, Sakamoto & Meszaros 2011).

It is therefore of paramount importance for many areas within astrophysics to construct and use accurate and reliable models of massive star evolution. We show below that the path to doing so appears long and is obstructed by (at least) three major obstacles: internal mixing, mass loss, and binarity, as well as possibly also by magnetic field effects, which form the focus of this review. Constructing accurate and reliable models will require the collection of the available observational and theoretical understanding of massive stars to derive a self-consistent picture of their presupernova evolution.

2. PHYSICAL PROCESSES: ROTATION

In the past decades, rotation has been identified as a parameter that may affect the evolution of stars as strongly as mass and metallicity (Maeder 1987; Langer 1991a; Meynet & Maeder 2000; Heger, Langer & Woosley 2000). This has been reviewed, e.g., by Maeder & Meynet (2000a) and Maeder (2009). In the following, we briefly discuss the main consequences of rotation in massive stars.

2.1. Centrifugal Force

The effect of centrifugal force on stellar structure has been investigated by various researchers, using different methods and approximations. Sweet & Roy (1953) investigated models of rigidly rotating main-sequence stars in the Cowling approximation. They were the first to show that rotation leads to a reduction of the stellar luminosity and to an increase of its central density and a reduced central temperature. In this respect, rotating main-sequence stars behave as if the centrifugal force leads to a reduced effective mass. This effect was later confirmed by more sophisticated models of rotating stars (e.g., Mark 1968, Endal & Sofia 1976, Meynet & Maeder 1997, Heger & Langer 2000) as well as in two-dimensional models (Bodenheimer 1971, Shindo et al. 1997, Roxburgh 2004).

Main-sequence star: a star or stellar model representing a star in the phase of core hydrogen burning

Because the centrifugal force is not spherically symmetric, it leads to a latitude dependence of the stellar structure. It was von Zeipel (1924) who showed that, assuming radiative energy transport, the local surface flux of a rotating star is proportional to its local effective surface gravity, leading to what is called gravity darkening near the stellar equator. For stars with convective envelopes, the effect is expected to be considerably weaker (Lucy 1967, Claret 1998). The picture that predicts that rapid rotators are brighter and, thus, hotter at their poles and cooler and dimmer at their equators has been confirmed by observations (Domiciano de Souza et al. 2003, 2005).

Centrifugal force also puts an upper limit on the rotation rate of hydrostatic stars. Considering only gravity and centrifugal acceleration leads to the concept of critical or break-up rotation when the two terms cancel each other at the equator. For stars near the so-called Eddington limit, at which continuum radiation pressure balances surface gravity, radiation pressure has to be included in the force balance (Eddington 1921, Langer 1997, Maeder 2009). Concerning the current implementation of the centrifugal force in stellar evolution codes, see Heger, Langer & Woosley (2000), Maeder & Meynet (2000a), and Maeder (2009).

2.2. Angular Momentum Transport

A number of instabilities can be triggered in rotating stars, which can lead to the transport of energy, angular momentum, and matter. Whereas they are all much less important than the most relevant thermal instability, convection, it has been shown that in particular the Eddington-Sweet flows, which are induced by the global thermal imbalance in rapidly rotating stars, and the shear instability in differentially rotating layers can induce significant effects, in particular in massive stars (Meynet & Maeder 2000; Heger, Langer & Woosley 2000).

Before considering angular momentum transport induced by these processes, we want to point out that efficient angular momentum transport from the core to the envelope in massive stars is in fact needed to avoid an angular momentum crisis. Similar to the star-formation process, where molecular cloud cores are enormously compressed on the way to forming main-sequence stars, the cores of massive stars grow in density by about nine orders of magnitude on their way to forming iron cores. The majority of massive stars rotate so rapidly, their cores would reach critical rotation if they could not share their angular momentum with a slowly rotating expanded stellar envelope during the post-main-sequence evolution.

This problem has been realized when constructing the first stellar evolution models with rotation leading to advanced evolutionary stages, where simple angular momentum transfer algorithms have been used (Kippenhahn, Meyer-Hofmeister & Thomas 1970; Meyer-Hofmeister 1972). Later on, Endal & Sofia (1976, 1978) included Eddington-Sweet currents and the shear instability, but did not find sufficient core-envelope coupling to alleviate the problem.

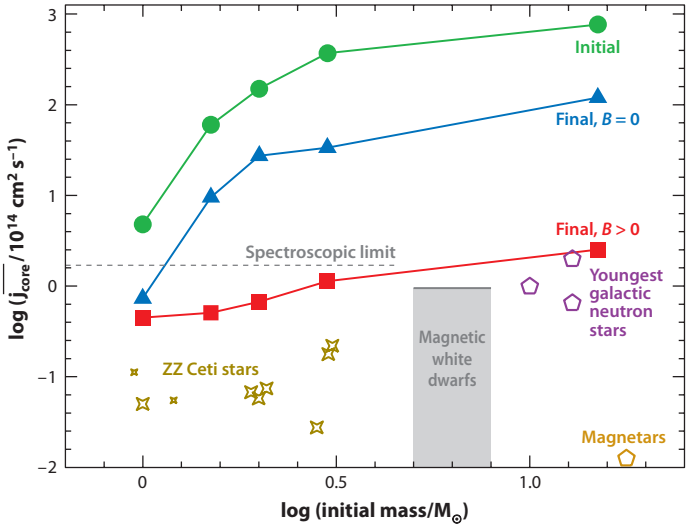

Figure 1

Average core specific angular momentum versus initial mass for the low- and intermediate-mass models of Suijs et al. (2008) and for the 15-$M_\odot$ model of Heger, Woosley & Spruit (2005) evolving from the zero-age main sequence to their end stages (*solid lines*). The upper line corresponds to the initial models. Filled triangles mark the final models of the nonmagnetic sequences, and filled squares indicate the final models of the magnetic sequences. The dashed horizontal line indicates the spectroscopic upper limit on the white dwarf spins obtained by Berger et al. (2005). Star symbols represent asteroseismic measurements from ZZ Ceti stars (Winget, Nather & Clemens 1994; Kepler et al. 1995; Kleinmann et al. 1998; Bradley 1998, 2001; Handler 2001; Handler, Romero-Colmenero & Montgomery 2002; Dolez et al. 2006), where smaller symbols correspond to less certain measurements. The gray shaded area is populated by magnetic white dwarfs (Ferrario & Wickramasinghe 2005; Brinkworth, Burleigh & Marsh 2007). The three purple open pentagons correspond to the youngest galactic neutron stars (Heger, Woosley & Spruit 2005), whereas the orange open pentagon is thought to roughly correspond to magnetars (Camilo et al. 2007). Figure adapted from Suijs et al. (2008).

In more recent calculations, by considering processes that reduce the effect of mean molecular weight barriers, the angular momentum transport is enhanced sufficiently to delay the problems of critically rotating cores to the stage of iron core collapse (Maeder & Zahn 1998; Heger, Langer & Woosley 2000; Hirschi, Meynet & Maeder 2004). However, in view of the slow spins of observed young neutron stars and white dwarfs, the core specific angular momentum in the mentioned stellar evolution models is still too large by about two orders of magnitude (Suijs et al. 2008, Hirschi & Maeder 2010). Therefore, additional angular momentum transport mechanisms are needed, and possible candidates include magnetic torques (Spruit 2002; Maeder & Meynet 2003, 2004) and gravity waves (Talon & Charbonnel 2005, 2008).

The stellar evolution models by Heger, Woosley & Spruit (2005) and Suijs et al. (2008) are so far the only ones that yield stellar remnant spins in rough agreement with observations (**Figure 1**). They rely on the model of Spruit (2002), who proposed that differential rotation would lead to significant toroidal magnetic fields that can exert torque to couple the rotation of the core with that of the stellar envelope. Although the model of Spruit has been criticized (see Section 4.1.2), notably, the slowly rotating core of the Sun can also be reproduced by models that include magnetic torques (Charbonneau & MacGregor 1993; Eggenberger, Maeder & Meynet 2005), although for this situation, gravity waves may be able to do the same (Charbonnel & Talon 2005).

2.3. Rotationally Induced Mixing

Whereas the fact that massive stars are generally rapid rotators may be motivation enough to study the effects of rotation in massive star models, the discovery of nitrogen and helium enhancements at the surface of massive main-sequence stars (e.g., Schönberner et al. 1988, Gies & Lambert 1992) has brought a major motivation to include rotational mixing in those models (see, however, Section 5.4).

The same processes that transport angular momentum in stars may also induce mixing. Endal & Sofia (1978) were the first to include rotationally induced mixing in massive star evolution models, whereas Maeder (1987) was among the first to connect rotational mixing with surface abundance changes on the main sequence. The current models (Heger & Langer 2000; Meynet & Maeder 2000; Hirschi, Meynet & Maeder 2004; Heger, Woosley & Spruit 2005; Frischknecht et al. 2010; Przybilla et al. 2010; Brott et al. 2011a) do reproduce the observed ranges of surface enrichments in massive main-sequence stars. The models that include magnetic torque (Heger, Woosley & Spruit 2005; Petrovic et al. 2005; Brott et al. 2011a) evolve close to rigid rotation and rely mostly on transport due to Eddington-Sweet circulations, whereas in the nonmagnetic models shear mixing is more important (cf. Heger, Langer & Woosley 2000; Maeder & Meynet 2005).

A critical ingredient in theories of rotationally induced chemical mixing is the treatment of mean molecular weight gradients. As stars fuse heavier nuclei in their cores, these gradients are generally opposed to mixing. Heger, Langer & Woosley (2000), Yoon, Langer & Norman (2006) and Brott et al. (2011a) parameterize this effect of mean molecular weight barriers, and Meynet & Maeder (2000), Hirschi, Meynet & Maeder (2004), and Frischknecht et al. (2010) argue that horizontal turbulence induced by the baroclinic instability reduces their effect. In all these models, the surface abundances of trace elements like boron (Section 5.4.2) or nitrogen (Section 5.4.1) are changed in sufficiently fast rotators. There is ambiguity, however, in how much helium can be mixed from the convective core of massive main-sequence stars to the stellar surface. Meynet & Maeder (2000) do find a substantial surface helium enrichment during the main-sequence phase of fast rotating massive stars, but the models of Brott et al. (2011b) show very little helium enrichment—unless the stars evolve chemically homogeneously (see below). Whereas the mixing of trace elements can be calibrated observationally (Brott et al. 2011b), there is not enough data to do the same for helium (Section 5.4.3).

The concept of rotational mixing is supported by more indirect observations, e.g., the number ratio of Wolf-Rayet (WR) to O stars or of blue to red supergiants (Maeder & Meynet 2000a) (see Section 6.4), the metallicity dependence of long gamma-ray bursts (Yoon, Langer & Norman 2006) (Section 7.4), or the nucleosynthesis signature of rotating massive stars in very metal-poor, galactic, low-mass stars (Chiappini et al. 2011). However, as we see below, direct evidence for rotational mixing, e.g., an observed correlation of surface enrichment with rotation in massive main-sequence stars that is unambiguously due to rotation in single stars, has not been found so far (see Section 5). This has two main reasons. First, the vast majority of the abundance determinations for massive main-sequence stars have been obtained for apparent slow rotators, where it is facilitated by the narrow widths of absorption lines in their spectra. And second, effects of binary evolution, of stellar wind mass loss, or of internal magnetic fields would need to be subtracted from the observations, which is difficult to do, as such effects might dominate the observational signal.

One of the most pregnant predictions of rotationally induced mixing is the so-called quasi-chemically homogeneous evolution—a concept already discussed by Eddington (1929). Once a chemical stratification is established in the stellar interior, the corresponding mean molecular weight gradients prevent efficient rotationally induced transport processes in the corresponding

Wolf-Rayet (WR) stars: stars that are hot ($\gtrsim$25,000 K) and luminous ($\log(L/L_\odot) \gtrsim 4.5$), with emission lines dominating their spectra, signifying an at least partly optically thick stellar wind

Supergiant: post-main-sequence stars with hydrogen-rich envelopes, where the ignition of the hydrogen burning shell source drives the stellar envelope to large radii

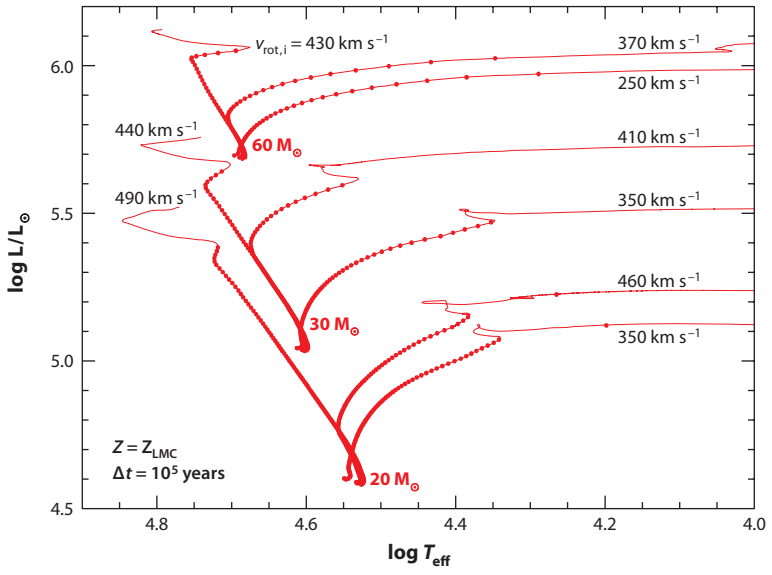

Figure 2

Evolutionary tracks of stars with initial masses of 20 $M_\odot$, 30 $M_\odot$, and 60 $M_\odot$, with Large Magellanic Cloud (LMC) metallicity, according to the models of Brott et al. (2011a), for three different initial rotational velocities, as indicated. The rotational velocities are chosen such that the lowest velocity at each mass is the first that shows the effect of truncated chemically homogeneous evolution, and the highest one is the first to show chemically homogeneous evolution until core hydrogen exhaustion.

layers. However, when the timescale of rotationally induced mixing becomes shorter than the nuclear timescale on which the star usually establishes a chemical stratification and evolves off the zero-age main sequence, a mean molecular weight barrier may never establish. As a consequence, the star evolves almost chemically homogeneously. As shown by Maeder (1987), for a given mass and metallicity, there is a discrete threshold rotational velocity above which chemically homogeneous evolution occurs and below which the star evolves in the normal way. Yoon, Langer & Norman (2006) and Brott et al. (2011a) demonstrated that due to the metallicity dependence of hot star winds (Mokiem et al. 2007b) and the associated angular momentum loss (Langer 1998), chemically homogeneous evolution occurs more easily at lower metallicity.

Owing to the angular momentum loss that is associated to stellar winds, it is also predicted that chemically homogeneous evolution may be truncated, i.e., that a chemically homogeneously evolving star transitions to normal evolution during core hydrogen burning. The surface helium abundance, which roughly corresponds to the central helium abundance at the time of the switch, remains more or less constant from that moment on, as mean molecular weight barriers prevent further efficient rotational mixing. **Figure 2** shows this behavior in recent models from Brott et al. (2011a). Three trends are seen in these models: Homogeneous evolution occurs at lower rotational velocity for higher initial mass, homogeneous evolution occurs at lower rotational velocity for lower metallicity, and the initial velocity range where truncated homogeneous evolution occurs for a given mass becomes wider for larger initial masses. The implication is that homogeneous as well as truncated homogeneous evolution is expected to occur more often at larger mass and lower metallicity.

3. PHYSICAL PROCESSES: BINARIES

3.1. Binary Evolution and Rotation

When considering rotation in massive stars, it is quite natural to look at massive close binaries, because binary interaction is a process that can move plenty of angular momentum to one of the components (Struve 1963, Huang 1966, Shu & Lubow 1981). It was Packet (1981) who showed that, neglecting angular momentum loss, a rigidly rotating main-sequence star that gains mass from a companion via an accretion disk reaches critical rotation at its surface after a mass increase of only ∼5–10%. Therefore, mass gainers in mass transfer binaries are expected to constitute the most rapidly rotating stars.

Among the many types of observed spun-up mass gainers in binary systems, from low-mass stars to millisecond pulsars, it is the Be/X-ray binaries that provide compelling evidence that the spin-up occurs also in accreting massive main-sequence stars. The Be stars are thought to be B-type main-sequence stars that spin close to critical rotation and are surrounded by an out-flowing disc of gas in Keplerian rotation (Porter & Rivinius 2003; Townsend, Owocki & Howarth 2004). Be/X-ray binaries contain an early-type Be star and a neutron star in a rather wide and eccentric orbit. The large majority of binaries consisting of a massive star and a compact object are in fact the Be/X-ray binaries (Liu, van Paradijs & van den Heuvel 2006). To understand the formation of these systems, one needs to assume that the neutron star progenitor sheds mass onto the now Be star before it experiences a supernova explosion (Tauris & van den Heuvel 2006). Most binary systems are expected to break up due to the kick imparted on the newly born neutron star during the supernova event (Eldridge, Langer & Tout 2011), thereby producing single Be stars. Only the binaries where the neutron star received a low kick, or a kick in a favorable direction, can remain bound and develop a Be/X-ray binary stage.

In detailed massive binary evolution models, mass transfer is generally accounted for but angular momentum transfer is largely ignored. With the advent of models for rotating massive single stars, however, massive binary models that include the same detailed physics of rotation are now being produced (Wellstein 2001; Langer et al. 2003; Petrovic et al. 2005; Petrovic, Langer & van der Hucht 2005; Cantiello et al. 2007; de Mink et al. 2009). In these models, the spin-up of the accretion star is indeed observed (**Figure 3**). The spin-up is found to be less dramatic in closer systems for two reasons. In close systems, when the mass gainer has a large enough radius, the accretion stream will directly impact on its surface without forming an accretion disk. When the impact parameter of the accretion stream is significantly smaller than the stellar radius, the specific angular momentum thus accreted by the star can be much smaller than it is in wider systems that accrete via a Keplerian disk (Lubow & Shu 1975). In addition, in close systems, tides may be efficient in slowing down the supersynchronously rotating mass gainer (Langer et al. 2003; Petrovic et al. 2005; Petrovic, Langer & van der Hucht 2005).

A solution of the angular momentum problem in binary evolution may well tie in with another unsolved key question in close binary evolution: What is the accretion efficiency during the mass transfer process, i.e., which fraction of the mass leaving the donor star ends up in the mass gainer (de Mink, Pols & Hilditch 2007)? Although most binary evolution models assume either a fixed accretion efficiency or an ad hoc dependence (cf. De Loore & De Greve 1992; Podsiadlowski, Joss & Hsu 1992; Wellstein, Langer & Braun 2001; Eldridge, Izzard & Tout 2008), angular momentum should make us consider this simple physical condition for the accretion efficiency: When the surface layers of the star are spun up to critical rotation, accretion will stop.

Whether this criterion is realized in accreting binary components is debatable. Once critical rotation is reached, the star can indeed gain no more angular momentum, so material attempting to

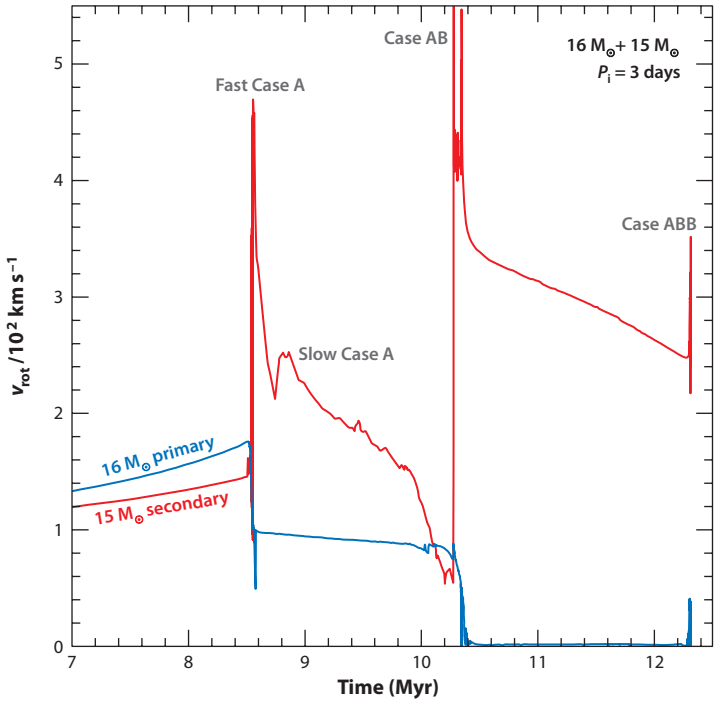

Figure 3

Evolution of the equatorial rotational velocity of both components of a binary system starting out with $16\,M_\odot$ and $15\,M_\odot$ and an orbital period of 3 days (cf. Wellstein 2001, Langer et al. 2003). The various mass transfer phases are indicated. Whereas the mass donor (primary, blue line) loses mass and angular momentum during each mass transfer event, the mass gainer is dramatically spun-up by the mass transfer and spun down in between by tides and stellar wind mass loss.

carry excess angular momentum into the star may be rejected. Within this scenario, an additional problem is to identify the force that carries this material away. The centrifugal force drops with $1/r^3$ assuming angular momentum conservation. Radiation pressure appears to be a more favorable candidate, decreasing outward with $1/r^2$, like gravity. The required task, however, is to push matter away at a rate of $\dot{M} \simeq M_{\rm donor}/\tau_{\rm th,donor}$, and it is questionable whether radiation can do this (van Marle, Owocki & Shaviv 2009). Perhaps, the material is first pushed to some finite distance, forming a ring or shell around the binary system, which is ablated on a longer timescale by the stellar photon fields or winds.

However, we know from accretion disks, which—in the case of Keplerian rotation—achieve critical rotation everywhere, that viscous coupling of adjacent radial fluid elements can transport angular momentum outward and mass inward (Pringle 1981). Popham & Narayan (1991) and Paczynski (1991) pointed out that this might apply as well to a critically rotating star that is coupled to an accretion disk via a boundary layer. To what extent critically rotating stars can keep accreting then depends obviously on the viscosities in the boundary layer as well as inside the star, which are uncertain.

In either case, it is interesting to consider the consequences of assuming the more restrictive criterion, i.e., that accretion is inhibited when critical rotation is achieved. **Figure 4** shows the resulting mass transfer and accretion rates in an initially very close ($P_i = 3$ d) system consisting of

Case A mass transfer: mass transfer from a core hydrogen burning donor star

Case B mass transfer: mass transfer from a hydrogen shell–burning star

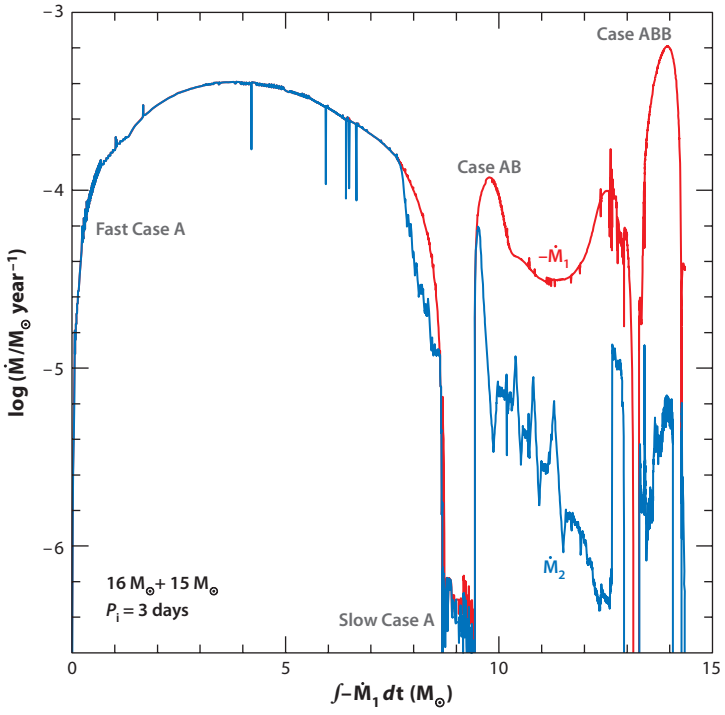

Figure 4

Mass transfer rate $-\dot{M}_1$ (*red*) and mass accumulation rate on the mass gainer $\dot{M}_2$ (*blue*) as functions of the transferred amount of mass, for the same binary system as shown in **Figure 3**. The various mass transfer phases are indicated. Fast and slow Case A mass transfer are almost conservative, but during Case AB and Case ABB less than 10% of the transferred matter is accreted by the mass gainer.

a 16-$M_\odot$ and a 15-$M_\odot$ star (Wellstein 2001, Langer et al. 2003). This system evolves through four separate mass transfer phases. It is evident that Case A mass transfer remains almost conservative, despite the fact that the donor star accretes much more than 10% of its initial mass (it grows from 15 $M_\odot$ to above 23 $M_\odot$), because the spin-up is mediated by the small impact parameter and by tides (see above). Only during the later mass transfer phases, when the orbital period has increased to 10 days or more, does the accretion become very inefficient within this model.

The donor stars of massive Case A binaries lose most of the remainder of their hydrogen-rich envelope during a thermal timescale mass transfer shortly after the ignition of the hydrogen burning shell source, which we call Case AB mass transfer. Some Case A or Case B systems initiate a further mass transfer after the ignition of the helium burning shell source, which we call Case ABB or Case BB, respectively.

It is evident that some observed post–mass transfer massive binary stars require close-to-conservative evolution (e.g., V729 Cygni and Wray 977; Langer et al. 2003), whereas others can only be understood through a low mass transfer efficiency (Petrovic, Langer & van der Hucht 2005; de Mink, Pols & Hilditch 2007; Mahy et al. 2011; Ritchie et al. 2012). The criterion that mass gainers stop accreting when critical rotation is reached leads to a mass accretion efficiency that drops for wider systems. It also leads to a decreasing mass accretion efficiency for more extreme mass ratios because lower mass companions can be spun-up to critical rotation by accreting a

smaller fraction of the mass lost from the donor star. Clearly, the latter trend has been confirmed through an analysis of close WR plus O star binaries (Petrovic, Langer & van der Hucht 2005).

The criterion discussed above leads to a strong time dependence of the mass transfer efficiency. In particular, as can be seen from the example displayed in **Figure 4**, it has the consequence that the mass that is transferred early may all be accreted, whereas what goes over late may be mostly expelled. Because the matter that is transferred at late times is more strongly enriched with nucleosynthesis products as it comes from deeper layers of the donor star (e.g., nitrogen and helium; de Mink et al. 2009), the mass gainer displayed in **Figure 4** will be much less enriched than a comparable mass gainer produced in a model with a constant accretion efficiency with a value equal to the average mass transfer efficiency as in our example binary. Dray & Tout (2007) show that the further evolution of a binary system may sensitively depend on the accreted amount of helium.

3.2. Surface Abundances of Mass Gainers

Researchers de Mink, Langer & Izzard (2011) showed recently that after a strong interaction (mass transfer or merger), the majority of massive close binaries are not recognizable as such. This is most evident for mergers, and for binaries where one component—usually the initially more massive star—has exploded as a supernova and thereby broken up the binary system. Even before the first supernova in a binary occurs, however, the mass gainer will often outshine its companion, as after the first mass transfer it is often much more massive than the mass donor. Additionally, the binary may have widened substantially due to the mass transfer (Wellstein, Langer & Braun 2001). Consequently, in an observed population of main-sequence stars, most mass gainers appear to be single stars.

Figure 5 shows the surface nitrogen enhancements of the core hydrogen burning mass gainers in short period binaries by conservative mass transfer. These enhancements come about by the accretion of CNO-processed material that was deep inside the mass donor before the mass transfer, which is then redistributed in the envelope of the mass gainer through thermohaline mixing operating on the thermal timescale of the star (Wellstein, Langer & Braun 2001). Rotation or rotational mixing is not included in these models. The surface nitrogen enhancement factors found in these conservative models are in the range of 3–6.

As discussed above, especially the evolution of wider binaries may be nonconservative, and the material with the highest fraction of CNO processed material in particular may be ejected from the binary. Therefore, mass gainers may also populate the range of nitrogen enhancement factors between 1 and 3 (Langer et al. 2008). The enhancement factors from conservative binary models also do not provide upper limits. For example, shortly after the mass transfer, before thermohaline mixing is complete, higher nitrogen abundances can be found (Langer et al. 2008). When weighing the obtained nitrogen enhancements with the corresponding lifetime, however, it appears that the range in predicted nitrogen surface enhancements in hydrogen burning mass gainers (without rotational mixing) is very similar to that produced by models of rotating single stars (Ekström et al. 2008, Brott et al. 2011a; see also Section 5). This fact, together with the expectation that mass gainers are often rapid rotators (Section 3.1), complicates observational tests of rotational mixing in massive main-sequence stars.

In addition to the pollution of the surface of the mass gainers by accretion, these stars are, of course, also prone to rotational mixing. Recent models that take this effect into account predict that nitrogen can be enhanced by up to another factor of 3 (Langer et al. 2008). Furthermore, it was shown by Cantiello et al. (2007) that—assuming efficient semiconvective mixing (cf. Section 4.3.2)—mass gainers can be spun-up sufficiently to completely mix during the accretion

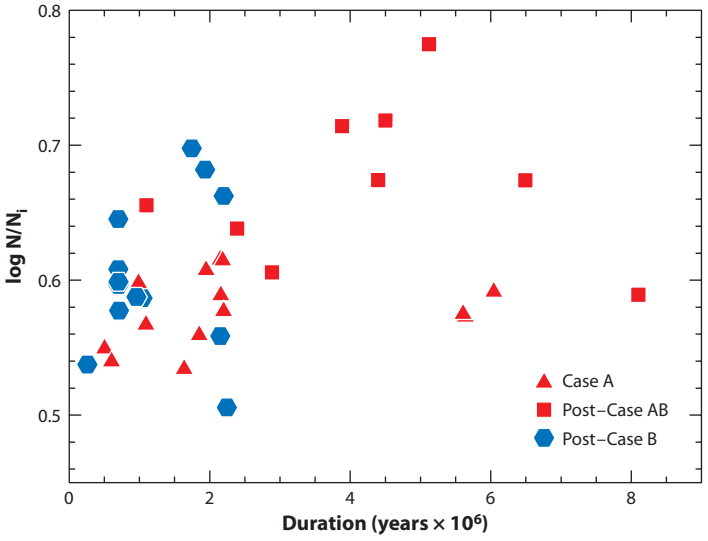

Figure 5

Time-averaged surface abundance of nitrogen during the various discrete post–mass transfer phases, relative to the initial nitrogen abundance, for the solar metallicity main sequence–type mass gainers in the binary models of Wellstein, Langer & Braun (2001), as a function of the duration of the post–mass transfer phases. The models are conservative, have 12 $M_\odot$ and 16 $M_\odot$ primaries, respectively, and have initial mass ratios larger than 0.5. Case A mass gainers during slow Case A mass transfer (Algol-type systems) are marked by triangles. The same stars appear as squares after Case AB mass transfer. Post–Case B mass gainers are marked by hexagons. The stars of the last two categories are unlikely to be identified as binary stars.

phase, as proposed by Vanbeveren & De Loore (1994). In fact, the 15-$M_\odot$ mass gainer studied by Cantiello et al. (2007) underwent chemically homogeneous evolution after the accretion event. This effect has not yet been investigated systematically, however. In addition to rotationally induced mixing, it is also conceivable that mass gainers in initially close binaries are mixed during the accretion phase by gravity waves that are excited by the impact of the accretion stream.

Most of the discussion above refers to mass gainers in massive binaries with short initial periods ($P_i \lesssim 10$ d), which may constitute more than half of all systems (cf. Section 3.6). The longest period systems that still interact strongly (with periods of several hundred days), to look at the other extreme, will undergo common envelope evolution, where mass and angular momentum loss leads to a close binary with a hydrogen-deficient core helium burning component (Taam & Sandquist 2000). In general, the initially less massive star is still on the main sequence. Because the main-sequence star is not accreting any substantial amount of mass due to the brevity of the common envelope phase, the luminosity ratio in such systems may be close to one. Consequently, and because their orbits are tight, they should be more easily recognized as binaries.

We know very few such systems. Some of the WR+O star binaries in the WR catalog of van der Hucht (2001) might be understood as post–common envelope binaries, but many of them are so massive that it is questionable whether they could have gone through a common envelope phase, as stars above 30 $M_\odot$ or so are thought not to evolve into the red supergiant regime (Humphreys & Davidson 1979; Langer et al. 1994; Vanbeveren, De Loore & Van Rensbergen 1998) (see Section 4.2). Lower mass OB stars with close helium star companions are not known, which could be owing to several reasons. Initially wide Case B and Case C systems might mostly merge, as suggested by Podsiadlowski, Joss & Hsu (1992). The merger stars are expected to form peculiar core helium burning supergiants, with helium cores that are undermassive for the total stellar

Case C mass transfer: mass transfer from a helium burning star

mass, likely making them blue supergiants (Braun & Langer 1995). Alternatively, helium star companions in the mass range of 2 $M_\odot$–5 $M_\odot$ might be difficult to observe, because they likely lack an optically thick stellar wind. This would prevent the shift of the flux maximum toward the optical wavelength range, unlike in more massive helium/WR stars. On top of this, the post-main-sequence lifetime of massive stars lasts only about 10% of the duration of core hydrogen burning. Helium stars below $\sim 3\ M_\odot$ can expand after core helium exhaustion (Yoon, Woosley & Langer 2010) and become optically bright. They could thus be caught observationally shortly before their supernova explosion.

3.3. Main-Sequence Mergers

When two core hydrogen burning stars merge in a Case A binary, the merger product will also be a core hydrogen burning star, i.e., a main-sequence object. According to Pols (1994) and Wellstein, Langer & Braun (2001), binaries with initial periods shorter than ∼2 days and with initial mass ratios smaller than ∼0.6 evolve into contact, with the likely consequence that many of them will merge. This concerns more than half of all Case A systems. Therefore, in practically any given population of massive main-sequence stars—e.g., in star clusters near the turn-off, or in a field population—we would expect up to 10% or more of the stars to be merger remnants (Podsiadlowski, Joss & Hsu 1992; de Mink, Langer & Izzard 2011; Eldridge, Langer & Tout 2011). Unfortunately, it is not yet clear what these merger stars look like. Peculiar properties may include the apparent age of the star, its surface abundances, its rotation rate, and its magnetic field.

Indeed, main-sequence mergers have been considered in the context of blue stragglers in old star clusters (Sills et al. 2002), i.e., main-sequence stars that reside above the turn-off in the Hertzsprung-Russell (HR) diagram and that have an apparent age that is younger than the cluster age. This is due to the steep mass-luminosity relation of main-sequence stars. This has the effect that the least massive of the merging stars has burnt much less fuel than what the more massive merger product would have consumed by the time of the merger if it had been born as massive and luminous as it comes out of the merger process. Whereas the mass-luminosity relation becomes shallower for high-mass stars (Gräfener et al. 2011), the effect as such prevails, unless there is excessive mass loss during the merger event (van Bever & Vanbeveren 1998). A similar effect is produced by mass accretion in close-to-conservative binary systems (cf. Section 3.1).

The amount of mixing expected in massive merger stars is rather unclear. In low-mass mergers, the amount of mixing is thought to be small (Lombardi, Rasio & Shapiro 1996). Gaburov, Lombardi & Portegies Zwart (2008) computed head-on collisions of massive stars, finding substantial mixing in equal mass mergers and little mixing in the case where the masses of the two colliding stars are substantially different. In contrast to those models, close binary mergers have a severe angular momentum surplus. This implies, on the one hand, that some mass needs to be lost in the merger process to carry away the excess angular momentum, while, on the other hand, that the merger remnant may be rapidly rotating, at least initially, and thus undergoes rotational mixing. Although quantitative predictions are not available, a nitrogen and perhaps helium surface enrichment is thus expected for massive main-sequence merger remnants.

As indicated above, the rotation rate of a main-sequence merger star is expected to be high, at least initially. The potential energy released in the merger event is thought to expand the merged star to radii well above its thermal equilibrium configuration (see Glebbeek & Pols 2008, for the case of low-mass mergers). The observations of an ongoing merger event described by Tylenda et al. (2011) provide observational evidence for this. It is conceivable that the merger product solves its angular momentum problem at this time by ejecting the high angular momentum material and that the merger remnant settles at subcritical rotation rates.

A further uncertainty is introduced by the possibility that the merger process may lead to the creation of a large-scale magnetic field owing to the strong differential rotation in the merger star. Tout et al. (2008) argue that magnetic white dwarfs gained their strong fields in a merger process, and Ferrario et al. (2009) proposed that large-scale magnetic fields in massive main-sequence stars (see Section 4.1) may be generated by the merger of pre-main-sequence stars. The mechanism discussed by Ferrario and colleagues may also work for the massive main-sequence mergers discussed here, which could thus turn out to produce magnetic main-sequence stars. As such, their rotation rates might be mediated after the merger process due to the interaction of the stellar wind with the magnetic field, which would lead to a spin down (ud-Doula, Owocki & Townsend 2008), as also observed among low-mass stars (Skumanich 1972).

3.4. Post-Main-Sequence Merger

In cases where one or both of the stars in a merging binary possess a hydrogen-free core, this core is not expected to mix with the hydrogen-rich material during the merger process due to its higher mean molecular weight and lower entropy. The merger star will therefore not be a core hydrogen burning star, even if one of the merging components is still a main-sequence object.

Depending on how much mass is lost during the merger process, the merger of a post-main-sequence star with a main-sequence component—which is the most likely case in a post-main-sequence merger—may lead to core helium burning stars, which have helium core masses that are too small for their total mass. In contrast to core hydrogen burning mergers or accretion stars, post-main-sequence mergers cannot rejuvenate, i.e., they cannot adapt, their core mass to the new total mass, due to the high entropy barrier generated by the hydrogen burning shell source. The structure of core helium burning stars with undermassive helium cores has been investigated by Braun & Langer (1995) and Claeys et al. (2011), who showed that these stars avoid the red supergiant stage, i.e., these stars not only perform all of core helium burning as blue supergiants, but they also explode in this stage (if they are not massive enough to transform into WR stars).

3.5. Merger Candidates

Whereas a galactic low-mass merger event has recently been observed (Tylenda et al. 2011), it is unlikely that massive mergers will be found nearby due to the short merger timescale and the scarcity of massive stars (although V838 Mon could have been a massive merger; cf. Munari et al. 2002). According to the most recent binary statistics (see Section 3.6 below), the rate of massive merger in the Milky Way may be of the order of 10–20% of the galactic supernova rate, i.e., one per 200 years. However, we can expect to find several stars that have merged recently and, thus, still display a gaseous circumstellar merger remnant, because the nebula dispersion timescale is expected to be of the order of 10^4 years, which is analogous to that of nebulae around luminous blue variable stars (LBVs) (Nota et al. 1995). In fact, there are two very good candidates.

The first one is the O6.5f?p star HD 148937, a bright nearby O star in the Ara OB1 association, which is surrounded by the expanding (350 km s^{-1}) nitrogen-rich (five times solar) bipolar circumstellar nebula RCW 107 (Leitherer & Chavarria 1987). Although the star is a giant, it appears to be too hot for its luminosity ($T_{\rm eff} = 41{,}000$ K, $\log(L/L_\odot) = 5.75$; Naze, Walborn & Martins 2008) to explain its nebula through an outburst during an LBV phase (Smith, Vink & de Koter 2004; Vink 2009). HD 148937 is one of three so-called Of?p stars that show recurrent spectral variations, for which strong magnetic fields (100–300 G) have been detected (Naze et al. 2010). With a rotation period of 7.2 days, it is a fast rotator among the OIII stars, and particularly among the Of?p stars (Naze et al. 2010).

Luminous blue variable (LVB): a star that evolves on the thermal timescale and when it reaches the Eddington limit or the Ω limit during post-main-sequence evolution

Interpreting HD 148937 as a merger remnant may provide an explanation for its massive (2 $M_\odot$) nitrogen-rich circumstellar nebula, its rapid rotation, and its strong magnetic field. Through the expansion age of the nebula, we can date the merger event as being only 3,000 years in the past (Leitherer & Chavarria 1987). The model of ud-Doula, Owocki & Townsend (2008) implies that the timescale for magnetic spin-down from the current configuration is two orders of magnitude larger. In this interpretation, we conclude that the merger process in HD 148937 found a way to carry away large amounts of mass (nebula) and angular momentum very fast, on a timescale that is short compared to the thermal timescale of the merger star. In order to carry away large amounts of angular momentum, a strong magnetic field might have been helpful. Therefore, the radius and perhaps the magnetic field strength could have been larger during and shortly after the merger process than they are at present. Due to the short derived time since the merger, which is comparable to the Kelvin-Helmholtz timescale of HD 148937, it is possible that the star has not yet reached thermal equilibrium, i.e., it may still be contracting and spinning up.

The second likely merger star is the B[e] supergiant R4 in the Small Magellanic Cloud (SMC). The B[e] star's position in the HR diagram coincides with the terminal-age main sequence (TAMS) position of 20-$M_\odot$ models (Zickgraf et al. 1996). The detection of a wide binary companion ($P \simeq 21$ years) allowed a dynamical mass determination yielding about 13 $M_\odot$ for both stars (the companion being an evolved star of spectral type A), with a normal luminosity-to-mass ratio (Zickgraf et al. 1996). As the luminosity ratio of both stars is $L(\mathrm{B[e]})/L(\mathrm{A}) = 7$, both objects can only have the same age if the B[e] star is a merger product (Pasquali et al. 2000). In fact, it requires that the system started out as a triple star with three components of rather similar mass: As we have reasons to assume that the merging happened very recently (see below), none of the components producing the B[e] star could have been more massive than the A star. However, the high luminosity of the B[e] star demands a high helium core mass fraction in both contributing components, which implies that their masses cannot have been significantly lower than that of the A star.

The implication that the merging event producing the B[e] star R4 happened recently stems from the spectroscopic discovery of an extended (2.4 pc) circumstellar nebula (Pasquali et al. 2000). As in the case of HD 148937, the nebula is bipolar, young (~12,000 years), and nitrogen-rich. Also like HD 148937, the B[e] star is too hot ($T_{\mathrm{eff}} = 27{,}000$ K; Zickgraf et al. 1996) to be considered a regular LBV. Being located in the SMC, R4 is too faint ($V = 13$ mag) to allow a direct detection of a magnetic field. However, Zickgraf and colleagues find prominent spectroscopic and photometric variability.

Further candidates for merger stars are the nitrogen-rich slowly rotating early B-type stars discussed in Section 5.4, and the hot nitrogen-rich slowly rotating B-supergiant (Section 6.1).

3.6. How Many Massive Binaries?

As discussed above, the mass gainers in close binary systems, and merger stars, will mostly be perceived as single stars. We have also seen that the predicted properties of these mass gainers may overlap significantly with those from models of rotationally mixed single stars. It will therefore be important to estimate the number of mass gainers that one may expect in a given ensemble of main-sequence stars.

In recent years, it has become evident that the fraction of massive stars that are members of a close binary system is very large. According to Mason et al. (2009) and Sana & Evans (2011), who review the O star binary fraction and binary distribution functions for young galactic clusters and for galactic field O stars, the fraction of O stars that have a spectroscopic companion is between 45% and 75%. Sana & Evans show, furthermore, that O star binaries have the tendency to form

very close binaries, with 60% of them at periods below 10 days and 90% with periods small enough to allow one of the stars to fill its Roche-lobe during its life. Because the companion stars are also often of spectral type O, about three-quarters of all O stars will have a strong binary interaction—mass transfer, common envelope evolution or merger—during their evolution, which for about half of them occurs during their core hydrogen burning phase of evolution. About one quarter of all O stars are expected to merge with their companion.

It is an immediate implication that when we observe a population of evolved massive stars, e.g., supergiants, WR stars, or supernovae, the average stellar properties may be largely determined by foregoing binary evolution effects (see Section 7). Depending on their age, even for main-sequence stars, the incidence of binary interaction can be so high that binary effects may produce the dominant signal. Single noninteracting O stars may be an exception. This is further discussed in Section 5.

4. FURTHER PHYSICAL PROCESSES

4.1. Magnetic Fields

As indicated above (Sections 2.2, 2.3, 3.3), magnetic fields are likely to be much more important in massive stars than generally acknowledged. Because this topic was recently reviewed (cf. Donati & Landstreet 2009), we only sketch the field here. We distinguish three different types of magnetic fields in the following, which may all play significant roles in massive stars.

4.1.1. Stable fields. A star may inherit a magnetic field from the material it formed from. This idea of fossil fields has been discussed, for example, by Moss (2003), who investigates the difficulty for such fields to survive a fully convective pre-main-sequence evolution. A comparable problem is to drag any magnetic field from the ISM into a star, because the material needs to go through an accretion disk. Significant accretion is only possible due to the high viscosity of the disc, which is thought to be produced by the magneto-rotational instability (Balbus & Hawley 1998). This instability might tangle the field through turbulent motion at such small spatial scales that reconnection processes could significantly reduce its flux, and no stable large-scale field configuration would emerge from this after the accretion process (M-M. Mac Low, private communication). This makes the idea of implanting fossil fields into main-sequence stars problematic.

There may be other ways to produce stable large-scale magnetic fields inside stars—i.e., fields that do not need a dynamo process to keep them up. According to observational evidence (Section 3.5), perhaps the most promising way is related to stellar mergers (Sections 3.3 and 3.4).

It was shown by Braithwate & Spruit (2004) that certain magnetic field configurations can be stable in the sense that their decay takes longer than the stellar lifetime. This holds in particular for poloidal fields that are stabilized by an embedded toroidal field. Although the fields in the magnetic fraction of intermediate-mass main-sequence stars (which are roughly 10%) appear, partly, to have a rather complex morphology (Donati et al. 2006), their structure appears to be simple compared to the fields of low-mass stars (Donati & Landstreet 2009). In the magnetic intermediate-mass stars, the fields are thought to be stable, i.e., not produced by any dynamo currently acting in the star. The reason is that many of these stars are slowly rotating, which excludes most potential dynamos, and that their convection zone—which could produce a field—lies in their cores (Donati & Landstreet 2009).

Such stable fields may also play a role in a significant fraction of massive main-sequence stars. Due to the small number of optical and near-IR spectral lines and wind effects on the photosphere structure, the detection of large-scale fields is more difficult in the hot massive main-sequence

stars (Schnerr et al. 2008, Donati & Landstreet 2009). Nevertheless, about two dozen OB stars have meanwhile been found to have quite strong fields of a few hundred Gauss (Petit, Massa & Marcolino 2011; Hubrig et al. 2011). We discuss possible indirect magnetic field indicators and evolutionary consequences of such fields in Section 5.

4.1.2. Dynamo fields. The second type of field that could be important for massive stars is dynamo-generated fields. As such, we designate fields that need a mechanism inside the star that reproduces them continuously, as they would decay quickly otherwise. Although the produced fields may or may not be fluctuating in time, the magnetic field would be present most of the time. Two different kinds of dynamo processes have been suggested to operate in massive main-sequence stars, one operating in convection zones, the second one operating in the radiative envelope.

According to current models, a magnetic field is produced in the convective cores of massive main-sequence stars and their vicinity—where it may well affect the transport of heat, angular momentum, and chemical elements (Charbonneau & MacGregor 2001; Brun, Browning & Toomre 2005). However, it appears unlikely that this field is transported deeply into the radiative envelope or even to the stellar surface (Charbonneau & MacGregor 2001, MacGregor & Cassinelli 2003, MacDonald & Mullan 2004).

Massive main-sequence stars also possess envelope convection zones very close to their surfaces (Stothers & Chin 1993), which are induced by the iron opacity peak (Iglesias, Rogers & Wilson 1992; Iglesias & Rogers 1996). These convection zones, for which various observational indications exist (Belkacem et al. 2009, Cantiello et al. 2009, Degroote et al. 2010), may also generate magnetic fields that reach the stellar surface (Cantiello et al. 2009) and may form bright magnetic spots (Cantiello et al. 2011, Cantiello & Braithwaite 2011). Such spots have been suggested to cause the ubiquitous DACs phenomenon (Cantiello et al. 2009), i.e., Discrete Absorption Components in UV lines of OB stars (Prinja & Howarth 1988; Kaper et al. 1997; Prinja, Massa & Fullerton 2002).

Spruit (2002) has suggested that a dynamo process can also work in differentially rotating radiative stellar envelopes. The main component of the produced magnetic field is toroidal, which is thought to counteract the differential rotation by producing a torque that transports angular momentum against the angular momentum gradient (cf. Section 2.2). Although the model of Spruit has been criticized (Zahn, Brun & Mathis 2007), the main effect has been confirmed in simplified magnetohydrodynamic models (Braithwaite 2006; see also Section 3.1).

4.1.3. Intermittent fields. The third type of magnetic fields that may be important in massive stars could be intermittent fields, i.e., fields that are enhanced inside the star by some nonstationary dynamo process and that exist at a strength to cause a significant effect only for a short time. For example, a possibility of magnetic fields to transport angular momentum in stars may be caused by winding up small fields by differential rotation without involving a dynamo process (R. Arlt, private communication; Arlt & Rüdiger 2011). The achieved magnetic torques could establish close-to-rigid rotation and then fade.

Furthermore, intermittent strong fields may be achieved in short-lived dynamical situations. In the case of a massive star merger, as discussed in Section 3.3, the expected strong differential rotation may boost the magnetic fields during the merger process, which decay to a weaker stable configuration thereafter. The short lifetime of these very strong fields would not imply that they are unimportant. As argued in Section 3.3, magnetic fields that are active during the merger process might be able to increase the amount of angular momentum that is carried away by the dynamical mass loss. However, it may be difficult to directly confirm such fields observationally,

as this basically requires catching a merger in the act. This is in fact currently attempted for the low-mass merger event V1309 Scorpii described by Tylenda et al. (2011).

4.2. Mass Loss

Due to the steep stellar mass-luminosity relation (Section 5.2), massive stars are very luminous ($>10^4$ $L_\odot$). This high luminosity gives rise to mass loss during all of the different evolutionary phases.

4.2.1. Mass loss from main-sequence stars. Mass loss from massive main-sequence stars was discovered by Morton (1967), who found blueshifted absorption lines in the UV spectra of OB stars. It is interpreted as being due to photon absorption in atmospheric UV lines, where a net outward force is exerted on the respective ions as the exciting photons are preferentially traveling outward but the direction of the re-emitted photons is random. The thereby accelerated ions couple with the other particles through scattering and electrostatic forces to drive the wind flow (Lucy & Solomon 1970; Castor, Abbott & Klein 1975; de Koter, Heap & Hubeny 1997; Kudritzki & Puls 2000).

The importance of these winds for the evolution of stars was realized quickly, as it was shown that stars could lose a substantial part of their initial mass through this process (De Loore, De Greve & Lamers 1977; Chiosi, Nasi & Sreenivasan 1978; Chiosi & Maeder 1986). The challenge is then to derive quantitative measures of the mass-loss rates, which can be used in stellar evolution calculations that are more accurate than a factor of two. Empirical approaches are severely complicated by the realization that the winds of hot stars are not smooth flows but highly structured or clumped (Hillier 1991; Eversberg, Lepine & Moffat 1998; Bouret et al. 2003; Mokiem et al. 2007b; Moffat 2008), as expected on theoretical grounds (Owocki, Castor & Rybicki 1988; Cantiello et al. 2009). Theoretical efforts require the treatment of the hydrodynamics of at least tens of thousands of spectral lines (Abbott & Lucy 1985; de Koter, Heap & Hubeny 1997; Vink, de Koter & Lamers 2001) and potentially clumping and porosity effects also (Muijres et al. 2011).

Nevertheless, the understanding of OB star winds is quite clear in that the mass-loss rates increase for more massive (i.e., more luminous) stars (Puls, Vink & Najarro 2008) and for more metal-rich stars (Mokiem et al. 2007b). This has the important implication that, at a given metallicity, radiation-driven winds are unimportant for the stellar mass budget of main-sequence stars below a certain initial mass. Using the mass-loss rate predictions of Vink, de Koter & Lamers (2001), Brott et al. (2011a) find that the stellar masses are reduced by less than 10% on the main sequence for stars below 28 $M_\odot$, 42 $M_\odot$, and 60 $M_\odot$, for galactic, Large Magellanic Cloud (LMC), and SMC metallicity, respectively. These numbers are evaluated for models with initial rotational velocities of 200 km s^{-1} and are lower for very fast rotators. Because the efficiency of the angular momentum loss that is associated with the stellar winds (disregarding magnetic fields) is about 10 times that of the mass loss (Langer 1998), the zero-age main sequence (ZAMS) masses—below which about 10% of the angular momentum of a star is lost during the main sequence evolution—are 9 $M_\odot$, 14 $M_\odot$, and 20 $M_\odot$, respectively, for the metallicities quoted above.

Mass loss becomes much more important for very massive stars ($M \gtrsim 60\,M_\odot$), where unfortunately the mass-loss rates become more uncertain, for a number of reasons. First, very massive stars are rare, such that there are only very few empirical constraints. The wind physics also becomes more challenging; as very massive stars are close to their Eddington limit (Ulmer & Fitzpatrick 1998), their atmospheres are often helium enriched (Herrero et al. 1992, Mokiem et al. 2006), their winds may become partly optically thick (de Koter, Heap & Hubeny 1997; Martins et al. 2008; Crowther et al. 2010b), their gravities do not reflect a simple mass-luminosity relation

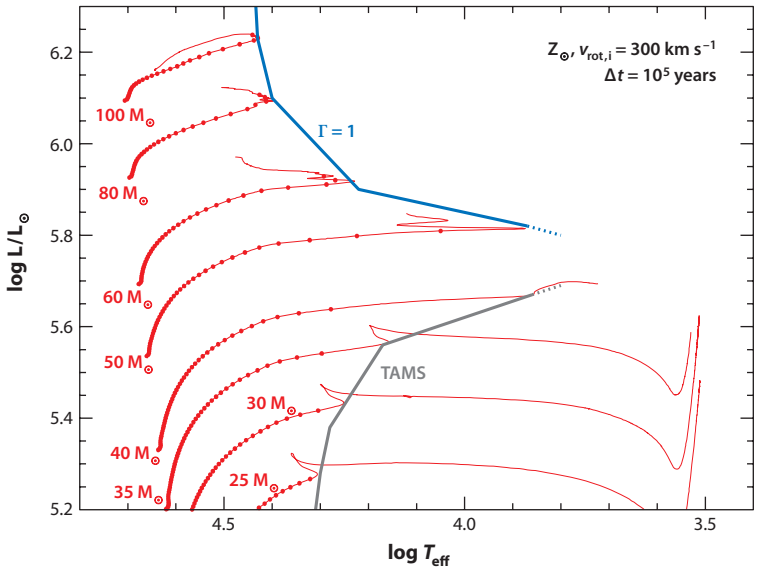

Figure 6

Evolutionary tracks of massive (Brott et al. 2011a) and very massive stars (K. Köhler, private communication) with solar metallicity, rotating initially at about 300 km s^{-1}, in the Hertzsprung-Russell diagram, starting at the zero age main sequence. The stars up to 40 $M_\odot$ were computed past core hydrogen exhaustion; the terminal age main sequence (TAMS) is drawn as a gray line. More massive stars are computed close to core hydrogen exhaustion, where they hit the Eddington limit (shown as $\Gamma = 1$). Red dots are placed on the evolutionary tracks with a time difference of 100,000 years.

(Gräfener et al. 2011), and their mass-loss rate may be influenced by the star's rotation (Friend & Abbott 1986, Langer 1998, Maeder & Meynet 2000b). Whereas mass-loss predictions for very massive stars start to emerge that identify the Eddington factor as the most relevant parameter controlling the mass-loss rate (Vink et al. 2011, Gräfener et al. 2011), those have not yet been used in stellar evolution models.

In addition, very massive stars may reach the Eddington limit during core hydrogen burning. This is shown in **Figure 6** for the example of the solar metallicity tracks of Brott et al. (2011a) and K. Köhler (private communication). In these models, which use an overshooting parameter of 0.3, it is assumed that the mass-loss rate increases proportional to $1/(1-\Gamma)^\alpha$ such that the models turn around near the Eddington limit. Here, $\Gamma = L/L_{\rm Edd}$ is the Eddington factor, and α is a positive exponent. In contrast to the situation where the Eddington limit is reached after core hydrogen exhaustion, which is the case when small or no convective core overshooting is assumed (Langer et al. 1994), the mass-loss rates required very near the Eddington limit are smaller than the thermal mass-loss rates $\dot{M}_{\rm th} = M/\tau_{\rm KH}$ because the evolutionary timescale is large ($\sim 10^5$ years). Therefore, the star can thermally adjust to the imposed mass loss, which means that although the star is close to the Eddington limit, its envelope may remain stable (Langer 1998).

The mass-loss process near the Eddington limit is complicated by the fact that all stars rotate, and therefore stars that do approach their Eddington limit will reach the Ω limit first, where gravity and radiative and centrifugal acceleration cancel each other (Langer 1997). Maeder & Meynet (2000b) showed that gravity darkening (Section 2.1) plays a role in defining a star's Ω limit, which is, however, difficult to assess because it was shown that even hot stars have convective envelopes when they are close to their Eddington limit (Langer 1997). The LBVs (Nota & Lamers 1997;

Smith, Vink & de Koter 2004; Vink 2009) are associated with stars near their Eddington limit, which show bipolar circumstellar nebulae (Nota et al. 1995) and are located near the theoretical Eddington limit in the HR diagram (Ulmer & Fitzpatrick 1998; see also **Figure 6**). Their eruptive mass loss, with the big eruption of η Carinae in the 1840s being perhaps the most violent example, may contribute significantly to the total amount of mass lost during the evolution of the most massive stars (Langer et al. 1994, Smith & Owocki 2006).

Observed star: a main-sequence star believed to be in the phase of core hydrogen burning

Although many questions about single-star mass loss near the Eddington limit remain open, we want to point out that this issue is also relevant for the evolution of very massive close binaries. It has been proposed that binary stars with primary masses high enough to reach the Eddington limit will not enter a common envelope evolution, because they would either undergo stable Case A/B mass transfer (short initial periods) or evolve like single stars (wider initial periods) (de Donder, Vanbeveren & van Bever 1997). The effective binding energies of the envelopes of massive stars near their Eddington limit may be as small as those of red supergiants, such that a common envelope evolution in this situation may in fact avoid a merger but rather lead to a common envelope ejection. The high-mass X-ray binary OAO 1657–415, which consists of a $\sim$15-$M_\odot$ Ofpe/WNL star with a high-mass neutron star companion in a $\sim$10 d orbit appears to support this scenario (Mason et al. 2012).

4.2.2. Post-main-sequence mass loss. Although the post-main-sequence lifetime of massive stars is generally only about 10% of their core hydrogen burning timescale, post-main-sequence mass loss is far from negligible because the mass loss rates can rise dramatically.

For blue supergiants, mass loss is generally described by the same methods as for hot main-sequence stars (Section 4.2.1; Vink, de Koter & Lamers 2001). However, some blue supergiants are Cepheids, i.e., large amplitude pulsators. Neilson & Lester (2008) proposed recently that Cepheid pulsations may greatly enhance the mass-loss rates of these stars. The total amount of mass loss by supergiant stars undergoing a blue loop evolution could thus be enhanced, which is suggested as a remedy for the longstanding Cepheid mass discrepancy (Neilson, Cantiello & Langer 2011).

The red supergiant mass-loss physics is not well understood (Bennett 2010), and the outflows of some of them are highly structured and variable (Smith, Hinkle & Ryde 2009; Tiffany et al. 2010). Therefore, the empirical mass-loss rates that have been used in stellar evolution models are quite uncertain. De Beck et al. (2010) and Mauron & Josselin (2011) review the available recipes and find disagreements of more than one order of magnitude. Mauron & Josselin conclude that the rate proposed by de Jager, Nieuwenhuijzen & van der Hucht (1988) still represents the available data best and should be favored over more recently suggested higher red supergiant mass-loss rates, despite the fact that it cannot reproduce all observed stars well. They also find evidence for supergiant mass-loss rates decreasing for lower metallicities, which might be expected if radiation pressure is playing a significant role.

Also, the WR mass-loss rates are not yet well understood, but evidence is accumulating that they may be explained by the same mechanism as the winds of O stars (Lucy & Abbott 1993, Gräfener & Hamann 2005, Vink et al. 2011, Gräfener et al. 2011). Both the presence of the iron opacity peak close to their stellar surface (Pistinner & Eichler 1995, Heger & Langer 1996) and their proximity to the Eddington limit (Gräfener & Hamann 2008) are related to their high mass fluxes. Furthermore, there is evidence that WR winds are highly clumped (Moffat et al. 1988, Marchenko et al. 2007). Hydrogen deficiency does not appear to be the key criterion for the emission of optically thick winds, as very hydrogen-rich WR stars have been identified (Martins et al. 2008, Gräfener et al. 2011), as well as hydrogen-free stars of lower luminosity with optically thin winds (Jeffery & Hamann 2010, Hamann 2010).

Similar to luminous main-sequence stars (Cantiello et al. 2009), subsurface convection zones in WR stars are expected to occur near the iron opacity peak. Their impact on the envelopes and winds of WR stars may be more dramatic than in massive main-sequence stars because the convection zone could reach up to the sonic point of the WR wind (Heger & Langer 1996; Petrovic, Pols & Langer 2006; Gräfener, Owocki & Vink 2012). Therefore, if (sub)surface convection zones do trigger wind clumping (Cantiello et al. 2009), WR stars are expected to show strongly clumped winds.

The metallicity dependence of the WR mass loss rates is of particular relevance, because the WR stars appear to be the immediate progenitors of long gamma-ray bursts, which are seen at high redshifts and often in low-metallicity environments (Section 7.4). Vink & de Koter (2005) have shown that the mass-loss rates of relatively cool WC-type stars ($T_{\rm eff} = 40{,}000$ K) decrease with metallicity down to a certain threshold ($\sim Z_{\odot}/1{,}000$), below which the winds are driven by carbon rather than by iron lines. However, Muijres et al. (2012) found that the winds of hot WR stars ($T_{\rm eff} \gtrsim 50{,}000$ K) may collapse altogether at low metallicity.

4.3. Thermally Induced Mixing

Although the focus in stellar evolution has been largely on the topic of rotationally induced mixing in the past decade, the fundamental uncertainties connected with the thermally induced mixing processes are still with us. This concerns two major process, overshooting and semiconvection. Whereas both processes may also transport energy and angular momentum, here we restrict our discussion on the probably more important transport of chemical elements.

4.3.1. Overshooting. Overshooting relates to the motion of convective fluid elements beyond the borderline between convectively unstable and radiatively stable layers. Whereas in multidimensional hydrodynamical models, this borderline is fluctuating in space and time (Brun, Browning & Toomre 2005), in one-dimensional stellar models without overshooting it is usually defined by the Schwarzschild criterion for convection. Usually, overshooting is simply applied in stellar models by increasing the convective region by a certain amount (e.g., Stothers & Chin 1985), although some groups describe the overshooting region by a diffusion approach (Herwig et al. 1997). Whereas overshooting is most often considered for convective cores of main-sequence stars (e.g., Stothers & Chin 1985), it may in principle apply to any stellar convection zone, although certainly with varying efficiency. For example, as helium burning convective cores usually grow in mass and are therefore bounded by a steep composition barrier, it is likely that overshooting is less efficient here compared to hydrogen burning convective cores that shrink in mass (Langer 1991c).

From the above it is clear that overshooting still poses many open problems. It may be easiest and most urgent to understand the efficiency of overshooting in the convective cores of massive main-sequence stars. Hydrodynamical models cannot resolve this question at present: Although they can obtain an overshooting distance for a fixed stellar background model (e.g., Dupree 2000), the thermal adaptation of the stellar model needs to be taken into account (Langer 1986), and hydrodynamical multidimensional models including convection cannot yet be evolved over a thermal timescale. Magnetohydrodynamic models, moreover, imply that magnetic fields generated in the rotating convective core of massive stars may influence convective core overshooting (Section 4.1.2).

Several attempts have been made to determine the efficiency of overshooting for main-sequence stars observationally. For low- and intermediate-mass stars, it is possible to determine the overshooting efficiency from the observed main sequence widths in star clusters, which is predicted

to be larger for larger overshooting (Stothers & Chin 1985). Mermilliod & Maeder (1986) and Maeder & Meynet (1987) found an overshooting of 0.25–0.3 pressure scale heights (H_P) from comparison with nonrotating stellar evolution models, whereas in the rotating models, Ekström et al. (2008) favor an overshooting of $0.1 H_P$. Schröder, Pols & Eggleton (1997) compared stellar evolution models without rotation to eclipsing binary stars in the mass range of $2.5-7\,M_\odot$ and derived an overshooting of about $0.3\,H_P$, whereas Ribas, Jordi & Gimenez (2000), Guinan et al. (2000), and Claret (2007), using the same method, find values between 0.1 and 0.6 H_P, with a systematic increase of the overshooting value for larger stellar masses. Briquet et al. (2007) used asteroseismological measurements to determine the overshooting in the β-Cephei variable θ Ophiuchi to $0.44 H_P$.

While most of the eclipsing binary work relates to stars of about $10\,M_\odot$ or less, the method to determine the overshooting from the observed main-sequence widening in the HR diagram cannot be applied to stars above $10\,M_\odot$ because the red edge of the main-sequence band merges with the blue supergiant distribution (Vink et al. 2010; Section 6). Nevertheless, Hunter et al. (2008b) and Brott et al. (2011a) used the sharp drop in the observed $v \sin i$–distribution of early B stars as a function of their surface gravity as an indicator of the red edge of the main-sequence band. In this way, they calibrated the overshooting in main-sequence models including rotation to be approximately $0.3\,H_P$ at a mass of $16\,M_\odot$.

Overall, the evidence is great that overshooting plays a significant role in massive main-sequence stars in addition to effects of rotation. If overshooting is really more efficient for more massive stars, its role in very massive main-sequence stars—for which we do not yet have an empirical assessment—could be quite large. As shown in **Figure 6**, for an overshooting distance of $0.3\,H_P$, the main-sequence phase of solar metallicity stars above $40\,M_\odot$ already extends all across the HR diagram (see also **Figure 2**).

4.3.2. Semiconvection. Semiconvection is an instability that occurs when a superadiabatic layer is stabilized by a chemical gradient (Kato 1966). In fact, semiconvection occurs if the Schwarzschild criterion for convection [comparing the temperature gradient in the star with the adiabatic temperature gradient, $dT/dr < (dT/dr)_{ad}$] is fulfilled but at the same time the Ledoux criterion [comparing density gradients, $d\rho/dr < (d\rho/dr)_{ad}$] is not fulfilled. As such, it is clear that in the presence of chemical gradients, the criterion for convection must be the Ledoux criterion.

Semiconvection in stars has been discussed initially in the context of massive core hydrogen burning stars, which can develop extended semiconvective regions above their convective core (Schwarzschild & Härm 1958; Chiosi & Summa 1970; Langer, El Eid & Fricke 1985). The timescale of semiconvection is the thermal timescale, which is short compared to the nuclear timescale in main-sequence stars but long compared to the timescale of convection. Therefore, it was found in the papers quoted above that the detailed treatment of semiconvection makes little difference for the main-sequence evolution of nonrotating massive stars. This is one of the reasons why until today in many stellar evolution calculations the Schwarzschild criterion for convection is used—which implies that semiconvective layers are mixed as rapidly as convective layers. This is, however, only a good approximation for such phases of stellar evolution, which have a timescale that is long compared to the thermal timescale.

However, semiconvection has a profound influence on the post-main-sequence evolution. It affects the convective mixing above the hydrogen shell source (Chiosi & Summa 1970), determines the appearance and extent of blue loops in the HR diagram during core helium burning, and is essential for defining the extent of the convective cores during core helium burning (Langer 1991c). It surely affects the late burning stages of massive stars, although this has not been investigated thoroughly. Cantiello et al. (2007) showed that semiconvection is also essential in models of rapidly

rotating binary stars, where they found that chemically homogeneous evolution (cf. Section 2.3) occurred only in the case of fast semiconvective mixing. In single stars, Yoon, Langer & Norman (2006) found chemically homogeneous evolution also to occur in the case of slow semiconvective mixing.

The local and linear regime of semiconvection (Kato 1966) is undebated and has been developed into a diffusion model (Langer, Sugimoto & Fricke 1983). Beyond the linear regime, semiconvective regions have been shown to break up into small convective layers bounded by small layers that contain the composition gradient (Spruit 1992). This picture emerges also from detailed stellar evolution models (Langer, El Eid & Fricke 1985; Langer 1991c). The overall mixing efficiency in this situation is still highly controversial (Shibahashi & Osaki 1976, Spruit 1992, Merryfield 1995, Zaussinger & Spruit 2011), with predicted mixing timescales ranging from values shorter than the thermal timescale (Merryfield 1995) to values larger than the nuclear timescale (Zaussinger & Spruit 2011). We conclude that the problem of semiconvection in massive stars is essentially unsolved.

4.3.3. Thermohaline mixing. Thermohaline mixing in stars occurs in thermally stable layers, i.e., in layers that have a subadiabatic temperature stratification, but which are destabilized by an inverted mean molecular weight gradient such that heavier particles are placed on top of lighter ones. In massive single stars, this situation happens rarely, because in the course of thermonuclear burning, the heaviest nuclei are formed in the deepest layers. An exception concerns the off-center ignition in semidegenerate cores (Siess 2009). Thermohaline mixing also has been found to be an important process in low-mass red giants, which may serve as the best suited benchmarks to probe this process (Charbonnel & Zahn 2007, Cantiello & Langer 2010).

In the context of massive main-sequence stars, thermohaline mixing is an essential process to consider in accreting binaries. Mass gainers generally accrete helium-enriched matter from their companions during Roche-lobe overflow. Because the timescale of thermohaline mixing is the thermal timescale, it can actually influence whether a binary system develops contact during a thermal timescale mass transfer, as the radius of the mass gainer depends on its surface helium content (Braun 1997). Thermohaline mixing is responsible for diluting the accreted matter throughout the envelope of the mass gainer up to the point that any inverse mean molecular weight gradient has disappeared (Wellstein, Langer & Braun 2001; Petrovic et al. 2005).

4.4. Microphysics

Stars are big, but their properties are often determined by quantum mechanical processes between elementary particles. Most relevant here are radiative opacities and thermonuclear reaction rates.

Accurate opacities for hot plasmas are available today through the OPAL (Rogers & Iglesias 1992, Iglesias & Rogers 1996) and OP (Seaton 2005) projects, which in particular produced the so-called iron opacity peaks (see Sections 4.1.2 and 4.2.2). The models of hot stars (i.e., massive main-sequence models) changed severely when these new opacities were included, such that models without them have to be considered with caution. Opacities for cool stellar atmospheres, where molecules and dust become important, are even more complex (Alexander & Ferguson 1994). As cool stars often have dynamical atmospheres and complex nonequilibrium chemistry, opacity calculations for those stars are difficult. For the current status, see Marigo & Aringer (2009).

The uncertainties of thermonuclear reaction rates in massive star models have been thoroughly investigated by Rauscher et al. (2002). Whereas the nucleosynthesis yields of various isotopes are sensitive to reaction rate uncertainties, the stellar evolution turns out to be little affected. Marked

exceptions are the C^{12} $(\alpha, \gamma)O^{16}$ rate (see Section 4.5) and perhaps the 3α rate (Tur, Heger & Austin 2010; Suda, Hirschi & Fujimoto 2011). Both rates are still considerably uncertain.

Type Ib/c supernova: a supernova showing no hydrogen that stems from a massive star with a stripped envelope

4.5. Advanced Core Evolution

The evolution of the cores of massive stars past the main-sequence stage has been relatively well understood for many decades. Following the Virial theorem (Kippenhahn & Weigert 1990), the cores evolve to ever increasing densities, and—in contrast to lower mass stars—increasing temperatures, as strong electron degeneracy is avoided. This leads massive star cores to evolve through the well-known sequence of hydrostatic helium, carbon, neon, oxygen and silicon burning (Arnett 1977 and references therein, Arnett & Thielemann 1985, Thielemann & Arnett 1985). This sequence is only abbreviated by the lowest masses, which undergo electron capture–induced collapse before core neon ignition (Nomoto 1984) (see Section 7.1), and by the highest masses where $e^{\pm}$-production can lead to a collapse of the core before oxygen ignition (Rakavy, Shaviv & Zinamon 1967; Heger & Woosley 2002; Heger et al. 2003) (Section 7.3).

These principles are well understood, but there are uncertainties during core helium burning. It brings up the question of whether the convective core during core helium burning can grow in mass or not. It is bounded by a composition discontinuity between the CO-rich gas inside the convective core and the layers above, which contain almost pure helium. Models with inefficient semiconvective mixing (Langer 1991c) end up with much smaller CO-cores than comparable models, which use fast semiconvective mixing (Woosley, Heger & Weaver 2002) or even the Schwarzschild criterion for convection (Meynet & Maeder 2000). This ambiguity has consequences for all subsequent burning stages, as well as for the bulk nucleosynthesis yields of massive stars (Langer & Henkel 1995) and the resulting compact remnants.

A second point is that the C^{12} $(\alpha, \gamma)O^{16}$ thermonuclear reaction rate is still quite uncertain. If this rate is slow, large amounts of carbon left after core helium exhaustion will ensure convective carbon and neon core burning stages. If the rate is fast, this may not be the case, which, among other things, may increase the borderline initial mass between neutron star and black hole formation (Tur, Heger & Austin 2007).

Also, binary effects during core helium burning have interesting consequences. In contrast to single stars, the helium core of a mass donor in a close binary, i.e., the progenitor of a Type Ib/c supernova (Section 7), cannot grow much in terms of its mass as it loses almost all its hydrogen in the mass transfer process, and consequently, the convective core also hardly grows. As a result, fewer α-particles are mixed into the core during core helium burning, which results in a higher final carbon fraction, because especially in the advanced stages of helium burning, most of the α-particles that are mixed into the convective core serve to convert carbon to oxygen. A high final carbon fraction from core helium burning implies a low–compact object mass, such that also quite massive Type Ib/c supernova progenitors may form neutron stars rather than black holes (Brown et al. 2001; Tauris, Langer & Kramer 2011).

The mixing processes during core helium burning are particularly uncertain at the lowest metallicities. Due to the lack of metals, hydrogen shell burning occurs at extremely low entropy, such that the entropy barrier between hydrogen and helium burning is significantly reduced compared to the situation at higher metallicity. This facilitates the mixing of protons into the helium burning layers, independent of the considered mixing process. Whereas rotational mixing has been suggested to lead to high yields of primary nitrogen and *s*-process elements in very metal-poor massive stars (Meynet & Maeder 2002; Yoon, Langer & Norman 2006; Chiappini et al. 2011; Yoon, Dierks & Langer 2012), thermally induced mixing may also play a major role in these stars (Heger, Woosley & Waters 2000).

In the burning stages beyond core helium exhaustion, the burning timescales become very short owing to the dominance of neutrino rather than photon cooling. This leads to substantial overadiabaticities in convection zones associated with the later burning stages, implying that the classical mixing length theory provides only a poor description of the transport of energy and chemicals, as suggested by multidimensional hydrodynamic models (e.g., Arnett & Meakin 2011). The consequences for nucleosynthesis, compact object formation, and supernovae have yet to be explored.

5. MODELS VERSUS OBSERVATIONS: MAIN SEQUENCE STARS

In view of the many uncertain physical processes that affect the evolution of massive stars, as discussed above, we review our current understanding of main-sequence stars here. Clearly, we can only hope to predict the advanced evolution of massive stars well with models that can reproduce the observed properties of main-sequence stars. As we see below, there are many problems, however.

A comparison with observations requires grids of detailed stellar evolution models. For metallicities equal to or larger than the SMC metallicity, single-star grids with up-to-date physics ingredients, including effects of rotation, have been produced by Meynet & Maeder (2000, 2003, 2005), Heger, Langer & Woosley (2000), Hirschi, Meynet & Maeder (2004), Heger, Woosley & Spruit (2005), Yoon, Langer & Norman (2006), Ekström et al. (2008) and Brott et al. (2011a). Recent grids describing the evolution of close binary stars were generated by Vanbeveren, De Loore & Van Rensbergen (1998), Wellstein, Langer & Braun (2001), de Mink, Pols & Hilditch (2007), Eldridge, Izzard & Tout (2008), and de Mink et al. (2009), and effects of rotation are included by Petrovic et al. (2005), Petrovic, Langer & van der Hucht (2005), Langer et al. (2008, 2010), de Mink et al. (2009), and Eldridge, Langer & Tout (2011).

5.1. Hertzsprung-Russell Diagram

For low- and intermediate-mass stars, we have a good understanding of the location of main-sequence stars in the HR diagram. The dispersion in the theoretical models has been small for many decades, and the qualitative and quantitative agreement with data on many star clusters is convincing (e.g., Chiosi, Bertelli & Bressan 1992). For stars above $\sim 10\,M_\odot$, however, the situation becomes more unclear and is getting worse the higher in mass we go.

There are two issues concerning the hot end of the main-sequence band. Massive stars are thought to already ignite core hydrogen burning during the star-formation phase when their mass is still increasing by accretion and while they are still hidden inside the molecular cloud from which they form (Yorke 1986, Zinnecker & Yorke 2007). Therefore, massive stars might appear in the HR diagram only after they have already consumed some hydrogen. However, because the evolutionary speed in the HR diagram is increasing during core hydrogen burning (e.g., **Figures 2** and **6**), this effect is rather small.

A second point concerns the hot edge of the main-sequence band. According to ZAMS stellar models, a maximum effective temperature is reached at a certain stellar mass. Above that, the ZAMS bends back toward cooler effective temperatures. This maximum temperature is about 46,000 K at a metallicity of $Z = 0.02$ and is achieved at about $120\,M_\odot$. It is higher and achieved at higher mass for lower metallicity (Ishii, Ueno & Kato 1999). At $Z = 0.004$, the maximum temperature of 56,000 K is reached at about $200\,M_\odot$. Petrovic, Pols & Langer (2006), who confirmed the finding of Ishi and colleagues for helium main-sequence stars (see Section 6.3), find that the maximum temperature may be higher for models that include mass loss.

The problem of identifying the cool edge of the main-sequence band in the HR diagram (the TAMS) is more severe for two reasons. First, there exists a population of blue supergiant stars of unknown evolutionary status, which appears to overlap with the main-sequence band for masses above 10–15 $M_\odot$ (Fitzpatrick & Garmany 1990, Larsen et al. 2011). As discussed in Section 4.3.1, this makes it impossible to calibrate the amount of mixing in massive main-sequence stars by, e.g., convective overshooting just based on the observed position of stars in the HR diagram (Vink et al. 2010).

Furthermore, models including the amount of overshooting suggested by recent observations lead to evolutionary tracks for stars above $\sim 40\,M_\odot$, which extend all the way to the red supergiant regime during core hydrogen burning (Brott et al. 2011a) (see **Figure 6**). Whether such an evolution is realized or whether the redward evolution is truncated by mass loss is currently not known. Certainly, stars that are slightly more massive will hit the Eddington limit before they can reach the red supergiant branch (**Figure 6**).

Stars of solar metallicity that are more massive than about $50\,M_\odot$ are expected to reach the Eddington limit or the Ω-limit (Section 4.2), leading to either stationary (Langer et al. 1994, Langer 1998) or eruptive enhanced mass loss (**Figure 6**). The line in the HR diagram at which the stellar models reach the Eddington limit depends somewhat on the initial rotation rate and the applied mass-loss rate. However, it agrees well with the location of the Eddington limit in the HR diagram as obtained from stellar model atmospheres. Ulmer & Fitzpatrick (1998) showed that this relates well to the observed upper luminosity boundary of stars in the LMC.

For stars above $\sim 20\,M_\odot$, it is also found that rotation can significantly affect the evolutionary track of a star in the HR diagram during core hydrogen burning (Meynet & Maeder 2000, Heger & Langer 2000, Brott et al. 2011a). In particular, the possibility of partial or complete chemically homogeneous evolution leads to tracks that remain close to the ZAMS but climb high in luminosity. Brott and colleagues found that this may strongly affect isochrones in the HR diagram for ages up to 10 Myr. The homogeneous stars behave somewhat like blue stragglers and may, if dated through isochrones based on nonrotating stellar models, appear a factor of two to three younger than they are. Observed potential examples are a nitrogen-rich O2 III(f) star in the SMC cluster, NGC 346 (Bouret et al. 2003), two further such stars found in the SMC by Walborn et al. (2004), three hydrogen-rich WN-type stars in the SMC (Martins et al. 2009), and the hydrogen-rich WN star VFTS 682 near R136 in the LMC (Bestenlehner et al. 2011).

Also, the high incidence of close binaries (Section 3.6) is expected to affect the distribution of main-sequence stars in the HR diagram substantially. Main-sequence accretion and mergers form stars with core and envelope masses as in single main-sequence stars by virtue of rejuvenation. The same effect makes them appear much younger, which again gives rise to the blue straggler phenomenon. These products of close binary evolution may be distinguishable from chemically homogeneously evolving stars as the latter are expected on, or even to the left of, the ZAMS, whereas the binary products are expected at some distance to the right of that line. Their position may overlap, however, with that of single stars that evolved partly chemically homogeneously but have already turned onto a normal evolutionary track (see **Figure 2**). Furthermore, as the binary mergers and accretion stars are expected to rotate very rapidly, at least initially, it is possible that chemically homogeneous evolution occurs, with the same effects as in single stars (Cantiello et al. 2007).

5.2. Mass-Luminosity Relation

Main-sequence stars are predicted to follow a well-defined mass-luminosity relation. Kippenhahn & Weigert (1990) showed analytically that a relation of the form $L \sim M^\alpha \mu^\beta$ is expected, with

$\alpha = 3$ and $\beta = 4$ for the case of an ideal gas and constant opacity. Here, μ is the (constant) mean molecular weight of the stellar gas. For massive stars for which radiation pressure becomes more important, α and β are predicted to decrease. It is $\alpha \to 1$ for $P_{\rm rad}/P \to 1$ ($P_{\rm rad}$ being the radiation pressure, and P the total pressure), which implies that the lifetime τ of the stars, assuming $\tau \sim M/L$, reaches an asymptotic lower limit.

These analytic predictions, as the mass-luminosity relation is based on detailed stellar model calculations (e.g., Gräfener et al. 2011), have been quantitatively confirmed by dynamical mass determinations of main-sequence stars in close binary systems, with good coverage up to 30 $M_\odot$ (Andersen 1991). Individual dynamical mass determinations have been achieved for stars up to about 100 $M_\odot$ (Bonanos et al. 2004, Rauw et al. 2004, Schnurr et al. 2008, Stroud et al. 2010). Higher masses have been derived for a number of stars (e.g., Figer et al. 1998, Figer 2005, Crowther et al. 2010b, Taylor et al. 2011) by applying the theoretical mass-luminosity relation.

5.3. Rotational Velocities

For massive stars of solar metallicity in the initial mass range of 10–15 $M_\odot$ or of SMC metallicity in the range of 10–25 $M_\odot$, the stellar evolution models predict a rather constant equatorial rotational velocity during the main-sequence evolution (Heger & Langer 2000, Meynet & Maeder 2000, Ekström et al. 2008, Brott et al. 2011a), independent of the employed detailed angular momentum transport mechanism. Shear mixing and Eddington-Sweet circulations as well as magnetic torques are efficient enough to transport angular momentum from the contracting core to the envelope, which would otherwise slow down as it grows in radius by a factor of three during core hydrogen burning. Angular momentum loss due to stellar winds (see Section 4.2) plays some role here, too, and may prevent a slight increase of the rotation rate for the larger stellar masses considered here (Meynet & Maeder 2000).

A comparison of these predictions with observations is not straightforward, as it requires age-dependent stellar samples. Huang, Gies & McSwain (2010) have achieved this for stars of about 9 $M_\odot$ and found rough agreement with the predictions, but they also suggested a contribution to the fastest rotators among the evolved main-sequence stars from close binary interaction (see below). The rotational velocity data for O and B stars from the VLT-FLAMES Survey of Massive Stars, as shown by Vink et al. (2010), implies that stars in the mass range of 10–20 $M_\odot$ cover the full range of rotational velocities, from slow rotation up to near-critical rotation, throughout their main-sequence lifetimes.

For more massive stars mass loss becomes more important (see Section 4.2), and the associated angular momentum loss even in nonmagnetic winds may lead to a significant slow-down of the rotation of the entire star (Meynet & Maeder 2000, Brott et al. 2011a). The sensitivity of the rotational velocity evolution to the mass-loss rate is well illustrated by the example of the solar-metallicity 60 $M_\odot$ models of Ekström et al. (2008; their figure 16). When the mass-loss rate of Vink, de Koter & Lamers (2001) is used, the 60-$M_\odot$ stars spin down, some quite drastically. Models computed with the mass-loss rate proposed by Kudritzki & Puls (2000), which is only about a factor of two lower than that of Vink and colleagues, keep about constant rotational velocity or even spin up, such that many of the models reach break-up rotation. Remarkably, the analysis of the rotation of about 100 galactic O and early B stars by Penny & Gies (2009) appears to be more consistent with the latter set of models. These results are tentative, however, because, e.g., the initial rotational velocity distribution for stars of a given mass range and metallicity may not be universal (e.g., Wolff et al. 2008).

Finally, we expect the distribution of rotational velocities of a massive star population to change as a function of age due to binary interactions. In particular, mass transfer and merger systems may enhance the number of fast rotators with time (cf. **Figure 3**), as suggested by Huang & Gies (2006) and Huang, Gies & McSwain (2010). It may even be conceivable that all very rapidly rotating massive stars are remnants of close binary interaction (Langer et al. 2008). This line of thought has an obvious connection to the question of the origin of Be stars. Whereas single-star models can explain many observational trends in Be stars (Ekström et al. 2008), a binary origin for most Be stars cannot be excluded (cf. Pols et al. 1991).

5.4. Surface Abundances

The surface abundances of massive main-sequence stars can change by three different means. First, mass loss can carry away such a large part of the hydrogen-rich envelope that material that experienced nuclear processing in or near the convective core of the star appears at the stellar surface. As the fraction of the star that is part of the convective core of main-sequence stars increases with stellar mass, as does the stellar wind mass-loss rate, this scenario applies to the most massive stars ($M \gtrsim 50\,M_\odot$ at solar metallicity; Brott et al. 2011a), although trace elements like boron can be blown off at substantially lower masses (Section 5.4.2). The limiting mass above which mass loss can lead to surface composition changes is furthermore larger for stars with lower metallicities, because their stellar wind mass-loss rates are smaller.

Second, mass accretion from a companion star can alter the surface abundances of a main-sequence star. Because in a mass transfer event the mass donor loses practically its entire hydrogen-rich envelope, it will always transfer enriched material from the bottom of the envelope, which is polluted with hydrogen burning products. Because in nonconservative models the mass transfer efficiency seems to decrease with time (see **Figure 4**), the enrichment may be strongest in the mass gainers of rather conservative systems. Furthermore, it is likely that the remnant of a merger of two main-sequence stars results in a main-sequence star that shows some hydrogen burning products at the surface (Section 3.3).

Last, the surface of a main-sequence star may be polluted by mixing processes occurring in the stellar interior. As thermally induced mixing (Section 4.3) cannot achieve this alone, rotational mixing processes are the strongest candidate (Section 2.3). Of course, a star needs to rotate faster than some threshold value to obtain a certain amount of surface pollution (Meynet & Maeder 2000, Heger & Langer 2000, Brott et al. 2011a, Köhler et al. 2012).

Needless to say, these three pollution mechanisms may also operate together. For example, merger or accretion stars may rotate fast and lose much more mass than comparable single stars. Also, stars that uncover enriched material by stellar wind mass loss usually lose so much angular momentum that rotational processes stop to play a major role. Still, as the mass-loss rate increases during the main-sequence evolution, rotational mixing could have affected the evolution prior to the stage where mass loss has removed large amounts of mass.

5.4.1. CNO. Main-sequence stars in the mass range of 8–25 $M_\odot$ are discussed here. Mass loss plays only a limited role, especially for LMC and SMC objects. As mentioned in Section 2.3, the finding that the surface of a fraction of massive main-sequence stars is enriched in nitrogen fostered the idea that rotational mixing can carry nitrogen from the edge of the convective core to the surface of the star. The accurate abundance determinations in early B-type main-sequence stars of Przybilla et al. (2010) clearly show that the CNO abundance pattern in these stars agrees with the prediction from CN-cycling: Nitrogen is enhanced, carbon is depleted, oxygen is hardly

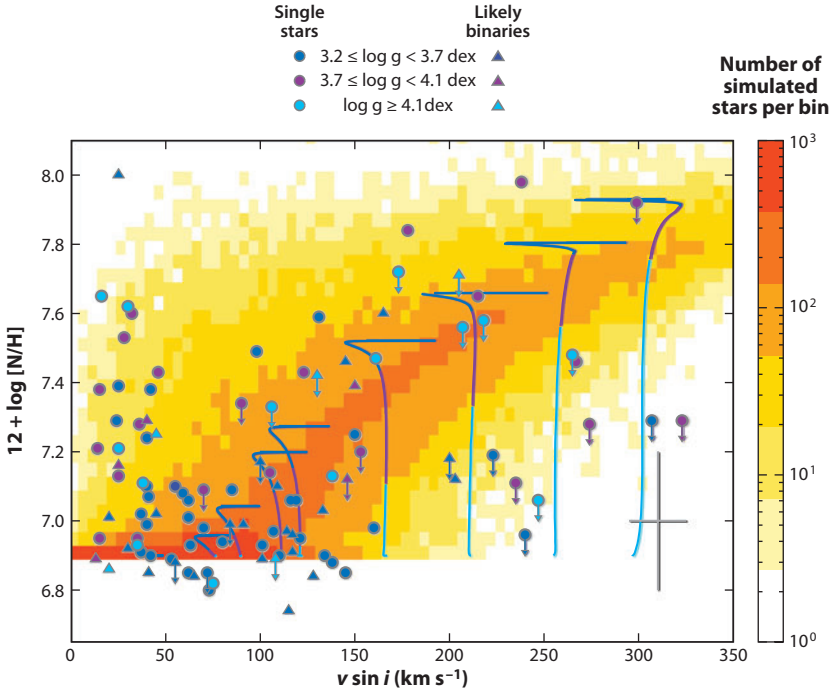

Figure 7

Hunter diagram for Large Magellanic Cloud early B-type stars from the VLT-FLAMES Survey of Massive Stars (*symbols*) showing projected rotational velocity against their nitrogen surface abundance. Single stars are plotted as circles, radial velocity variables as triangles; different colors indicate the surface gravities of the observed stars. A population synthesis simulation based on single-star evolution models with rotational mixing (Brott et al. 2011a) is shown as a density plot in the background. The color coding corresponds to the number of predicted stars per pixel. Theoretical evolutionary tracks of 13-$M_{\odot}$ stars, corresponding to the average mass of the sample stars, are shown (*lines*) with their surface gravity coded by the same colors as the observations. The corresponding rotational velocities have been multiplied by $\pi/4$ to account for the average projection effect. The cross in the lower right corner shows the typical error on the observations. Adapted from Brott et al. (2011b).

affected, and the sum of CNO nuclei is constant. In this respect, the results of Przybilla and colleagues provide a breakthrough.

To interpret these results as the consequence of rotational mixing is problematic, however, as the analyzed stars hardly rotate. At least their $v \sin i$'s are smaller than 30 km s^{-1}, which is why a highly accurate abundance analysis was possible. The reasoning that these stars are slow rotators (rather than fast rotators viewed almost pole-on) is due to the discovery of a slowly rotating nitrogen-rich subgroup of the early B-type stars in the LMC, which comprises about 15% of all stars (Hunter et al. 2008b, Brott et al. 2011b). Galactic counterparts have been identified by Morel et al. (2006) and Morel, Hubrig & Briquet (2008), who also found that stars of this subgroup have a high incidence of magnetic fields.

Hunter diagram: a key diagram for analyzing rotating massive main-sequence stars that shows the nitrogen surface abundance of stars versus their projected rotational velocity

The subgroup of nitrogen-rich slowly rotating early B stars shows up most clearly in the Hunter diagram, which is shown for a sample of ∼100 LMC stars in **Figure 7**, for $v \sin i < 50$ km s^{-1} (Brott et al. 2011b). The inclination angles for these stars are unknown, but the clear gap of nitrogen-rich stars between $v \sin i \simeq 50$ km s^{-1} and $v \sin i \simeq 100$ km s^{-1} implies that most N-rich low-$v \sin i$ stars are true slow rotators.

Meynet, Eggenberger & Maeder (2011) explore magnetic braking models, where the stars start out rapidly rotating and undergo rotational mixing before they slow down to their current low velocities by the interaction of the stellar wind with the stellar magnetic fields (ud-Doula, Owocki & Townsend 2008). They find satisfactory solutions when allowing for differential rotation inside the star, but the more likely case of close-to-rigid rotation, which is thought to be enforced by the magnetic field inside the star, allowed very little mixing.

Alternatively, the slowly rotating nitrogen-rich early B stars could be the remnants of stellar mergers. As discussed in Section 3.3, massive main-sequence mergers are expected to show CNO-processed material at their surface, and the merger process may lead to the generation of a large-scale magnetic field—as perhaps demonstrated by HD 148937 (Section 3.5). The nitrogen enhancement would thus not require rotational mixing, and the star can spin down quickly after the merger. Morel, Hubrig & Briquet (2008) argue that the current magnetic fields of the slowly rotating nitrogen-rich early B stars are too weak to allow significant spin down. This could imply that their magnetic fields were stronger shortly after the merger. Main-sequence mergers also appear to occur frequently enough to explain the order of magnitude of the observed number of nitrogen-rich slow rotators (Section 3.3). Further, it is remarkable that the well-analyzed galactic nitrogen-rich slow rotators all appear to be single stars, except for β Cephei, which has a companion with an orbital period of 90 years (Morel, Hubrig & Briquet 2008). The binary incidence is also small for the nitrogen-rich slowly rotating LMC stars discussed above (see **Figure 7**).

The discussion above shows that in order to test the predictions of rotationally induced mixing theories, one needs to compare to a sample of stars that rotate reasonably fast. The VLT-FLAMES Survey of Massive Stars (Evans et al. 2005) recently provided the first statistically significant sample fulfilling this constraint. As shown in **Figure 7**, the area of rapid rotation and nitrogen enrichment, which represents the predictions of rotational mixing highlighted by the color shading, is populated with stars. This supports the underlying theory of rotationally induced mixing (Hunter et al. 2008b). The interpretation of the Hunter diagram is nevertheless complicated by two issues.

Firstly, as **Figure 7** shows, about 10% of the observed stars are fast rotators, but they do not show an appreciable nitrogen enhancement. Köhler et al. (2012) show in a star-by-star analysis that the lack of a strong nitrogen enrichment in these stars cannot be explained as an age effect, because all of them appear to be evolved main-sequence objects. These stars are therefore contradicting the predictions of rotational mixing in single stars. Perhaps nonconservative binary evolution can explain these stars (Langer et al. 2008).

Secondly, as mentioned in Section 3.2, the production of rapidly rotating nitrogen-rich main-sequence stars is one of the prime predictions of current models of massive close binaries. As shown in **Figure 5**, the range of nitrogen enrichment factors in conservative models is three to five for a galactic initial CNO pattern. This corresponds well to the range of nitrogen abundances observed in the rapid rotators ($v \sin i > 100$ km s^{-1}) shown in **Figure 7**. Given the large fraction of massive stars in close binaries (Section 3.6), the nitrogen-rich fast rotators might thus correspond to mass transfer remnants. In fact, the mass transfer remnants ought to show up somewhere in the Hunter diagram.

In view of these issues, we conclude that at the present time, there is still no unambiguous evidence for rotational mixing in massive stars. Due to the degeneracy between the predictions of rotational mixing and close binary evolution, such evidence is also difficult to achieve. To collect data for "proven" single stars does not help, because most close binaries will look like single stars after their main interaction (de Mink, Langer & Izzard 2011). Certainly, obtaining more quantitative and statistically complete predictions from binary evolution models is desirable. A surprising albeit difficult alternative way has been outlined by de Mink et al. (2009) and de Mink,

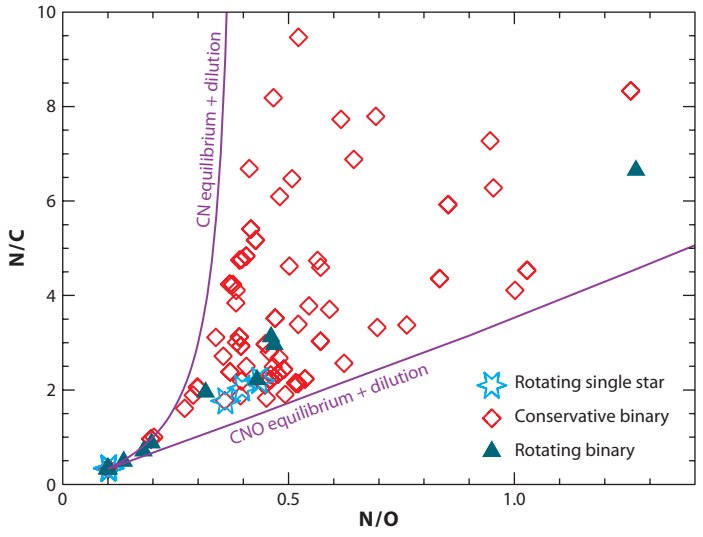

Figure 8

Location of various types of stellar evolution models in the plane defined by the surface abundance ratios N/O (*x*-axis) and N/C (*y*-axis). Each symbol represents the time average abundances during a long-lasting evolutionary stage. Blue star symbols correspond to the 12 $M_\odot$, 15 $M_\odot$ and 20 $M_\odot$ models, respectively, of Heger & Langer (2000) rotating with roughly 300 km s^{-1}, red diamonds represent the conservative binary evolution models of Wellstein, Langer & Braun (2001), and green triangles show the rotating nonconservative binary models of Wellstein (2001) and Langer et al. (2003). The upper purple line is defined through the dilution of material that has reached CN equilibrium with unprocessed matter. The lower purple line is analogous for matter that has reached CNO equilibrium.

Langer & Izzard (2011): We must analyze stars in recognized close binaries, because for those one can easily rule out that binary interaction has already happened.

A further diagnostic diagram to be explored in the near future is the N/C-N/O-diagram, which contains the surface abundances of all three CNO elements. The permitted part in this diagram is bounded by the two lines corresponding to diluted CN- and CNO-equilibrium abundances. As shown in **Figure 8**, the models of conservative close binary evolution appear to be able to fill up the entire permitted area. Models of rotating single stars with rotationally induced mixing tend to populate the lower part of the diagram (see also Przybilla et al. 2010). The same holds for the few nonconservative binary models with rotation that are available so far. For main-sequence merger stars, there exist no quantitative predictions yet.

5.4.2. Boron. The CNO elements probe the transport of matter from the stellar core to the surface. In contrast, the surface abundances of the light elements Li, Be, and B are sensitive to rather shallow mixing in the stellar envelope, where only much less restrictive mean molecular weight gradients are expected. Whereas all three elements can be measured in low-mass main-sequence stars (Pinsonneault 1997), suitable lines in the spectra of hot upper main-sequence stars are only available for boron (Mendel et al. 2006). Both stable boron isotopes are rather fragile. In a 10-$M_\odot$ star, their lifetimes against proton capture equal the stellar lifetime at about 7×10^6 K, which means that boron is completely destroyed in most of the star early during the main-sequence evolution. It can only survive in the outer one or two solar masses of the envelope of massive main-sequence stars. Because these layers might be ejected by a stellar wind for stars

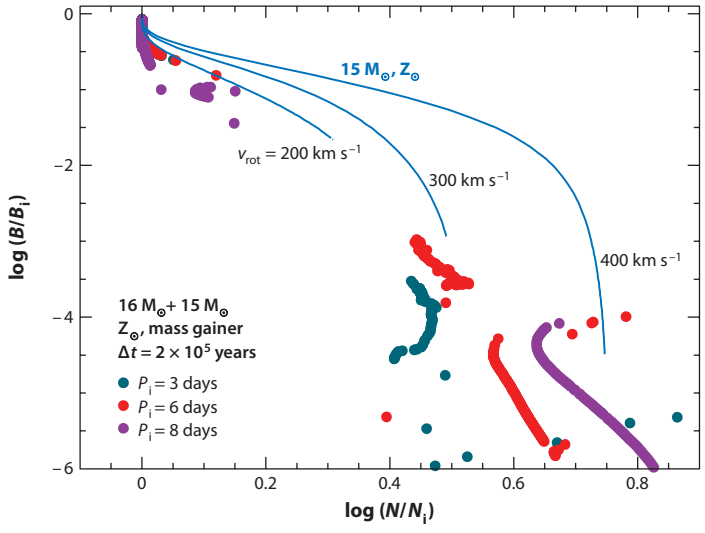

Figure 9

Surface boron depletion factor versus surface nitrogen enhancement factor for models of rotating single and binary stars including rotational mixing. The blue lines represent galactic 15 $M_\odot$ stars during core hydrogen burning from Brott et al. (2011a), with different initial rotational velocities as indicated. The colored dots represent the rotating nonconservative binary models of Wellstein (2001) and Langer et al. (2003), where each dot represents 2×10^4 years of evolution. Shown are only the results for the mass gainer, which will be the easier, or even the only, observable star after the mass transfer. The legend gives the initial period of the three binary evolution models.

more massive than ~20 $M_\odot$, an analysis of internal mixing processes through boron abundances is facilitated by looking at stars below this mass.

First predictions of the effect of rotationally induced mixing on the surface boron abundances of massive stars were given by Fliegner, Langer & Venn (1996) and Heger & Langer (2000), who showed that a depletion of boron by more than a factor of three is achieved in stars rotating initially only with a velocity of ~100 km s^{-1}. Fliegner and colleagues also investigated the boron-nitrogen anticorrelation, which occurs due to rotationally induced mixing, and found that during the main-sequence evolution of sufficiently fast rotating stars, boron is first depleted by at least a factor of three or so before nitrogen starts to be enhanced. They suggested that boron might be a key element in distinguishing binary effects from rotational mixing in single stars. Further detailed models of rotating single stars including boron depletion by rotational mixing have been provided by Frischknecht et al. (2010), Langer et al. (2010), and Brott et al. (2011a). Also, predictions from mass-transferring binary models are available, although these models are far from covering the whole binary parameter space. The current picture is summarized in **Figure 9**. Single-star models show a continuous depletion of boron with time, but the nonconservative binary models predict a pronounced gap because the major mass transfer events occur on a very short timescale (~10^4 years).

Whereas the surface abundances of boron and other elements have been determined for about two dozen galactic early B- and late O-type main-sequence stars (Venn, Lambert & Lemke 1996; Venn et al. 2002; Mendel et al. 2006), and in some cases even boron isotope ratios are measured (Proffitt et al. 1999, Proffitt & Quigley 2001), all measurements are for apparent slow rotators. Most of the boron-depleted stars are also found to be nitrogen enriched (Morel, Hubrig

& Briquet 2008), and it appears that the boron analyses have been performed for stars of the same subgroup of likely true slow rotators that was discussed in the context of the CNO surface abundances (Section 5.4.1). A comparison with models of rotationally mixed single stars, as performed in most of the papers quoted above, may therefore not be very meaningful. Being aware of this situation, Morel and colleagues conclude that a mechanism other than rotational mixing appears to be required to explain the observations. A prominent gap in the observed boron abundance distribution, separating stars with more or less normal surface abundances from stars where boron is depleted by more than one order of magnitude—for which mostly only upper limits on the boron abundance are available (Mendel et al. 2006; Morel, Hubrig & Briquet 2008)—could be in support of scenarios where many of the boron-depleted stars are close binary remnants. This is suggested by **Figure 9**, in line with the discussion on surface nitrogen abundances above.

5.4.3. Helium. Helium measurements for massive main-sequence stars have been obtained mostly for O-type stars. As mentioned above, for those stars it is difficult to separate the effects of mass loss on the helium abundance from those of mixing or binarity. Helium surface abundances are also more difficult to interpret because the predicted relative change for this element is much smaller than that for nitrogen or boron.

A helium surface enrichment has been found in a significant fraction of galactic (Herrero et al. 1992; Herrero, Puls & Najarro 2002) and LMC/SMC O stars (Mokiem et al. 2006, 2007a). Independent of the origin of the helium enrichment, Langer (1992) showed that a helium-rich main-sequence star will be overluminous with respect to its current mass, according to the μ-dependence in the mass-luminosity relation (Section 5.2). The effect is tentatively confirmed by the analyses of Mokiem et al. (2006, 2007a). It is expected to be strongest in chemically homogeneously evolving stars (Brott et al. 2011a, Gräfener et al. 2011).

Systematic trends are found showing larger helium surface abundances for larger mass (or luminosity) and lower gravity (e.g., Mokiem et al. 2007a), which is expected from all helium enrichment mechanisms. Helium abundances have also been derived for rapidly rotating O stars, and a high fraction of them have been found to be helium-enriched (Herrero & Lennon 2004, Mokiem et al. 2006). Curiously, Herrero & Lennon find it a challenge for the rotationally mixed single-stars models to recover the helium-enriched fast rotators, as most of the models have already spun down significantly before a helium enrichment occurs at the surface (Howarth & Smith 2001). These helium-rich rapid rotators, so-called On stars (Walborn et al. 2010, 2011), could be correlated with a high runaway fraction, as suggested by Langer et al. (2007b).

However, very slowly rotating helium-rich stars have also been identified, which are reminiscent of the nitrogen-rich slowly rotating early B-type stars. In the SMC sample of the VLT-FLAMES Survey of Massive Stars, they appear to relate to the so-called OVz stars, which are found very close to the ZAMS (Walborn 2009), and three out of three have been found helium-rich by Mokiem et al. (2006), as shown in Langer et al. (2007b). These small number statistics will hopefully soon be improved, as dozens of OVz stars have been found in the frame of the VLT-FLAMES Tarantula Survey (Evans et al. 2011) and are currently being analyzed.

In view of this situation, it is difficult not to relate helium enrichment in massive O stars with close binary physics. The slow rotators might again be connected to main-sequence mergers, and runaway O stars are produced by post–mass transfer systems (Eldridge, Langer & Tout 2011). Given the high fraction of O stars that are expected to interact with a companion star (Section 3.6), this may not be surprising. The role of rotational mixing in O-type stars remains still to be identified.

6. MODELS VERSUS OBSERVATIONS: POST-MAIN-SEQUENCE EVOLUTION

6.1. Blue and Red Supergiants

Observationally, supergiants are defined as stars of luminosity class I in the MK system (Morgan & Keenan 1973). These stars indicate the weakest gravities (i.e., largest radii, at a given mass) from gravity-sensitive spectroscopic absorption lines in a given spectral type (cf. Kudritzki et al. 2008). Large radii, at a given temperature (or spectral type), imply large luminosities; luminosity class I stars are the most luminous stars within a spectral type. Although our theoretical definition of a supergiant (see Section 2.3) mostly coincides with the observational definition, in particular O-type luminosity class I stars may still undergo core hydrogen burning and are, thus, main-sequence stars in the language used in this review (Section 5).

At near solar metallicity, most current massive star evolution models predict that after core hydrogen exhaustion, stars below the LBV limit (Section 6.2) expand all the way to the red supergiant stage (e.g., Brott et al. 2011a). There is, however, no unambiguous observational evidence that this really happens. As shown by El Eid (1995) and Langer & Maeder (1995), plausible parameter choices for convection, semiconvection, and overshooting may also lead to models that stop their expansion in the blue supergiant stage and have the stars burn a fraction of their helium there before moving to the red supergiant stage (see also Schaller et al. 1992, Ekström et al. 2008).

The models that form red supergiants after core hydrogen exhaustion may or may not undergo so-called blue loops in the HR diagram: After burning a significant fraction of helium in the red supergiant stage, most models move to the blue supergiant stage on a thermal timescale and perform the rest of core helium burning as such before evolving back to the red supergiant branch. Whether a star evolves through a blue loop is again sensitively dependent on the assumptions on internal mixing. In particular, Stothers & Chin (1991) showed that blue loops can be induced by assuming overshooting from the convective red supergiant envelope.

In summary, the post-main-sequence radius and effective temperature evolution of massive single stars is little understood. In addition, massive binary evolution models show that in particular mass receivers in mass transfer systems and Case B mergers (where the more massive star in the binary already has a hydrogen-free helium core) can produce stars that have significantly smaller helium cores than single stars of the same total mass (Section 3.4). For mass transfer systems, inefficient semiconvective mixing can prevent the rejuvenation of many mass gainers (Braun & Langer 1995), which leads to undermassive helium cores. In the HR diagram, such core helium burning stars are found in the region of blue supergiants, with some overlap even to the main-sequence band (Braun & Langer 1995; Claeys et al. 2011; Wellstein, Langer & Braun 2001).

Looking at observed supergiant distributions in the HR diagram (e.g., Humphreys & McElroy 1984, Fitzpatrick & Garmany 1990, Massey et al. 1995, Hunter et al. 2008a) allows two conclusions. First, although predicted by most single-star models, there is no clear evidence for a gap between the main-sequence band and the location of the blue supergiants. This means most likely that either blue loops reach a hotter temperature than most models predict or that the gap is filled by binary products. This may well be possible given the high binary fraction of massive stars (see Section 3.6).

The recently identified population of slowly rotating nitrogen-rich and likely magnetic massive main-sequence stars (Section 5.4) offers a third way to obtain helium burning stars with undermassive helium cores. Their internal magnetic field might hinder core convection to the extent that they produce a smaller helium core than nonmagnetic main-sequence stars of the same mass. In this case they would likely spend core helium burning as hot blue supergiants, similar to the Case B mergers mentioned above.

Surface abundance analyses cannot easily resolve this ambiguity. Many blue supergiants, which are located redward of the predicted red edge of the main-sequence band, are nitrogen-rich (Herrero & Lennon 2004; Crowther, Lennon & Walborn 2006; Vink et al. 2010). This could, however, be due to convective dredge-up in a foregoing red supergiant stage, owing to a mass transfer or merger processes or due to the enrichment in the main-sequence progenitor. Finding close companions to blue supergiants would challenge all three scenarios, because those would not be expected in either case, unless the companion is a low-mass helium star or even white dwarf (Wellstein, Langer & Braun 2001). Those are, however, hard to detect. Searching for those potential companions might be rewarding, as finding them would settle the case. The low rotational velocity of nearly all blue supergiants (Vink et al. 2010) may favor the post–red supergiant scenario, unless these stars have spun down due to magnetic fields, as presumed for the slowly rotating early B dwarfs (Section 5.4). A study of magnetic fields in galactic B-type supergiants, as well as an assessment of their binary fraction, would constitute tests of the above scenarios. It would also shed new light on the unsolved question why SN 1987A exploded as a blue supergiant and how frequent 1987A-type supernovae occur (Parthasarathy et al. 2006).

Remarkably, the gap predicted in the HR diagram between blue and red supergiants by most stellar evolution models (e.g., Langer 1991c, Schaller et al. 1992) is prominently present in observed supergiant distributions for stars between $10\,M_\odot$ and $30\,M_\odot$ (Humphreys & McElroy 1984, Fitzpatrick & Garmany 1990). It may relate to models of supergiant envelopes at intermediate effective temperatures being thermally unstable. Only core helium burning models undergoing rather short blue loops (i.e., rather yellow loops; this occurs typically at $10\,M_\odot$ or below), and former red supergiants whose convective red supergiant envelope becomes very low in mass or very helium rich (occurring typically above $20-30\,M_\odot$), can form thermally stable yellow supergiant models.

6.2. Luminous Blue Variables

Observationally, LBVs are identified as luminous, hot, unstable supergiants (Section 6.1) that suffer irregular eruptions like S Dor and AG Car or more rarely giant eruptions like P Cyg and η Car (Humphreys & Davidson 1994). Here, we consider stellar models corresponding to the LBV stage (see also Sections 3.5 and 4.2).

After core hydrogen exhaustion, massive stars at solar metallicity tend to expand toward the red supergiant branch (Section 6.1). Galactic red supergiants, however, have an upper luminosity limit of about $\log(L/L_\odot) = 5.8$ (Humphreys & Davidson 1979, 1994). This coincides with the fact that more luminous stars reach their Eddington limit when they expand toward cool surface temperatures, due to an increase in the opacity in the outer layers of the star (see Section 4.2 and **Figure 6**). As discussed in Section 5.1, this may even already happen toward the end of core hydrogen burning. If not, it occurs after core hydrogen exhaustion, as long as the surface composition is not already so helium rich that a further expansion can be avoided. If so, the star would be a bona fide WR star (Section 6.3).

It is thought that when stars do reach their Eddington limit while evolving on their thermal timescale, their surfaces may become unstable and the star may undergo episodic mass-loss events. Whereas many detailed stellar evolution models do not show this behavior (also due to numerical limitations), the idea is fostered by the proximity of the LBVs to the location of the Eddington limit in the HR diagram (Ulmer & Fitzpatrick 1998).

Although the LBV phenomenon is quite diverse (see Vink 2009 for a recent review), we follow the strategy below to identify an evolutionary stage with an LBV phase when the star does reach its Eddington or Ω limit and when the evolutionary stage is short, i.e., the evolution proceeds on

the thermal rather than on the nuclear timescale, because stellar models that reach the Ω limit during core hydrogen burning have evolved without any unstable behavior (Langer 1998).

6.3. Wolf-Rayet Stars

Depending on the predominance of nitrogen versus carbon and oxygen emission lines, WR stars are divided into a nitrogen sequence (WN stars) and a carbon sequence (WC stars), with a subdivision into the apparently hotter early-type objects (WNE stars, with subtypes WN2···WN6, and WCE stars with subtypes WO, WC4–WC6) and the apparently cooler late-type objects (WNL stars, with subtypes WN6–WN9, and WCL stars with subtypes WC7–WC9; see Crowther 2007).

In the Milky Way, single stars above 20–25 $M_\odot$ are thought to evolve into WR stars (Hamann, Gräfener & Liermann 2006) (see **Figure 10**). This mass limit is expected to be larger at lower metallicity (Meynet & Maeder 2005). In close binary systems, however, WR stars are thought to be produced from stars with initial masses of 10 $M_\odot$ or less (Section 6.3.2). Originally it was presumed that all WR stars are hydrogen deficient, but it has become clear in recent years that

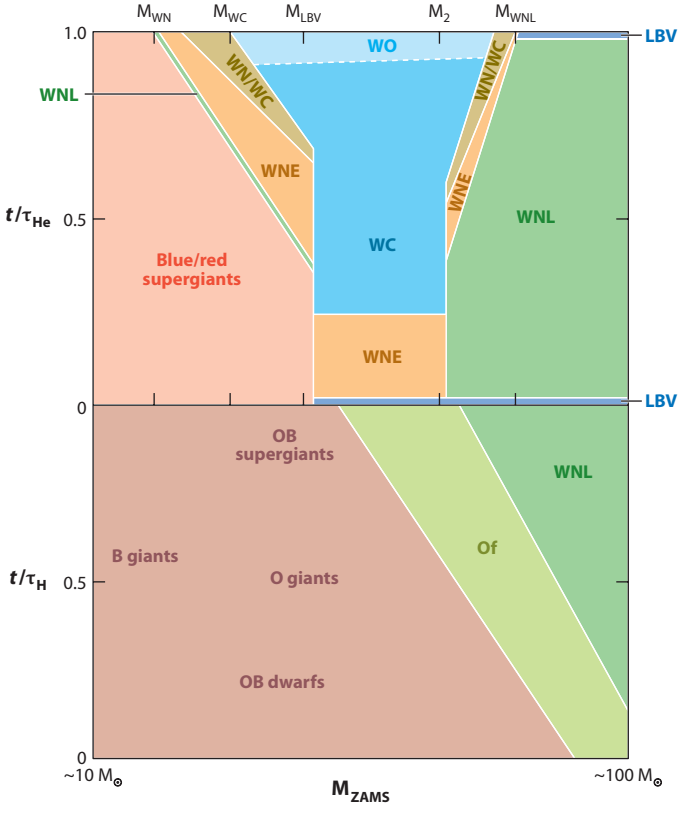

Figure 10

Schematic phase diagram for the main-sequence (*lower part*) and post-main-sequence (*upper part*) evolution of massive stars at solar metallicity. A star of a given zero-age main sequence mass (abscissa) evolves vertically upward in this diagram. The vertical stretch spent in a certain region is a measure of the fraction of core hydrogen or core helium burning spent in the corresponding phase, according to the scenario outlined in the text. This is an extended version of a diagram from Langer (1987).

the most massive and most luminous main-sequence stars may be classified as late-type WR stars (WNL) even when their helium surface abundance is not enhanced (Martins et al. 2008, 2009; Gräfener et al. 2011).

WN/WC star: a star showing strong lines of nitrogen and carbon in its spectra; a few percent of all WR stars are WN/WC stars, and they do not represent WN+WC binaries, but rather stars that have shown a surface composition enriched in nitrogen and carbon

The early-type (hotter) WNE stars are hydrogen deficient, and many of them do not show any sign of hydrogen (Hamann, Gräfener & Liermann 2006). Some of them, however, do show small amounts of hydrogen (Crowther, Smith & Hillier 1995), which may explain the considerable spread in temperature of these stars (Hamann, Gräfener & Liermann 2006), which is not expected theoretically for hydrogen-free stars independent of their evolutionary origin (Langer 1989a). The WNE stars contain so-called weak-lined and strong-lined stars. Some of them apparently have the same temperature, luminosity, and hydrogen surface abundance (e.g., none), but mass-loss rates that differ by an order of magnitude (Crowther, Smith & Hillier 1995; Hamann, Gräfener & Liermann 2006). This is in contradiction to theoretical expectations, particularly due to the tight predicted mass-luminosity and mass-radius relations for helium stars (Langer 1989a, 1989b; Gräfener et al. 2011), unless rotation or magnetic fields are important in one of the two classes (Section 6.3.1).

A WN/WC star transition phase is predicted in evolutionary models due to semiconvective mixing in the growing superadiabatic but chemically stratified part at the top of the helium burning convective core (Langer 1991b), as well as due to rotationally induced mixing between the helium burning convective core and the helium mantle (Meynet & Maeder 2003). In order to produce a nitrogen- and carbon-rich transition layer by semiconvective mixing, the superadiabatic part of the helium core would need to grow for some time after helium ignition, which would favor WN/WC phases in stars where the helium core is covered by a hydrogen-containing layer during the early stages of core helium burning. Most WN/WC stars appear to show a surface carbon mass fraction of only a few percent (Crowther, Smith & Willis 1995; Sander, Hamann & Todt 2012). The most luminous one, WR 26, appears to have a carbon abundance of the order of 20% by mass (Sander, Hamann & Todt 2012), which may be related to the properties of the WO stars (see Section 6.3.1).

The recent analysis of galactic WC and WO stars by Sander, Hamann & Todt (2012) shows that the temperatures of the WC stars appear to be quite similar to those of the WNE group, which is to be expected from WR star models that include partial recombination of carbon and oxygen and opacities that take the high carbon and oxygen abundances into account (Langer et al. 1988, Langer 1989a). Curiously, unexpected trends are found at the low-luminosity end, where the models predict the WC stars to be hotter than the WNE stars, but Sander and colleagues find that the WC9 stars even overlap with the main sequence in the HR diagram. And also at the high luminosity end, the two WO stars analyzed by Sander and colleagues appear very hot (200,000 K), whereas the most luminous WC/WO stars are expected to be cooler than the WNE stars (Langer 1989a)—unless they already contract toward carbon burning (Langer et al. 1988). Though this may appear unlikely at first due to the short lifetime of this stage (~10,000 years), there are other arguments that these luminous WO stars are close to core helium exhaustion (see below).

6.3.1. Evolutionary connections. Putting the observed WR subtypes and those of their potential progenitors and descendants in evolutionary sequences is a high aim and has been attempted many times. A key for doing this successfully is certainly to know of the bolometric luminosities of the WR stars. Those, however, are difficult to assess: WR stars are so hot that they radiate the overwhelming part of their energy at UV wavelength, which is largely unaccessible. Huge bolometric corrections are thus required (Crowther 2007). A second reason is that in order to derive evolutionary connections, one requires statistically meaningful samples. The largest sample

is that of the galactic WR stars (van der Hucht 2001), where, however, the distances to many WR stars are uncertain or unknown.

It may therefore be not surprising that the derived luminosities of most galactic WR stars have been changing significantly in the past decade or so, by up to one order of magnitude. Most recently, the luminosities of both types of WN stars (WNL and WNE) have been largely corrected, mostly to higher values (Hamann, Koesterke & Wessolowski 1995; Hamann, Gräfener & Liermann 2006), with luminosities now up to $\log(L/L_\odot) = 6.8$. The derived luminosities of WC stars have not changed by so much (Koesterke & Hamann 1995; Sander, Hamann & Todt 2012), but their spectra are less understood than those of the WN stars (Sander, Hamann & Todt 2012). Being aware that the luminosities are still uncertain, our discussion below is based on the most recent analyses (Hamann, Gräfener & Liermann 2006; Crowther 2007; Sander, Hamann & Todt 2012).

There is growing evidence that many of the most luminous WR stars, the WNLs, which may develop from the most massive O stars (Crowther et al. 2010b) or were even born as WNL stars (Martins et al. 2008, 2009; Gräfener et al. 2011), do not transform into other WR subtypes before ending their lives. Hamann, Gräfener & Liermann (2006) find that the WNE group [$\log(L/L_\odot) < 5.8$] practically does not overlap in luminosity with the WNL group [$\log(L/L_\odot) > 6.0$], with very few exceptions. Therefore, unless the WNL stars evolve to the much lower luminosity of the WNE stars on a timescale short enough to make this effectively unobservable, they cannot be WNE progenitors (Hamann, Gräfener & Liermann 2006).

However, the most massive stars also need to lose most of their hydrogen-rich envelope, because the internal evolution drives these stars to the cool side of the HR diagram. Because the clumping-corrected mass-loss rates of O stars are not thought to be powerful enough to remove the hydrogen-rich envelope (Mokiem et al. 2007b), these stars are likely to be driven to their Eddington or Ω limit during core hydrogen burning (**Figure 6**; Langer 1998). Consequently, their mass loss may be enhanced (Vink et al. 2011, Gräfener et al. 2011) by a factor of a few (Langer 1998), which may produce P Cygni or emission lines and make the stars appear as Of stars or, at the highest luminosities, as hydrogen-rich WNL stars. Due to slow evolution on the nuclear timescale, there may be no need for these stars to develop LBV-type instabilities despite their proximity to the Eddington limit (Section 6.2). Once the hydrogen surface abundance drops, the star may become more compact, which would, at a constant mass-loss rate, increase the wind density and make the appearance more WR-like.

During the past two decades, the adopted mass-loss rates in stellar evolution calculations were higher than what is proposed today (Section 4.2), with the consequence that the most massive stars would end their lives as hydrogen-free WR stars (Schaller et al. 1992, Meynet et al. 1994, Heger et al. 2003, Eldridge & Tout 2004, Georgy et al. 2009). A reason for these stars to potentially not reduce their surface hydrogen abundance much further during the post-main-sequence evolution has been proposed by Langer (1987). Very massive stars have, initially, huge convective cores, but these cores also decrease rapidly in mass during core hydrogen burning. As long as the convective core mass decreases faster than the stellar mass (e.g., Langer & El Eid 1986), a massive envelope with rather low hydrogen concentration covers the helium core after core hydrogen exhaustion. Langer (1987) argued that such an envelope is helium rich enough to allow a thermal equilibrium position in the hot part of the HR diagram during core helium burning, and that it is massive enough such that it will not be lost completely during the remaining post-main-sequence lifetime of $\sim 3 \times 10^5$ years, with the prediction that the most luminous stars end their lives as WNL stars (**Figure 10**).

Within this scenario, the star is expected to undergo rapid evolutionary changes at the transition from core hydrogen to core helium burning and at core helium exhaustion. Both transitions

could involve excursions to cooler surface temperatures and, therefore, trigger LBV instabilities. We discuss in Section 7 that recent evidence for very luminous hydrogen-rich supernovae and presupernova LBV-type mass ejections supports this line of thought. The 100-$M_\odot$ evolution model of Langer & El Eid (1986) comes close to representing this scenario. The reason that current stellar evolution models fail to reproduce this might be the assumptions of too high mass-loss rates or too strong internal mixing—by rotation or convective overshooting (for the latter, see again Langer & El Eid 1986).

This scenario has an interesting implication: The least massive stars that follow the scenario outlined above may, after a brief transition phase, develop into WC-type stars toward the end of their core helium burning evolution (**Figure 10**). At this stage, the composition uncovered from the helium burning convective core will be quite helium poor and oxygen rich, which resembles the composition of WO stars. Indeed, the two galactic WO stars analyzed by Sander, Hamann & Todt (2012) fit this picture quite well, as their luminosities are among the highest of all galactic WC/WO stars. Because our "least massive WNL star" had the longest possible time to enrich its helium layer above the convective helium burning core with carbon, the transition between the WNL and the brief WO phase may not be of type WNE but rather of type WN/WC (**Figure 10**). The WN/WC star WR 26 in Sander and colleagues' sample, with a luminosity even larger than that of the WO stars, fits this picture very well. Also, the very high carbon abundance in WR 26 is in support of this scenario. Finally, the very high temperature of the two WO stars agrees with the idea that they are at the end of their core helium burning stage or even beyond.

The fact that the hydrogen mass fraction in the layers above the helium core increases for smaller masses implies a critical mass, below which a thermal equilibrium position in the hot part of the HR diagram during core helium burning is not possible. The star is then forced to expand and reaches the Eddington limit after core hydrogen exhaustion, where it would be forced to lose its entire hydrogen envelope in a short LBV stage (Langer 1987, Langer et al. 1994, Meynet & Maeder 2003). These stars would thus not go through a WNL stage during helium burning, but emerge from the LBV stage as WNE stars (**Figure 10**). This scenario agrees with the observation that the galactic WNL and WNE stars practically do not overlap in luminosity (Hamann, Gräfener & Liermann 2006). As the stars considered here uncover their helium core early during core helium burning, they are likely to be able to lose their helium mantle to uncover CO-rich layers during core helium burning, which implies that they may evolve further into WC stars.

At even lower initial mass, post-main-sequence stars have low enough luminosities to evolve to the cool side of the HR diagram without hitting their Eddington limit (**Figure 6**). At solar metallicity, these stars are expected to evolve into red supergiants (Ekström et al. 2008, Brott et al. 2011a). The deep convective envelope at this stage produces a very high hydrogen mass fraction in the layers covering the helium core. Consequently, the more massive stars in this mass range, which have a sufficiently strong red supergiant mass loss to remove the whole envelope, will move to the WR stage only when almost all hydrogen has been lost. Therefore, these stars are also not expected to display a WNL phase (Langer 1987; see **Figure 10**). The most massive of these stars may evolve further into WC/WO stars, which may be preceded by a WN/WC transition phase, because there was plenty of time for mixing carbon into the helium layer.

Within this picture, two different types of WNE stars are produced. The ones that form from higher initial masses would be post–LBV stars in an early phase of core helium burning. Their mass and luminosity range might overlap significantly with that of the post–red supergiant WNE stars, as the helium core of the latter can grow in mass before being uncovered, whereas the helium core of the post–LBV WNE stars is uncovered at the beginning of core helium burning. A consequence of the late uncovering of the post–red supergiant WNE stars could be that their

rotation is strongly reduced by magnetic coupling (Heger, Woosley & Spruit 2005) or shear mixing (Meynet & Maeder 2003), owing to the strong differential rotation between core and envelope in the red supergiant stage. The post–LBV WNE stars, in contrast, might rotate rather fast initially before they are spun down by their own mass loss. Crowther et al. (1995) suggested the distinction between strong-lined and weak-lined WNE stars might occur because they have different progenitors, i.e., LBVs and red supergiants.

Wolf-Rayet (WR) binary: a stellar binary system that contains at least one Wolf-Rayet star

The initial mass range of WNE progenitors can be estimated from the luminosities that are derived for the galactic WNE stars (Hamann, Gräfener & Liermann 2006). The upper limit is close to $\log(L/L_\odot) = 6$, which implies a helium star mass of about $30\,M_\odot$ (Langer 1989a). In the post–LBV scenario, this mass should correspond to the initial mass of the helium core, which translates to a ZAMS mass of about $60\,M_\odot$ (Hamann, Gräfener & Liermann 2006; Brott et al. 2011a), depending somewhat on convective core overshooting and rotational mixing. As outlined above, current evolutionary models do not reproduce this limit.

The lower luminosity limit found for WNE stars is about $\log(L/L_\odot) = 5.3$ (Hamann, Gräfener & Liermann 2006), corresponding to about 10-$M_\odot$ helium star models, which implies an initial mass of roughly $25\,M_\odot$. For their rotationally mixed models, Meynet & Maeder (2003) find this mass is the lower limit to produce WR stars, and in particular WN-type stars. According to Hamann, Gräfener & Liermann (2006), however, these models are too hydrogen rich to correspond to the WNE class, although they are post–red supergiant WN models. Perhaps, the rather high hydrogen mass fraction in the post–red supergiant models of Meynet & Maeder (2003) originates from the efficient mixing during the main-sequence phase. If so, this might either argue against such mixing or imply that most stars in the corresponding mass range rotate slower than Meynet & Maeder's models. A low hydrogen mass fraction in the post–red supergiant models would also help to bring the predicted WNL/WNE ratio of the quoted models in better agreement with the galactic population (Hamann, Gräfener & Liermann 2006). At the same time, this seems required for lower mass WN models to develop into WC stars and thereby reach the observed low luminosities of galactic WC stars (Sander, Hamann & Todt 2012).

Sander, Hamann & Todt (2012) argue, based on the derived lower luminosity limit of WC stars of $\log(L/L_\odot) = 4.9$, that the evolutionary tracks of Vanbeveren et al. (1998)—which assume much higher red supergiant mass-loss rates than recommended by recent analyses (Section 4.2)—fit the WR star observations well. Whereas they do reproduce the lowest WR star luminosities, their models would also predict WN stars in the luminosity range of $4.9 < \log(L/L_\odot) < 5.3$, where Hamann, Gräfener & Liermann (2006) find none. Enhanced red supergiant mass-loss rates are therefore not a likely solution.

As each observed WC star must have a somewhat more luminous (as well as more massive) WNE phase (except perhaps the most massive ones; see **Figure 10**), the observed WC population has to evolve from the observed WNE population. The lower luminosity limit for WC stars may therefore put some lower limit on the time-averaged mass-loss rate of WC stars.

6.3.2. Wolf-Rayet binaries. Most WR binary stars contain an O star companion. Three WR stars are found to have compact companions (Crowther et al. 2010a). No binary consisting of two WR stars has yet been found.

The discussion in the previous section ignored any contribution of close binary evolution. Hamann, Gräfener & Liermann (2006) and Sander, Hamann & Todt (2012) carefully removed known galactic WR binaries from their samples. Ignoring binaries, however, is only justified if close binary evolution does not produce WR stars that are apparent single stars, i.e., in which the binary companion is either gone or very hard to detect. Indeed, it turns out that not many binary-produced apparently single WR stars are expected.

One possible contribution to the WR population may come from stellar mergers. As discussed in Sections 3.3 and 3.4, during their core helium burning evolution, merger products may have helium cores that are smaller than those of single stars of the same mass. As a result, they may have surface temperatures of B stars during core helium burning. As such, they would lose less mass during core helium burning compared to their single-star counterparts, which are driven either to the red supergiant or the LBV stage. This may prevent merger stars up to quite high mass (perhaps $\sim 40\,M_\odot$) from ever developing a WR stage. Mergers of even higher mass, however, might contribute to the most massive stars, which do not lose all their hydrogen and end their lives as WNL stars or LBVs. Whereas there are no detailed stellar models available to test this hypothesis (cf. Eldridge, Izzard & Tout 2008), the clear separation in luminosity between the WNL and the WNE stars found by Hamann, Gräfener & Liermann (2006) implies that the high-mass WNL population is, in any case, dominated by genuine single stars.

The most common avenue to produce a WR star in a close binary system is Case A/B mass transfer (Section 3.1). If, initially, the masses of the two stars are too different, the mass transfer would be unstable and the system would merge (see Sections 3.3 and 3.4). The evolution of the merger product may differ from that of ordinary single stars, but there is no immediate implication for the WR stage. If the initial mass ratio is close to unity, the mass ratio after the mass transfer will mostly imply that the mass donor, which may be a WR star at that stage, is less luminous than its OB star companion. Because most WR stars are also hotter than OB stars, the O star cannot be missed in optical observations. Only very massive close binaries with rather unequal initial masses can produce WR binary stars where the O star is somewhat less luminous than the WR star (Petrovic, Langer & van der Hucht 2005), through highly nonconservative evolution. Even then, however, the O star is likely to be detected.

In fact, the problem is the other way around: WR companions of O stars can easily be so much dimmer than the O stars that many O stars could have such companions without us knowing (Section 3.2) (de Mink, Langer & Izzard 2011). This does not change the analysis of the WR stars in Section 6.3.1, but it leads to an interesting consideration. There is no lower limit to the masses of WR or helium stars produced by close binaries. It is thus interesting to consider the lowest-mass WR star found in binaries, which appears to be about $9\,M_\odot$ (Crowther 2007). This corresponds roughly to the mass of the least luminous galactic single WR star (Sander, Hamann & Todt 2012). This implies a large population of undetected galactic WR stars in close binaries.

There can, indeed, be no doubt about the existence of such a population, because we know many progenitor systems. Massive Algol-type systems have already performed the fast Case A mass transfer during which most of the mass is transferred (Section 3.1) and which are currently in the slow Case A mass transfer. The spectral type of the mass donor is still OB or at most Of/WNL at this stage (e.g., Harries, Hilditch & Hill 1997; Rauw, Vreux & Bohannan 1999). These systems must undergo Case AB mass transfer in the future, which will remove most of the remaining hydrogen envelope of the donor star. We also know two types of descendants of the undetected WR+O star population. These are the Be/X-ray binaries (Liu, van Paradijs & van den Heuvel 2006; Section 3.1) and the Type Ib/c supernovae (Section 7). Even when the emission-line signature of the WR component will fade for lower mass WR or helium stars, these so-far undetected systems should be spectroscopically identifiable with current telescopes because the expected radial velocity shifts in their O star companions are typically above 10 km s^{-1} (Wellstein, Langer & Braun 2001).

At low metallicity, spin-up by mass transfer in close binaries may induce chemically homogeneous evolution due to rotational mixing (Sections 3.1 and 3.2). This might produce rapidly rotating WR stars. After the supernova explosion of their binary companion these stars would evolve in isolation (Cantiello et al. 2007). As they might resemble the rapidly rotating single stars that also evolve chemically homogeneously, we discuss them together in Section 6.4.

6.4. Wolf-Rayet Star Statistics

To validate stellar models, it has been popular to compare the predicted number ratios of certain spectroscopic types with the corresponding observed values. Whereas this can in principle be quite meaningful, these statistical comparisons may be highly affected by observational biases, by the difficulty of assigning spectral types to stellar models, and by the often unknown star-formation history and initial mass function.

One of the perhaps better defined numbers is the galactic WC/WN ratio. Empirically, this is found to be about 0.9, independent of whether all known WR stars are counted (van der Hucht 2001) or only those that are presumed single stars (Hamann, Gräfener & Liermann 2006). The single-star models without rotation of Meynet & Maeder (2003) and Eldridge, Izzard & Tout (2008) reproduce this ratio quite well. Eldridge and colleagues find that including binary evolution may decrease the WC/WN ratio by a factor of two, due to the formation of long-lived and rather low-mass WN stars. It remains uninvestigated, however, whether such stars, which will mostly have much brighter O star companions, would actually be detected (see Section 6.3.2). Meynet & Maeder (2003) find a similar reduction of the predicted WC/WN ratio when rotation is included in their models. Therefore, the galactic WC/WN ratio per se does not support rotation. Meynet & Maeder argue, however, that their value obtained with rotation (which is 0.35) nevertheless fits well into the general trend of the observed WC/WN ratio as a function of metallicity.

What indeed appears undisputed is that the observed WC/WN ratio is increasing with metallicity (cf. Meynet & Maeder 2005). For example, out of 12 WR stars in the SMC, 11 are of type WN. For subsolar metallicity, Eldridge & Vink (2006) explain that this is due to the metallicity dependence of the WR mass-loss rates (Section 4.2.2). Indeed, for increasing WNE mass-loss rates, the WNE lifetimes must decrease and the WC lifetimes must increase. As this is true for single and binary stars, this trend is expected to persist to low metallicity, where the binary channel of WR star formation may dominate.

The number ratio of WR- to O-type stars, even though it is difficult to establish for large galaxies, is also found to increase with metallicity. Whereas the trend is clear when looking at the Local Group galaxies (Meynet & Maeder 2005), it continues to smaller metallicities as found from the study of dwarf galaxies with WR wind features in their spectra, so-called WR galaxies (Brinchmann, Kunth & Durret 2008). For the smallest metallicities, however, i.e., $Z_{\odot}/50$ in I Zw 18, there appear to be more WR stars, in particular of type WN, than expected from extrapolations of single-star evolution models at higher metallicity (Crowther & Hadfield 2006; Brinchmann, Kunth & Durret 2008). This could imply that WR stars produced by binaries dominate the WR population at the lowest metallicities considered (Eldridge, Izzard & Tout 2008), even though Foellmi, Moffat & Guerrero (2003a) still find a normal binary fraction among the WR stars in the SMC. Alternatively, Foellmi, Moffat & Guerrero (2003b) suggest that the effects of stellar rotation could become much stronger at very low metallicity. Indeed, according to Yoon, Langer & Norman (2006), chemically homogeneous evolution induced by rapid rotation in single stars might be able to explain these observations.

7. MODELS VERSUS OBSERVATIONS: SUPERNOVAE AND GAMMA-RAY BURSTS

The recent and ongoing large supernova and transient surveys, together with targeted efforts, have dramatically changed our view on the final stage of massive star evolution, including their collapse and explosions. Long-term surveys like LOSS (Li et al. 2011) and CHASE (Pignata et al. 2009) target nearby massive galaxies and provide a nearly complete supernova inventory of these

high-metallicity systems (Li et al. 2011, Smith et al. 2011a). These results are augmented by successful detections of supernova progenitor stars in archival data (Li et al. 2007, Smartt et al. 2009), and by high redshift surveys aiming at Type Ia supernova cosmology (e.g., SNLS; Guy et al. 2010).

Furthermore, new untargeted surveys—e.g., PTF (Law et al. 2009) and the SDSS Supernova Search (e.g., Modjaz et al. 2008)—opened a new window to supernovae from low-metallicity dwarf galaxies and unexpectedly found a stunning number of new types of supernovae as well as exciting trends of number ratios of various supernova types with galaxy type and metallicity (Arcavi et al. 2010). Together with new high- (Racusin et al. 2011) and low-energy views (Soderberg et al. 2010) of stellar explosions, these observations provide important clues to the supernova progenitor evolution of massive stars.

Observationally, supernovae are classified into various types based on their spectra or light curves (for details see Smartt 2009), and it is often difficult to relate a given type of supernova to a certain type of progenitor (see below), because the observable properties are dominated by the stellar envelopes, whereas it is the cores of the progenitors that define the different explosion types.

Type Ia supernova: a supernova showing no hydrogen that is thought to originate from exploding white dwarfs

Electron-capture supernovae (ECSNe): produced from electron-degenerate ONeMg-cores, which collapse when electron captures set in at densities above 10^9 g cm^{-3}, and are thought to form in stars within a narrow mass range near about 9 $M_\odot$

7.1. Electron-Capture Supernovae

As mentioned in Section 4.5, the lowest mass supernova progenitors may not evolve all the way to form iron cores. Instead, their ONeMg cores collapse due to electron captures (Nomoto 1984; Wheeler, Cowan & Hillebrandt 1998) (**Figure 11**). Computing the advanced evolution of such stars is difficult and plagued with uncertainties (Siess 2007, 2010). Based on synthetic models for solar metallicity, Poelarends et al. (2008) estimate that the initial-mass range for electron-capture supernovae (ECSNe) is only about 0.25 $M_\odot$ wide, which would imply that some 4% of all supernovae would be of this type. These supernovae are thought to produce at most 10–20% of the kinetic energy of ordinary core collapse supernovae, to have very low nickel and metal yields (Kitaura, Janka & Hillebrandt 2006), and to produce low-kick neutron stars (Podsiadlowski et al. 2004). Therefore, we anticipate that such supernovae, which are expected to occur in massive asymptotic giant branch (AGB) stars (Siess 2007, Poelarends et al. 2008), are faint and slow. Several such supernovae have been found recently, for which ECSNe provide one possible explanation (Kasliwal et al. 2011).

It was found by van Veelen (2010), who simulated the interaction of the supernova ejecta with the previously emitted AGB wind, that the interaction luminosity could make ECSNe quite bright despite their low kinetic energy if the ejecta mass is small. Furthermore, the interaction of the supernova with its circumstellar medium could produce emission that persists for several decades, as found, e.g., for the supernova 1988Z (Schlegel & Petre 2006).

The metallicity dependence of the frequency of ECSNe is subject to two main uncertainties. First, it is open whether the winds of AGB stars are decreasing for low metallicity, which would allow the degenerate cores of massive AGB stars to grow to high masses, enabling more ECSNe. Second, the efficiency of the so-called third dredge-up is uncertain, which digs up core material into the convective AGB envelope (Siess 2010). The third dredge-up reduces the rate of core growth and, thus, diminishes the expected number of ECSNe. According to Poelarends (2007), the mass range of ECSNe at low metallicity may widen to such an extent that these events may have been the most frequent type of supernovae at metallicities below $Z_\odot/100$ (**Figure 12**). The low neutron star kicks imposed in such events might explain the high number of neutron stars in globular clusters.

As discussed by Podsiadlowski et al. (2004), ECSNe may occur much more frequently in close binary systems than in single stars, because the second dredge-up, which reduces the helium core

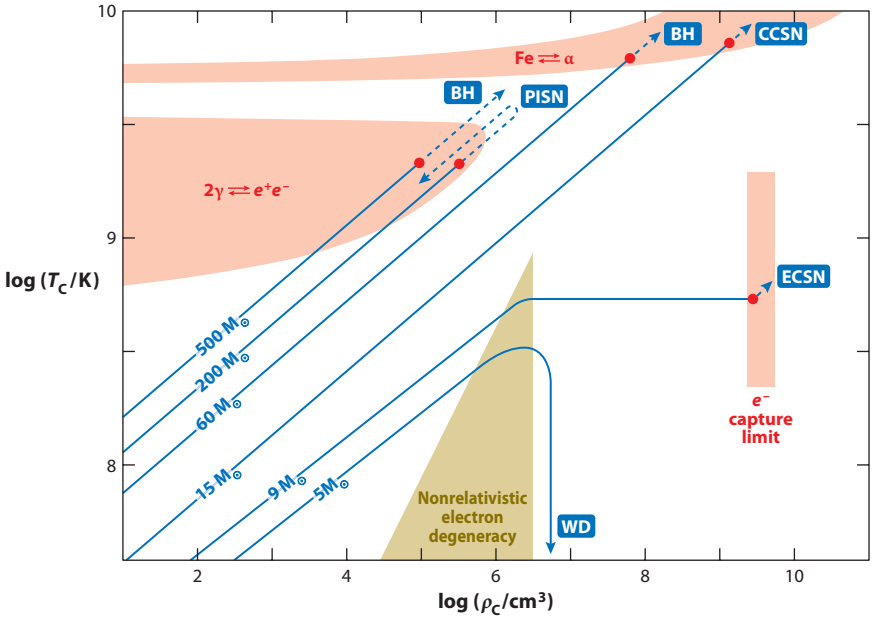

Figure 11

Schematic evolutionary tracks of the centers of single stars of various masses in the temperature-density plane (*blue lines*), representing the different final fates of stellar evolution. Solid lines indicate hydrostatic evolution, big red dots indicate the start of the collapse of the core, and dashed lines imply hydrodynamic evolution, i.e., collapse or explosion. In the three light red areas, the stellar core is prone to collapse, whereas the brown area represents nonrelativistic electron degeneracy. Labels on the evolutionary tracks indicate the initial mass and the final fate. At high metallicity, mass loss may prevent the most massive stars from entering the region of $e^{\pm}$-production, whereas at very low metallicity, rotational mixing may lead stars above 60 $M_{\odot}$ into the pair-unstable regime. Rapid rotation could also lead to the formation of long-duration gamma-ray bursts for those stars that produce black holes or neutron stars (Section 7.4). Abbreviations: BH, black hole; CCSN, iron core-collapse supernova (Section 7.2); ECSN, electron-capture supernova (Section 7.1); PISN, pair-instability supernova (Section 7.3); WD, white dwarf.

mass in intermediate-mass single stars below the Chandrasekhar mass, can be avoided. Due to the lack of a massive and extended hydrogen envelope in the corresponding supernova progenitor stars, such electron-capture explosions are likely to be fast and faint transients, which might be hard to detect.

7.2. Core-Collapse Supernovae

Iron core collapse supernova (CCSN): the stellar explosion from a massive star that has developed an iron core at the end of its evolution

Type II supernova: a supernova that shows hydrogen

Iron core collapse supernovae (CCSNe), which can occur in stars covered with a hydrogen envelope (Type II supernovae) or in stars where hydrogen is almost or completely missing (Type Ib/c supernovae), show a large variety in properties. Much of the diversity in their spectra and light curves reflects differences of the envelope properties of the progenitor stars, e.g., the envelope mass, radius, and chemical composition (Young 2004). However, a large range of explosion energies, radioactive nickel masses, and ejecta geometries are also inferred from observations, which are thought to be determined by the properties of the core of the progenitors: its mass, density structure, spin, and magnetic field (Woosley, Heger & Weaver 2002).

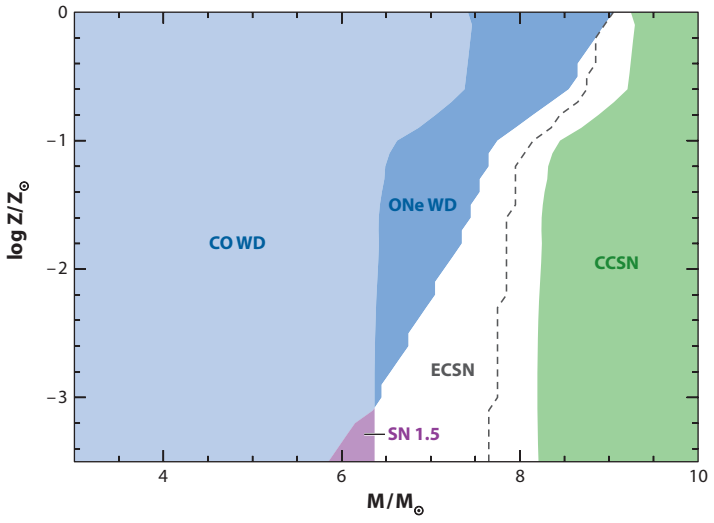

Figure 12

Final outcome of the evolution of stars in the initial mass range of 3 $M_\odot$ to 10 $M_\odot$ as a function of their initial metallicity, according to the synthetic evolution models of Poelarends (2007) and Poelarends et al. (2008). This realization is using the asymptotic giant branch (AGB) mass-loss rate of van Loon et al. (2005) with an added metallicity dependence, assuming that the AGB mass-loss rates decrease for lower metallicity, and a parameterized third dredge-up efficiency. The diagram is divided into four regions according to the different predicted final fate, i.e., carbon oxygen white dwarfs (CO WD, *light blue*; $M_{\rm c,init} < 1.06\,M_\odot$), oxygen neon white dwarfs (ONe WD, *dark blue*; $1.06 < M_{\rm c,init}/M_\odot < 1.375$), electron capture supernova (ECSN, *white*), and iron core collapse supernova (CCSN, *green*; $M_{\rm c,init} > 1.375$). The purple shaded region indicates the range of so-called Type 1.5 supernovae, i.e., carbon deflagrations in stars with a substantial hydrogen envelope. The dashed gray line represents the borderline between CCSN and ECSN for the case where the assumption of the metallicity dependence of the AGB mass-loss rate is dropped. Adapted from Poelarends (2007).

Type IIP supernova: a supernova that shows hydrogen and is identified by a plateau in its light curve; they are by far the largest subgroup

Type IIL supernova: a supernova that shows hydrogen and has a linear decay of its light curve

Type IIb supernova: a supernova that shows a very little hydrogen that can be seen only early on and looks similar to a Type Ib/c supernova afterward

7.2.1. Type IIP and IIL supernovae. Type IIP supernovae are the most frequent type of core-collapse supernovae. They make up about 50% to 75% of all supernovae associated with massive stars (Smartt 2009, Arcavi et al. 2010, Smith et al. 2011a). About one dozen red supergiant progenitors of Type IIP supernovae have been identified so far (Li et al. 2007, Smartt 2009). Calculations of Type IIP supernovae light curves and spectra based on red supergiant models also show good agreement with typical Type IIP supernova observations (e.g., Dessart & Hillier 2011). Clearly, these supernovae are produced from red supergiants with a hydrogen-rich envelope of many solar masses. Based on the observed progenitor brightnesses, Type IIP supernovae are produced from stars of up to ∼17 $M_\odot$ (Smartt 2009), which could form 65% of all massive star supernovae.

According to theoretical light curve studies (e.g., Young 2004), decreasing the mass of the hydrogen-rich envelope of a red supergiant could transform the light curve from a plateau-shape (Type IIP) to a more linear decay (Type IIL supernova) and further to supernovae that show hydrogen lines only at early time (Type IIb supernova). The latter make up about 6% and 11% of all massive star supernovae according to Smith et al. (2011a). These numbers imply that single stars up to about 22 $M_\odot$ might die as red supergiants. This is roughly consistent with the idea that WR stars are formed from single stars with masses above 20–25 $M_\odot$ (see Section 6.3) (Sander, Hamann & Todt 2012).

7.2.2. Type IIn supernovae. Our discussion in Section 6 relates to the recently identified class of Type IIn supernovae. These objects show narrow emission lines at early time. Although this class is quite diverse, Type IIn supernovae are generally bright and are thought to originate from very massive stars that lost large amounts of mass shortly before exploding (Grasberg & Nadezhin 1986, Gal-Yam et al. 2007, Smith et al. 2011a). This conclusion is reinforced by the tentative detection of very luminous progenitor stars (Gal-Yam & Leonard 2009, Smith et al. 2011b). It was found that the narrow emission lines could correspond to shells with velocities of ∼100 km s^{-1}, which would point toward blue supergiant progenitor stars. These observations, together with periodic radio emission that could be explained by the interaction of the supernova ejecta with previously lost shells of material with regular time spacing (Kotak & Vink 2006, Gal-Yam et al. 2007) lead to the idea that LBVs could be immediate supernova progenitors.

Type IIn supernova: a hydrogen-rich supernova showing narrow emission lines due to a dense circumstellar medium

The suggestion that Type IIn supernovae represent explosions of very massive stars has two implications (Smith et al. 2011b). First, it implies that such stars, even in metal-rich large galaxies, do not lose their hydrogen envelope completely before they end their lives. Whereas this contradicts the current detailed stellar evolution models (see Section 6), it agrees with the finding of Hamann, Gräfener & Liermann (2006) that the very massive and hydrogen-rich WNL stars appear not to evolve into the much less luminous hydrogen-free WNE and WC stars, as suggested by Langer (1987). According to Smith et al. (2011b), about $9 \pm 3\%$ of all CCSNe are of Type IIn, which, adopting a Salpeter initial mass function from $8\,M_\odot$ to $150\,M_\odot$, would correspond to all stars initially more massive than $42\,M_\odot$. The results of Hamann, Gräfener & Liermann (2006) suggest that stars above $\sim 60\,M_\odot$ end as WNL stars, which would be about 5% of all massive stars. These two results appear to be compatible.

The second implication of very massive stars being progenitors of Type IIn supernovae is that, apparently, not all very massive stars die quietly by falling into the black hole that we expect they produce in their center (**Figure 11**). In fact, the number fraction of Type IIn supernovae is so large that perhaps all very massive stars explode as luminous supernovae (see above). This brings up the question of the explosion mechanism in those stars that likely form massive black holes, which might require a different explosion mechanism than that of classical CCSNe (Moriya et al. 2010) (Section 7.2.3). Whereas the neutrino-wind appears to be essential to explode the more typical, lower mass stars (Janka et al. 2007), rotation and magnetic fields may play a key role in exploding very massive stars (e.g., Piro & Ott 2011). This is also likely the case in the long-duration gamma-ray bursts (Section 7.4).

7.2.3. Type Ib/c supernovae. Type Ib/c supernovae contain little or no hydrogen. They might be produced from massive and metal-rich single stars through stellar mass loss ($M > 20 - 25\,M_\odot$; see Section 6.3), as shown by Woosley, Langer & Weaver (1993), Woosley, Heger & Weaver (2002), Maeder & Meynet (2003, 2005) and Eldridge & Tout (2004). Alternatively, the mass donors in close binary systems at any metallicity that are initially above $\sim 8\,M_\odot$ (Section 3.1) can be presupernova stars with little or no hydrogen (Woosley, Langer & Weaver 1995; Wellstein & Langer 1999; Eldridge & Tout 2004; Yoon, Woosley & Langer 2010; Dessart et al. 2011).

Smith et al. (2011a) argue that, based on the observed fraction of Type Ib/c supernovae (∼25% of all massive star explosions; see also Smartt 2009), they cannot all originate from single stars. However, Smith and colleagues use $34\,M_\odot$ as the lower mass limit for WR star formation from single stars (based on Heger et al. 2003), whereas the galactic WR population seems to require a value in the range $20–25\,M_\odot$ (Section 6.3). This would allow all Type Ib/c supernovae to be produced from single stars. Nevertheless, there are several arguments supporting the idea that binary progenitors contribute significantly, or even dominate, the Type Ib/c supernovae population.

Hypernovae: consist of a small fraction of Type Ic supernovae that lack helium lines, but show very broad emission lines, and some are associated with long-duration gamma-ray bursts

Pair-instability supernova (PISN): a supernova generated when pair production induces the collapse of the oxygen core, and the oxygen then ignites explosively. This disrupts the whole star without leaving a compact remnant

Pulsation pair instability: stars near the lower mass limit of pair instability are thought to produce oxygen explosions too weak to disrupt the whole star; after the ejection of some envelope material, the star may recollapse, and this may occur repeatedly within the same star, leading to the formation of an iron core and ending in an iron core collapse

First, the Type Ic supernovae especially show a large range of ejecta masses. In particular, the very energetic broad-line Type Ics can show high values ($\sim$10 $M_\odot$; e.g., Mazzali, Iwamoto & Nomoto 2000), whereas some of them have very low ejecta masses ($\sim$1 $M_\odot$; Smartt 2009, Mazzali et al. 2010). The latter are unlikely to be produced from single stars, as the observed WR stars have masses above 8–9 $M_\odot$ (Section 6.3; Crowther 2007). Instead, Type Ib/c supernovae with low ejecta masses are likely to originate from the WR or helium star descendants of donor stars in close binary systems with initial masses in the range 8–20 $M_\odot$. These have been argued to exist in large numbers in the Milky Way (Section 6.3.2), but have not yet been identified observationally. The close binary models of Wellstein & Langer (1999) and Yoon, Woosley & Langer (2010) predict that Type Ic supernovae should indeed have low and high ejecta masses, with Type Ib supernovae covering the middle ground.

A second argument against Type Ib/c supernovae being solely due to single stars is the observation of several of them having a very low kinetic energy and a very low nickel mass. These supernovae are thought to suffer from fallback, which would lead the nickel-rich inner layers first ejected by the supernova core to fall back on the proto-neutron star, possibly thereby producing a black hole (Fryer et al. 2009). Such supernovae are often of Type Ib/c, as with the record holder, SN 2008ha, with a derived kinetic energy of only 0.1% of the canonical value of 10^{51} erg (Moriya et al. 2010a). Nomoto et al. (2006) argue that progenitors with initial masses below 20 $M_\odot$ provide supernovae with mostly about 10^{51} erg in kinetic energy. Above 20–25 $M_\odot$, however, Nomoto and colleagues find a high-energy branch that contains the so-called broad-line Type Ic supernovae or hypernovae is perhaps connected to long-duration gamma-ray bursts (Section 7.4), and may reach up to initial masses of $\sim$80 $M_\odot$ (Section 7.2.2) (Moriya et al. 2010). In addition, they find a low-energy branch that contains the fallback supernovae. This behavior might be connected with the expectation that above initial masses of 20–25 $M_\odot$, black holes are formed in the supernova core (Fryer & Kalogera 2001; Tauris, Langer & Kramer 2011). If this idea is right, it might be that most WR star descendants of single stars produce no or only very faint supernovae, and only those that contain rapidly spinning cores or strong magnetic fields are seen as hypernovae or even gamma-ray bursts (Section 7.4).

7.3. Pair-Instability Supernovae

As mentioned in Section 4.5, the most massive stars may develop pair-unstable oxygen cores before oxygen ignition that may subsequently collapse (**Figure 11**). Thereby, oxygen ignites explosively and a thermonuclear explosion may disperse the whole star, unless its mass was so big that the collapse proceeds to form a black hole. Unlike for CCSNe, the explosion mechanism of pair-instability supernovae (PISNe) is robust and has been confirmed by many groups (El Eid & Langer 1986, Heger & Woosley 2002, Waldman 2008). The only condition to be fulfilled in the absence of rotation is that the helium core at the end of core helium burning needs to be more massive than about 60 $M_\odot$ (Heger & Woosley 2002). For helium core masses between 40 $M_\odot$ and 60 $M_\odot$, Heger & Woosley find pulsational pair instability, where violent thermonuclear pulsations may lead to mass ejections and the star ends up in a CCSN (see also Woosley, Blinnikov & Heger 2007; Waldman 2008).

Whether a very massive star in the local Universe can maintain a sufficiently high helium core mass to form a PISN depends primarily on its mass-loss history. Even for mass-losing stars, the mass of the helium core is only growing as long as it is covered with a hydrogen envelope. Langer et al. (2007a) reached the conclusion that, based on the currently available mass-loss rates—which have to be extrapolated to the regime of very massive stars—PISNe may occur in the local Universe in stars with a metallicity smaller than $Z_\odot/3$, leading to 1 in 1,000 supernovae being of

this type. The conclusion reached in Section 6.3 that the most massive stars may die covered by a hydrogen envelope, however, has the consequence that PISNe might be possible even in our Milky Way. To reach the required helium core mass, the initial mass of the star would need to be about 100–140 $M_\odot$ (El Eid & Langer 1986, Heger & Woosley 2002), depending on assumed overshooting and rotational mixing efficiencies.

In recent years, several observational counterparts of PISNe have been suggested. The best candidate may be SN 2007bi (Gal-Yam et al. 2009), whose nucleosynthesis, light curve, and spectral evolution agree very well with the predictions of PISN models (Heger & Woosley 2002; Scannapieco et al. 2005; Kasen, Woosley & Heger 2011), although a hypernova model provides an alternative explanation (Umeda & Nomoto 2008). Supernova 2007bi, however, was a Type Ic supernova, i.e., it did not contain hydrogen. This event, which occurred at subsolar metallicity, does not fit easily into the scheme of massive star evolution at solar metallicity outlined above (see Section 7.5).

A further PISN candidate is SN 2006gy (Ofek et al. 2007, Smith et al. 2007), the most luminous supernova discovered until then, which is of Type IIn (Section 7.2.2). Woosley, Blinnikov & Heger (2007) and Smith et al. (2010) argue that this interaction-powered supernova could be consistent with a pulsational pair-instability event. Finally, Quimby et al. (2011) present the newly discovered class of hydrogen-poor superluminous supernovae, for which they also discuss the emission being powered by the collision of the supernova with previously ejected hydrogen-poor shells, which could have been formed by the pulsational pair-instability mechanism. Clearly, more supernova progenitor and explosion models of very massive stars are needed to evaluate these possibilities.

The majority of PISNe are not expected to be bright. In fact, hardly any ^{56}Ni is predicted to form in such supernovae from stars below ~180 $M_\odot$ (see figure 1 in Heger & Woosley 2002). This is confirmed by detailed light curve modeling of such events (Herzig et al. 1990, Scannapieco et al. 2005). This implies that many such supernovae could occur (see above), but most would not be detected observationally. As each of these events produces as much metal as a whole generation of core collapse supernovae, PISNe might play a significant role for nucleosynthesis, even in the local Universe.

7.4. Long-Duration Gamma-Ray Bursts

The origin of long-duration gamma-ray bursts remained unclear for a long time. Today, there is overwhelming evidence that massive stars are their progenitors (Woosley & Bloom 2006; Gehrels, Ramirez-Ruiz & Fox 2009)—either due to the formation of a rapidly rotating black hole in the so-called collapsar scenario (Woosley 1993) or within the millisecond-magnetar model, where an almost critically rotating highly magnetized neutron star produces a pointing flux–dominated explosion (Lyutikov & Blackman 2001). In both cases, the progenitor star needs to develop a rapidly rotating iron core. A further constraint from those models is that the dimension of the immediate progenitor star is smaller than the distance that a relativistic jet can travel during the central engine lifetime, which leaves only WR stars as possible progenitors. This prediction was verified by several associations of Type Ic supernovae with gamma-ray bursts (e.g., Hjorth et al. 2003).

Because at least the single stars in the Solar Neighborhood are likely to end up with rather slowly rotating cores (Section 2.2), and because WR stars would quickly spin down due to their strong winds, various scenarios have been proposed to lead to late production and spin-up of a WR star in a close binary system (Fryer & Heger 2005, Podsiadlowski et al. 2010, Tout et al. 2011). These scenarios involve complex binary physics and will apply only to a limited number of binary systems, but they have the advantage of being able to produce long duration gamma-ray bursts even at high metallicity.

Long-duration gamma-ray bursts: seconds- to minutes-long flashes of time-variable gamma-ray emission found to emerge at cosmological distance and thought to be produced by the deaths of rapidly rotating WR stars; most are associated with X-ray flashes, and a fraction of them also show optical or radio afterglows, presumably due to interaction with circumstellar material

Most long duration gamma-ray bursts appear to occur at low metallicity (Fruchter et al. 2006, Modjaz et al. 2008), perhaps even those that occur in galaxies with high average metallicity (Niino 2011). The local ratio of long duration gamma-ray bursts to supernovae is low (about 1:1,000). A low-metallicity bias implies, however, that at a given low metallicity, this ratio must be much higher, because low-metallicity massive stars are rare in the local Universe (Langer & Norman 2006). Exotic binary channels could then explain at most a small fraction of the events.

An alternative long duration gamma-ray burst progenitor model is provided by the scenario of quasi-chemically homogeneous evolution induced by rapid rotation (Section 2.3) (Yoon & Langer 2005, Woosley & Heger 2006). Because in this picture a core-envelope structure is avoided, the helium core is not spun down by a slowly rotating hydrogen-rich envelope. Because the WR star is formed early on, low metallicity appears to be required to avoid wind-induced spin down. Brott et al. (2011a) find quasi-chemically homogeneous evolution to be possible for stars initially more massive than $20\,M_\odot$ at LMC metallicity (see **Figure 2**).

7.5. The Picture at Low Metallicity

As discussed throughout this review, we are currently still struggling to obtain stellar evolution models for massive stars in our Galaxy that are consistent with the available observations and to pin down which physical processes are most relevant to consider. Of course, this does not stop us from providing evolutionary models for low-metallicity massive stars, for which observational constraints are much scarcer. There is no space here to discuss low-metallicity massive stars in detail. It is interesting to realize, however, that the recent supernova data suggests that massive stars do end their evolution quite differently at low metallicity.

It has been shown by Prantzos & Boissier (2003) that the ratio of Type Ib/c to Type II supernovae is decreasing with decreasing metallicity. This may be connected with the decreasing ratio of O to WR stars (Section 6.3). Arcavi et al. (2010) report the opposite trend for broad-lined Type Ic supernovae, which are mostly found in dwarf galaxies. As mentioned above, in the local Universe long gamma-ray bursts also occur preferentially in dwarf galaxies. All this may reflect that stellar winds become less important and rotation becomes more important with decreasing metallicity.

8. OUTLOOK

The sections above give a status report on our current understanding of massive stars. Large progress has been achieved in the past decade, mainly, but not exclusively, for main-sequence stars, WR stars, and supernovae. It was also shown that there are still many uncertain physical processes to be considered in massive star evolution. In the following, we point out several paths that might be fruitful to take in the near future.

- Mass loss remains one of the largest uncertainties for massive star evolution except for main-sequence stars below about $28\,M_\odot$ (Milky Way) to $60\,M_\odot$ (SMC) (see Section 4.2.1). For more massive main-sequence stars, the mass-loss rates are well understood until the stars reach the Eddington or Ω limit (see **Figure 6**). The mass loss of red supergiants, LBVs, and WR stars is not yet well understood, and empirical mass-loss rates for these types of stars are uncertain. The initial-final mass relation for stars above $\sim 25\,M_\odot$ is therefore not yet well determined.
- Rotation has been identified as an important ingredient in massive star evolution. Surprisingly, this appears now to be most clear for the end stages of massive star evolution. Long-duration gamma-ray bursts and hypernovae, as well as peculiar bright Type II and

Type Ib/c supernovae, cannot be understood without invoking rapid rotation (Section 7). Effects of rotation appear further to increase toward low metallicity (Section 7.5). However, the effects of rotational mixing in ordinary massive main-sequence stars are not clearly identified (Sections 5.4 and 6.3.1). Resolving this issue will require a large-scale observational campaign of rapidly rotating stars with respect to their surface abundances and their binary status.

- One of the current mysteries is the unknown origin of slowly rotating massive main-sequence stars that have surfaces enriched in hydrogen burning products and which may all be magnetic (Section 5.4.1). We need to investigate the binary fraction and companion properties of these stars in order to test whether they could indeed be products of stellar mergers (Section 3.3).
- There are currently indications that of the order of 10% of the massive main-sequence stars are magnetic (Sections 2.2, 2.3, and 3.3). The long-standing question of the origin of the magnetic fields in Ap/Bp stars is now extended to massive stars. Modeling the effects of such fields on the evolution of these stars may help to pin down, or disprove, evolutionary connections between various types of stars, as magnetic main-sequence stars, hot slowly rotating B supergiants, or magnetars (Section 3.4).
- It will be of key importance to derive statistically sound correlations of surface nitrogen and helium abundances in O-type stars with their rotational velocities, their radial velocities, and their binary properties. A key to understanding very massive main-sequence stars may lie in the enigmatic OVz and On stars (Section 5.4.3).
- In order to understand the role of rotation in massive stars, it will help to investigate the origin of the distribution of their rotational velocities. One goal to pursue is to separate the effect of binary evolution on this distribution on one side, and that of magnetic spin-down on the other side, which both could be considerable (Section 5.3).
- The origin of the hot, slowly rotating nitrogen-rich B supergiants is currently unknown (Section 6.1). We need stellar models with undermassive helium cores, due to either a post-main-sequence merger or magnetic field effects in their main-sequence progenitors, to test the corresponding ideas. At the same time, searches for magnetic fields in these stars and for close binary companions may provide essential constraints.
- For most of the points mentioned above, it would be helpful to have detailed quantitative predictions from stellar evolution grids for massive close binary stars (Section 3), which are so far available only in very limited number, and for small parts of the binary parameter space.
- Observations of very massive stars and their explosions have led to the new paradigm that the most massive stars may not lose their hydrogen envelopes completely during their lives (Sections 6.3.1 and 7.2.2). This is consistent with the evidence that mass-loss rates might have been overestimated in the past and agrees with simple concepts of massive star evolution. We need new detailed model grids for single stars to verify this concept. Also, the implications for the evolution of metal-poor very massive stars still have to be worked out.
- One consequence of hydrogen-rich explosions from very massive stars is that PISNe may occur even at high metallicity (Section 7.3). So far, very few models for PISNe for metal-rich stars exist, which makes a comparison with the recently observed spectacularly bright massive star explosions difficult.
- There appears to be evidence for many (but not all!) stars with initial masses above $\sim 25\ M_{\odot}$ producing bright supernovae, either as broad-lined Type Ic (Section 7.2.3) or as Type IIn supernovae (Section 7.2.2). To explode such massive stars may require rapidly rotating or

highly magnetized cores (Section 7). Evolutionary models leading to those cores need to be identified.

- Long-duration gamma-ray bursts, which may preferentially occur at low metallicity, have massive hydrogen-free progenitors (Section 7.4). Their initial mass range and preferred progenitor evolution remains to be identified unambiguously. Whether chemically homogeneous evolution (Section 2.3) provides such a path can be tested through observations of O- and WR-type stars in the Magellanic Clouds.

DISCLOSURE STATEMENT

The author is not aware of any affiliations, memberships, funding, or financial holdings that might be perceived as affecting the objectivity of this review.

ACKNOWLEDGMENTS

This review profited from constructive remarks by Alexander Heger, Alex de Koter, Selma de Mink, Thomas Tauris, and Sung-Chul Yoon. The author is grateful to Andreas Sander, Wolf-Rainer Hamann, and Helge Todt for making their results available before publication, and to my colleagues at the Argelander-Institute and in the VLT-FLAMES Tarantula Survey for many inspiring discussions.

LITERATURE CITED

Abbott DC, Lucy LB. 1985. *Ap. J.* 288:679
Alexander DR, Ferguson JW. 1994. *Ap. J.* 437:879
Andersen J. 1991. *Astron. Astrophys. Rev.* 3:91
Arcavi I, Gal-Yam A, Kasliwal MM, Quimby RM, Ofek EO, et al. 2010. *Ap. J.* 721:777
Arnett WD. 1977. *Ap. J. Suppl.* 35:145
Arnett WD, Thielemann F-K. 1985. *Ap. J.* 295:589
Arnett WD, Meakin C. 2011. *Ap. J.* 733:78
Arlt R, Rüdiger G. 2011. *MNRAS* 412:107
Balbus SA, Hawley JF. 1998. *Rev. Mod. Phys.* 70:1–53
Berger L, Koester D, Napiwotzki R, Reid IN, Zuckerman B. 2005. *Astron. Astrophys.* 444:565
Belkacem K, Samadi R, Goupil M, Lefevre L, Baudin F, et al. 2009. *Science* 324:1540
Bennett PD. 2010. *ASP Conf. Ser.* 425:181
Bestenlehner JM, Vink JS, Gräfener G, Najarro F, Evans CJ, et al. 2011. *Astron. Astrophys.* 530:L14
Bodenheimer P. 1971. *Ap. J.* 167:153
Bonanos AZ, Stanek KZ, Udalski A, Wyrzykowski L, Zebrun K, et al. 2004. *Ap. J.* 611:L33
Bouret J-C, Lanz T, Hillier DJ, Heap SR, Hubeny I, et al. 2003. *Ap. J.* 595:1182
Bradley PA. 1998. *Ap. J. Suppl.* 116:307
Bradley PA. 2001. *Ap. J.* 552:326
Braithwaite J. 2006. *Astron. Astrophys.* 449:451
Braithwaite J, Spruit HC. 2004. *Nature* 431:819
Braun H. 1997. *Mischprozesse und Nukleosynthese in den Komponenten massereicher enger Binärsysteme*. PhD thesis. Ludwig Maximilian Univ., München. 152 pp.
Braun H, Langer N. 1995. *Astron. Astrophys.* 297:483
Bresolin F, Kudritzki R-P, Mendez RH, Przybilla N. 2001. *Ap. J. Lett.* 548:L159–63
Brinchmann J, Kunth D, Durret F. 2008. *Astron. Astrophys.* 485:657
Brinkworth CS, Burleigh MR, Marsh TR. 2007. *ASP Conf. Ser.* 372:183
Briquet M, Morel T, Thoul A, Scuflaire R, Miglio A, et al. 2007. *MNRAS* 381:1482

Brott I, de Mink SE, Cantiello M, Langer N, de Koter A, et al. 2011a. *Astron. Astrophys.* 530:A115
Brott I, Evans CJ, Hunter I, de Koter A, Langer N, et al. 2011b. *Astron. Astrophys.* 530:A116
Brown GE, Heger A, Langer N, Lee C-H, Wellstein S, Bethe HA. 2001. *New Astron.* 6:457
Brun AS, Browning MK, Toomre J. 2005. *Ap. J.* 629:461
Camilo F, Ransom SM, Halpern JP, Reynolds J. 2007. *Ap. J.* 666:L93
Cantiello M, Langer N. 2010. *Astron. Astrophys.* 521:A9
Cantiello M, Braithwaite J. 2011. *Astron. Astrophys.* 534:A140
Cantiello M, Yoon S-C, Langer N, Livio M. 2007. *Astron. Astrophys.* 465:L29
Cantiello M, Langer N, Brott I, de Koter A, Shore SN, et al. 2009. *Astron. Astrophys.* 499:279
Cantiello M, Braithwaite J, Brandenburg A, Del Sordo F, Käpylä P, Langer N. 2011. *IAU Symp.* 273:200
Castor JI, Abbott DC, Klein RI. 1975. *Ap. J.* 195:157
Charbonneau P, MacGregor KB. 1993. *Ap. J.* 417:762
Charbonneau P, MacGregor KB. 2001. *Ap. J.* 559:1094
Charbonnel C, Talon S. 2005. *Science* 309:2189
Charbonnel C, Zahn J-P. 2007. *Astron. Astrophys.* 467:L15
Chiappini C, Frischknecht U, Meynet G, Hirschi R, Barbuy B, et al. 2011. *Nature* 472:454
Chiosi C, Summa C. 1970. *Astrophys. Space Sci.* 8:478
Chiosi C, Maeder A. 1986. *Annu. Rev. Astron. Astrophys.* 24:329
Chiosi C, Nasi E, Sreenivasan SR. 1978. *Astron. Astrophys.* 63:103
Chiosi C, Bertelli G, Bressan A. 1992. *Annu. Rev. Astron. Astrophys.* 30:235
Claeys JSW, de Mink SE, Pols OR, Eldridge JJ, Baes M. 2011. *Astron. Astrophys.* 528:A131
Claret A. 1998. *Astron. Astrophys. Suppl.* 131:395
Claret A. 2007. *Astron. Astrophys.* 475:1019
Crowther PA. 2007. *Annu. Rev. Astron. Astrophys.* 45:177
Crowther PA, Barnard R, Carpano S, Clark JS, Dhillon VS, Pollock AMT. 2010a. *MNRAS* 403:L41
Crowther PA, Hadfield LJ. 2006. *Astron. Astrophys.* 449:711
Crowther PA, Lennon DJ, Walborn NR. 2006. *Astron. Astrophys.* 446:279
Crowther PA, Schnurr O, Hirschi R, Yusof N, Parker RJ, et al. 2010b. *MNRAS* 408:731–51
Crowther PA, Smith LJ, Hillier DJ. 1995. *Astron. Astrophys.* 302:457
Crowther PA, Smith LJ, Hillier DJ, Schmutz W. 1995. *Astron. Astrophys.* 293:427
Crowther PA, Smith LJ, Willis AJ. 1995. *Astron. Astrophys.* 304:269
De Beck E, Decin L, de Koter A, Justtanont K, Verhoelst T, et al. 2010. *Astron. Astrophys.* 523:A18
De Donder E, Vanbeveren D, van Bever J. 1997. *Astron. Astrophys.* 318:812
Degroote P, Briquet M, Auvergne M, Simon-Diaz S, Aerts C, et al. 2010. *Astron. Astrophys.* 519:A38
de Jager C, Nieuwenhuijzen H, van der Hucht KA. 1988. *Astron. Astrophys. Suppl.* 72:259
de Koter A, Heap SR, Hubeny I. 1997. *Ap. J.* 477:792
De Loore C, De Greve JP. 1992. *Astron. Astrophys. Suppl.* 94:453
De Loore C, De Greve JP, Lamers HJGLM. 1977. *Astron. Astrophys.* 61:251
de Mink SE, Cantiello M, Langer N, Pols OR, Brott I, Yoon S-C. 2009. *Astron. Astrophys.* 497:243
de Mink SE, Langer N, Izzard RG. 2011. *Bull. Societe Royale des Sci. Liege* 80:543–48
de Mink SE, Pols OR, Hilditch RW. 2007. *Astron. Astrophys.* 467:1181
Dessart L, Hillier DJ. 2011. *MNRAS* 410:1739
Dessart L, Hillier DJ, Livne E, Yoon S-C, Woosley S, et al. 2011. *MNRAS* 414:2985
Dolez N, Vauclair G, Kleinman SJ, Chevreton M, Fu JN, et al. 2006. *Astron. Astrophys.* 446:237
Domiciano de Souza A, Kervella P, Jankov S, Abe L, Vakili F, et al. 2003. *Astron. Astrophys.* 407:L47
Domiciano de Souza A, Kervella P, Jankov S, Ohishi N, Nordgren TE, Abe L. 2005. *Astron. Astrophys.* 442:567
Donati J-F, Howarth ID, Jardine MM, Petit P, Catala C, et al. 2006. *MNRAS* 370:629
Donati J-F, Landstreet JD. 2009. *Annu. Rev. Astron. Astrophys.* 47:333
Douglas LS, Bremer MN, Lehnert MD, Stanway ER, Milvang-Jensen B. 2010. *MNRAS* 409:1155–71
Dray LM, Tout CA. 2007. *MNRAS* 376:61
Deupree RG. 2000. *Ap. J.* 543:395
Eddington AS. 1921. *Zs. Phys.* 7:351
Eddington AS. 1929. *MNRAS* 90:54

Eggenberger P, Maeder A, Meynet G. 2005. *Astron. Astrophys.* 440:L9
Ekström S, Meynet G, Maeder A, Barblan F. 2008. *Astron. Astrophys.* 478:467
Eldridge JJ, Izzard RG, Tout CA. 2008. *MNRAS* 384:1109
Eldridge JJ, Langer N, Tout CA. 2011. *MNRAS* 414:3501
Eldridge JJ, Tout CA. 2004. *MNRAS* 353:87
Eldridge JJ, Vink JS. 2006. *Astron. Astrophys.* 452:295
El Eid MF. 1995. *MNRAS* 275:983
El Eid MF, Langer N. 1986. *Astron. Astrophys.* 167:274
Endal AS, Sofia S. 1976. *Ap. J.* 210:184–98
Endal AS, Sofia S. 1978. *Ap. J.* 220:279–90
Evans CJ, Smartt SJ, Lee J-K, Lennon DJ, Kaufer A, et al. 2005. *Astron. Astrophys.* 437:467
Evans CJ, Taylor WD, Henault-Brunet V, Sana H, de Koter A, et al. 2011. *Astron. Astrophys.* 530:A108
Eversberg T, Lepine S, Moffat AFJ. 1998. *Ap. J.* 494:799
Ferrario L, Pringle JE, Tout CA, Wickramasinghe DT. 2009. *MNRAS* 400:L71
Ferrario L, Wickramasinghe DT. 2005. *MNRAS* 356:615
Figer DF. 2005. *Nature* 434:192
Figer DF, Najarro F, Morris M, McLean IS, Geballe TR, et al. 1998. *Ap. J.* 506:384
Fitzpatrick EL, Garmany CD. 1990. *Ap. J.* 363:119
Fliegner J, Langer N, Venn KA. 1996. *Astron. Astrophys.* 308:L13
Foellmi C, Moffat AFJ, Guerrero MA. 2003a. *MNRAS* 338:1025
Foellmi C, Moffat AFJ, Guerrero MA. 2003b. *MNRAS* 338:360
Fryer CL, Brown PJ, Bufano F, Dahl JA, Fontes CJ, et al. 2009. *Ap. J.* 707:193
Fryer CL, Heger A. 2005. *Ap. J.* 623:302
Fryer CL, Kalogera V. 2001. *Ap. J.* 554:548
Friend DB, Abbott DC. 1986. *Ap. J.* 311:701
Frischknecht U, Hirschi R, Meynet G, Ekström S, Georgy C, et al. 2010. *Astron. Astrophys.* 522:A39
Fruchter AS, Levan AJ, Strolger L, Vreeswijk PM, Thorsett SE, et al. 2006. *Nature* 441:463
Gaburov E, Lombardi JC, Portegies Zwart S. 2008. *MNRAS* 383:L5
Gal-Yam A, Leonard DC. 2009. *Nature* 458:865
Gal-Yam A, Leonard DC, Fox DB, Cenko SB, Soderberg AM, et al. 2007. *Ap. J.* 656:372
Gal-Yam A, Mazzali P, Ofek EO, Nugent PE, Kulkarni SR, et al. 2009. *Nature* 462:624
Gehrels N, Ramirez-Ruiz E, Fox DB. 2009. *Annu. Rev. Astron. Astrophys.* 47:567
Georgy G, Meynet G, Walder R, Folini D, Maeder A. 2009. *Astron. Astrophys.* 502:611
Gies D, Lambert DL. 1992. *Ap. J.* 387:673
Glebbeek E, Pols O. 2008. *Astron. Astrophys.* 488:1017
Gräfener G, Hamann W-R. 2005. *Astron. Astrophys.* 432:633
Gräfener G, Hamann W-R. 2008. *Astron. Astrophys.* 482:945
Gräfener G, Owocki SP, Vink JS. 2012. *Astron. Astrophys.* 538:A40
Gräfener G, Vink JS, de Koter A, Langer N. 2011. *Astron. Astrophys.* 535:A56
Grasberg EK, Nadezhin DK. 1986. *Sov. Astron. Lett.* 12:68
Guinan EF, Ribas I, Fitzpatrick EL, Gimenez A, Jordi C, et al. 2000. *Ap. J.* 544:409
Guy J, Sullivan M, Conley A, Regnault N, Astier P, et al. 2010. *Astron. Astrophys.* 523:A7
Haiman Z, Loeb A. 1997. *Ap. J.* 483:21
Hamann W-R. 2010. *Astrophys. Space Sci.* 329:151
Hamann W-R, Gräfener G, Liermann A. 2006. *Astron. Astrophys.* 457:1015
Hamann W-R, Koesterke L, Wessolowski U. 1995. *Astron. Astrophys.* 299:151
Handler G. 2001. *MNRAS* 323:L43
Handler G, Romero-Colmenero E, Montgomery MH. 2002. *MNRAS* 335:399
Harries TJ, Hilditch RW, Hill G. 1997. *MNRAS* 285:277
Heger A, Fryer CL, Woosley SE, Langer N, Hartmann DH. 2003. *Ap. J.* 591:288
Heger A, Langer N. 1996. *Astron. Astrophys.* 315:421
Heger A, Langer N. 2000. *Ap. J.* 544:1016–35
Heger A, Langer N, Woosley SE. 2000. *Ap. J.* 528:368–96

Heger A, Woosley SE. 2002. *Ap. J.* 567:532
Heger A, Woosley SE, Waters R. 2000. *The First Stars: Proc. MPA/ESO Workshop, ESO Astrophys. Symp.*, ed. A Weiss, TG Abel, V Hill, pp. 121. Berlin: Springer
Heger A, Woosley SE, Spruit HC. 2005. *Ap. J.* 626:350
Herrero A, Kudritzki RP, Vilchez JM, Kunze D, Butler K, Haser S. 1992. *Astron. Astrophys.* 261:209
Herrero A, Lennon DJ. 2004. *IAU Symp.* 215:209
Herrero A, Puls J, Najarro F. 2002. *Astron. Astrophys.* 396:949
Herwig F, Bloecker T, Schoenberner D, El Eid MF. 1997. *Astron. Astrophys.* 324:L81
Herzig K, El Eid MF, Fricke KJ, Langer N. 1990. *Astron. Astrophys.* 233:462
Hillier DJ. 1991. *Astron. Astrophys.* 247:455
Hirschi R, Maeder A. 2010. *Astron. Astrophys.* 519:A16
Hirschi R, Meynet G, Maeder A. 2004. *Astron. Astrophys.* 425:649
Hjorth J, Sollerman J, Moller P, Fynbo JPU, Woosley SE, et al. 2003. *Nature* 423:847
Howarth ID, Smith KC. 2001. *MNRAS* 327:353
Huang S-S. 1966. *Annu. Rev. Astron. Astrophys.* 4:35
Huang W, Gies DR. 2006. *Ap. J.* 648:580
Huang W, Gies DR, McSwain MV. 2010. *Ap. J.* 722:605
Hubrig S, Schöller M, Kharchenko NV. 2011. *Astron. Astrophys.* 528:A151
Humphreys RM, Davidson K. 1979. *Ap. J.* 232:409
Humphreys RM, Davidson K. 1994. *Publ. Astron. Soc. Pac.* 106:1025
Humphreys RM, McElroy DB. 1984. *Ap. J.* 284:565
Hunter I, Brott I, Lennon DJ, Langer N, Dufton PL, et al. 2008b. *Ap. J. Lett.* 676:L29
Hunter I, Lennon DJ, Dufton PL, Trundle C, Simon-Diaz S, et al. 2008a. *Astron. Astrophys.* 479:541
Iglesias CA, Rogers FJ. 1996. *Ap. J.* 464:943
Iglesias CA, Rogers FJ, Wilson BG. 1992. *Ap. J.* 397:717
Ishii M, Ueno M, Kato M. 1999. *Publ. Astron. Soc. Jpn.* 51:417
Janka H-T, Langanke K, Marek A, Martinez-Pinedo G, Müller B. 2007. *Phys. Rev.* 442:38
Jeffery CS, Hamann W. 2010. *MNRAS* 404:1698
Kaper L, Henrichs HF, Fullerton AW, Ando H, Bjorkman KS, et al. 1997. *Astron. Astrophys.* 327:281
Kasen D, Woosley SE, Heger A. 2011. *Ap. J.* 734:102
Kasliwal MM, Kulkarni SR, Arcav I, Quimby RM, Ofek EO, et al. 2011. *Ap. J.* 730:134
Kato S. 1966. *Publ. Astron. Soc. Jpn.* 18:374
Kepler SO, Giovannini O, Wood MA, Nather RE, Winget DE, et al. 1995. *Ap. J.* 447:874
Kippenhahn R, Meyer-Hofmeister E, Thomas HC. 1970. *Astron. Astrophys.* 5:155
Kippenhahn R, Weigert A. 1990. *Stellar Structure and Evolution*. Berlin: Springer
Kitaura FS, Janka H-T, Hillebrandt W. 2006. *Astron. Astrophys.* 450:345
Kleinman SJ, Nather RE, Winget DE, Clemens JC, Bradley PA, et al. 1998. *Ap. J.* 495:424
Koesterke L, Hamann W-R. 1995. *Astron. Astrophys.* 299:503
Köhler K, Borzyszkowski M, Brott I, Langer N, de Koter A. 2012. *Astron. Astrophys.* In press (DOI: 10.1051/0004-6361/201118352)
Kotak R, Vink JS. 2006. *Astron. Astrophys.* 460:L5
Kudritzki R-P. 2010. *A.N.* 331:459–73
Kudritzki R-P, Puls J. 2000. *Annu. Rev. Astron. Astrophys.* 38:613
Kudritzki R-P, Urbaneja MA, Bresolin F, Przybilla N, Gieren W, Pietrzynski G. 2008. *Ap. J.* 681:269
Langer N. 1986. *Astron. Astrophys.* 164:45
Langer N. 1987. *Astron. Astrophys.* 171:L1
Langer N. 1989a. *Astron. Astrophys.* 210:93
Langer N. 1989b. *Astron. Astrophys.* 220:135
Langer N. 1991a. *Astron. Astrophys.* 243:155
Langer N. 1991b. *Astron. Astrophys.* 248:531
Langer N. 1991c. *Astron. Astrophys.* 252:669
Langer N. 1992. *Astron. Astrophys.* 265:L17
Langer N. 1997. *ASP Conf. Ser.* 120:83

Langer N. 1998. *Astron. Astrophys.* 329:551
Langer N, Brott I, Cantiello M, de Mink SE, Izzard RG, Yoon S-C. 2010. *IAU Symp.* 268:411
Langer N, Cantiello M, Yoon S-C, Hunter I, Brott I, et al. 2008. *IAU Symp.* 250:167
Langer N, El Eid MF. 1986. *Astron. Astrophys.* 167:265
Langer N, El Eid MF, Fricke KJ. 1985. *Astron. Astrophys.* 145:179
Langer N, Hamann W-R, Lennon M, Najarro F, Pauldrach AWA, Puls J. 1994. *Astron. Astrophys.* 290:819
Langer N, Henkel C. 1995. *AIP Conf. Ser.* 327:413
Langer N, Kiriakidis M, El Eid MF, Fricke KJ, Weiss A. 1988. *Astron. Astrophys.* 192:177
Langer N, Maeder A. 1995. *Astron. Astrophys.* 295:685
Langer N, Norman CA. 2006. *Ap. J. Lett.* 638:L63
Langer N, Norman CA, de Koter A, Vink JS, Cantiello M, Yoon S-C. 2007a. *Astron. Astrophys.* 475:L19
Langer N, Sugimoto D, Fricke KJ. 1983. *Astron. Astrophys.* 126:207
Langer N, van Marle AJ, Poelarends AJT, Yoon SC. 2007b. *ASP Conf. Ser.* 374:37
Langer N, Yoon S-C, Petrovic J, Heger A. 2003. *IAU Symp.* 215:535
Larsen SS, de Mink SE, Eldridge JJ, Langer N, Bastian N, et al. 2011. *Astron. Astrophys.* 532:A147
Law NM, Kulkarni SR, Dekany RG, Ofek EO, Quimby RM, et al. 2009. *Publ. Astron. Soc. Pac.* 121:1395
Leitherer C, Chavarria KC. 1987. *Astron. Astrophys.* 175:208
Li W, Leaman J, Chornock R, Filippenko AV, Poznanski D, et al. 2011. *MNRAS* 412:1441
Li W, Wang X, Van Dyk SD, Cuillandre J-C, Foley RJ, Filippenko AV. 2007. *Ap. J.* 661:1013
Liu QZ, van Paradijs J, van den Heuvel EPJ. 2006. *Astron. Astrophys.* 455:1165
Lombardi JC Jr, Rasio FA, Shapiro SL. 1996. *Ap. J.* 468:797
Lubow SH, Shu FH. 1975. *Ap. J.* 198:383
Lucy LB. 1967. *Zeit. Astrophys.* 65:89
Lucy LB, Abbott DC. 1993. *Ap. J.* 405:738
Lucy LB, Solomon PM. 1970. *Ap. J.* 159:879
Lyutikov M, Blackman EG. 2001. *MNRAS* 321:177
MacDonald J, Mullan DJ. 2004. *MNRAS* 348:702
MacGregor KB, Cassinelli JP. 2003. *Ap. J.* 586:480
Mac Low M-M, Balsara DS, Kim J, de Avillez MA. 2005. *Ap. J.* 626:864
Maeder A. 1987. *Astron. Astrophys.* 178:159
Maeder A. 2009. *Physics, Formation and Evolution of Rotating Stars*. Berlin: Springer
Maeder A, Meynet G. 1987. *Astron. Astrophys.* 182:243
Maeder A, Meynet G. 2000a. *Annu. Rev. Astron. Astrophys.* 38:143–90
Maeder A, Meynet G. 2000b. *Astron. Astrophys.* 361:159
Maeder A, Meynet G. 2003. *Astron. Astrophys.* 411:543
Maeder A, Meynet G. 2004. *Astron. Astrophys.* 422:225
Maeder A, Meynet G. 2005. *Astron. Astrophys.* 440:1041
Maeder A, Zahn J-P. 1998. *Astron. Astrophys.* 334:1000
Mahy L, Martins F, Machado C, Donati J-F, Bouret J-C. 2011. *Astron. Astrophys.* 533:A9
Marchenko SV, Foellmi C, Moffat AFJ, Martins F, Bouret J-C, Depagne E. 2007. *Ap. J. Lett.* 656:L77
Marigo P, Aringer B. 2009. *Astron. Astrophys.* 508:1539
Mark JW-K. 1968. *Ap. J.* 154:627–43
Martins F, Hillier DJ, Bouret JC, Depagne E, Foellmi C, et al. 2009. *Astron. Astrophys.* 495:257
Martins F, Hillier DJ, Paumard T, Eisenhauer F, Ott T, Genzel R. 2008. *Astron. Astrophys.* 478:219
Mason AB, Clark JS, Norton AJ, Crowther PA, Tauris TM, et al. 2012. *MNRAS.* 422(1):199
Mason BD, Hartkopf WI, Gies DR, Henry TJ, Helsel JW. 2009. *Astron. J.* 137:3358
Massey P, Armandroff TE, Pyke R, Patel K, Wilson CD. 1995. *Astron. J.* 110:2715
Mauron N, Josselin E. 2011. *Astron. Astrophys.* 526:A156
Mazzali PA, Iwamoto K, Nomoto K. 2000. *Ap. J.* 545:407
Mazzali PA, Maurer I, Valenti S, Kotak R, Hunter D. 2010. *MNRAS* 408:87
Mendel JT, Venn KA, Proffitt CR, Brooks AM, Lambert DL. 2006. *Ap. J.* 640:1039
Mermilliod J-C, Maeder A. 1986. *Astron. Astrophys.* 158:45
Merryfield WJ. 1995. *Ap. J.* 444:318

Meyer-Hofmeister E. 1972. *Astron. Astrophys.* 16:282
Meynet G, Eggenberger P, Maeder A. 2011. *Astron. Astrophys.* 525:L11
Meynet G, Maeder A. 1997. *Astron. Astrophys.* 321:465
Meynet G, Maeder A. 2000. *Astron. Astrophys.* 361:101
Meynet G, Maeder A. 2002. *Astron. Astrophys.* 381:L25
Meynet G, Maeder A. 2003. *Astron. Astrophys.* 404:975
Meynet G, Maeder A. 2005. *Astron. Astrophys.* 429:581
Meynet G, Maeder A, Schaller G, Schaerer D, Charbonnel C. 1994. *Astron. Astrophys. Suppl.* 103:97
Modjaz M, Kewley L, Kirshner RP, Stanek KZ, Challis P, et al. 2008. *Astron. J.* 135:1136
Moffat AFJ. 2008. In *Proceedings: Clumping in Hot Star Winds*, ed. W-R Hamamm, A Feldmeier, LM Oskinova, p. 17. Potsdam: Univ.-Verl.
Moffat AFJ, Drissen L, Lamontagne R, Robert C. 1988. *Ap. J.* 334:1038
Mokiem MR, de Koter A, Evans CJ, Puls J, Smartt SJ, et al. 2006. *Astron. Astrophys.* 456:1131
Mokiem MR, de Koter A, Evans CJ, Puls J, Smartt SJ, et al. 2007a. *Astron. Astrophys.* 465:1003
Mokiem MR, de Koter A, Vink JS, Puls J, Evans CJ, et al. 2007b. *Astron. Astrophys.* 473:603
Morel T, Butler K, Aerts C, Neiner C, Briquet M. 2006. *Astron. Astrophys.* 457:651
Morel T, Hubrig S, Briquet M. 2008. *Astron. Astrophys.* 481:453
Morgan WW, Keenan PC. 1973. *Annu. Rev. Astron. Astrophys.* 11:29
Moriya T, Tominaga N, Tanaka M, Maeda K, Nomoto K. 2010. *Ap. J. Lett.* 717:83
Moriya T, Tominaga N, Tanaka M, Nomoto K, Sauer DN, et al. 2010a. *Ap. J.* 719:1445
Morton DC. 1967. *Ap. J.* 147:1017
Moss D. 2003. *Astron. Astrophys.* 403:693
Muijres L. 2010. *The physics of line-driven winds of hot massive stars*. PhD thesis. Univ. Amst. 149 pp.
Muijres LE, de Koter A, Vink JS, Krticka J, Kubat J, Langer N. 2011. *Astron. Astrophys.* 526:A32
Munari U, Henden A, Kiyota S, Laney D, Marang F, et al. 2002. *Astron. Astrophys.* 389:L51
Naze Y, ud-Doula A, Spano M, Rauw G, De Becker M, Walborn NR. 2010. *Astron. Astrophys.* 520:59
Naze Y, Walborn NR, Martins F. 2008. *Rev. Mex.* 44:331
Neilson HR, Cantiello M, Langer N. 2011. *Astron. Astrophys.* 529:L9
Neilson HR, Lester JB. 2008. *Ap. J.* 684:569
Niino Y. 2011. *MNRAS* 417:567
Nomoto K. 1984. *Ap. J.* 277:791
Nomoto K, Tominaga N, Tanaka M, Maeda K, Suzuki T, et al. 2006. *Il Nuovo Cimento B* 121:1207
Nota A, Lamers HJGLM, eds. 1997. *Luminous Blue Variables: Massive Stars in Transition*, *ASP Conf. Ser.* Vol. 120. San Francisco: ASP. 396 pp.
Nota A, Livio M, Clampin M, Schulte-Ladbeck R. 1995. *Ap. J.* 448:788
Ofek EO, Cameron PB, Kasliwal MM, Gal-Yam A, Rau A, et al. 2007. *Ap. J. Lett.* 659:13
Owocki SP, Castor JI, Rybicki GB. 1988. *Ap. J.* 335:914
Packet W. 1981. *Astron. Astrophys.* 102:17
Paczynski B. 1971. *Annu. Rev. Astron. Astrophys.* 9:183
Paczynski B. 1991. *Ap. J.* 370:597
Parthasarathy M, Branch D, Baron E, Jeffery DJ. 2006. *Bull. Astron. Soc. India* 34:385
Pasquali A, Nota A, Langer N, Schulte-Ladbeck RE, Clampin M. 2000. *Astron. J.* 119:1352
Penny LR, Gies DR. 2009. *Ap. J.* 700:844
Petit V, Massa DL, Marcolino WLF. 2011. *MNRAS* 412:L45
Petrovic J, Langer N, van der Hucht KA. 2005. *Astron. Astrophys.* 435:1013
Petrovic J, Langer N, Yoon S-C, Heger A. 2005. *Astron. Astrophys.* 435:247
Petrovic J, Pols O, Langer N. 2006. *Astron. Astrophys.* 450:219
Pignata G, Maza J, Hamuy M, Antezana R, Gonzales L. 2009. *Rev. Mex.* 35:317
Pinsonneault MH. 1997. *Annu. Rev. Astron. Astrophys.* 35:557
Piro AL, Ott CD. 2011. *Ap. J.* 736:108
Pistinner S, Eichler D. 1995. *Ap. J.* 454:404
Podsiadlowski P, Ivanova N, Justham S, Rappaport S. 2010. *MNRAS* 406:840
Podsiadlowski P, Joss PC, Hsu JJL. 1992. *Ap. J.* 391:246

Podsiadlowski P, Langer N, Poelarends AJT, Rappaport S, Heger A, Pfahl E. 2004. *Ap. J.* 612:1044
Poelarends AJT. 2007. *Stellar evolution at the borderline of white dwarf and neutron star formation*. PhD thesis, Utrecht University, Utrecht, The Netherlands. 133 pp.
Poelarends AJT, Herwig F, Langer N, Heger A. 2008. *Ap. J.* 675:614
Pols OR. 1994. *Astron. Astrophys.* 290:119
Pols OR, Cote J, Waters LBFM, Heise J. 1991. *Astron. Astrophys.* 241:419
Popham R, Narayan R. 1991. *Ap. J.* 370:604
Porter JM, Rivinius T. 2003. *Publ. Astron. Soc. Pac.* 115:1153
Prantzos N, Boissier S. 2003. *Astron. Astrophys.* 406:259
Pringle JE. 1981. *Annu. Rev. Astron. Astrophys.* 19:137
Prinja RK, Howarth ID. 1988. *MNRAS* 233:123
Prinja RK, Massa D, Fullerton AW. 2002. *Astron. Astrophys.* 388:587
Proffitt CR, Jönsson P, Litzen U, Pickering JC, Wahlgren GM. 1999. *Ap. J.* 516:342
Proffitt CR, Quigley MF. 2001. *Ap. J.* 548:429
Przybilla N, Firnstein M, Nieva MF, Meynet G, Maeder A. 2010. *Astron. Astrophys.* 517:A38
Puls J, Vink JS, Najarro F. 2008. *Astron. Astrophys. Rev.* 16:209
Quimby RM, Kulkarni SR, Kasliwal MM, Gal-Yam A, Arcavi I, et al. 2011. *Nature* 474:487
Racusin JL, Oates SR, Schady P, Burrows DN, de Pasquale M, et al. 2011. *Ap. J.* 738:138
Rakavy G, Shaviv G, Zinamon Z. 1967. *Ap. J.* 150:131
Rauscher T, Heger A, Hoffman RD, Woosley SE. 2002. *Ap. J.* 576:323
Rauw G, De Becker M, Naze Y, Crowther PA, Gosset E, et al. 2004. *Astron. Astrophys.* 420:L9
Rauw G, Vreux J-M, Bohannan B. 1999. *Ap. J.* 517:416
Ribas I, Jordi C, Gimenez A. 2000. *MNRAS* 318:L55
Ritchie BW, Stroud VE, Evans CJ, Clark JS, Hunter I, et al. 2012. *Astron. Astrophys.* 537:A29
Rogers FJ, Iglesias CA. 1992. *Ap. J.* 401:361
Roxburgh IW. 2004. *Astron. Astrophys.* 428:171
Salvaterra R, Della Valle M, Campana S, Chincarini G, Covino S, et al. 2009. *Nature* 461:1258–60
Sana H, Evans CJ. 2011. *IAU Symp.* 272:474
Sander A, Hamann W-R, Todt H. 2012. *Astron. Astrophys.* 540:A144
Savaglio S, Glazebrook K, Le Borgne D. 2009. *Ap. J.* 691:182–211
Scannapieco E, Madau P, Woosley SE, Heger A, Ferrara A. 2005. *Ap. J.* 633:1031
Schaller G, Schaerer D, Meynet G, Maeder A. 1992. *Astron. Astrophys. Suppl.* 96:269
Schlegel EM, Petre R. 2006. *Ap. J.* 646:378
Schnerr RS, Henrichs HF, Neiner C, Verdugo E, de Jong J, et al. 2008. *Astron. Astrophys.* 483:857
Schnurr O, Casoli J, Chene A-N, Moffat AFJ, St-Louis N. 2008. *MNRAS* 389:L38
Schönberner D, Herrero A, Becker S, Eber F, Butler K, et al. 1988. *Astron. Astrophys.* 197:209
Schröder K-P, Pols OR, Eggleton PP. 1997. *MNRAS* 285:696
Schwarzschild M, Härm R. 1958. *Ap. J.* 128:348
Seaton MJ. 2005. *MNRAS* 362:L1
Shindo M, Hashimoto M, Eriguchi Y, Müller E. 1997. *Astron. Astrophys.* 326:177–86
Shibahashi H, Osaki Y. 1976. *Publ. Astron. Soc. Jpn.* 28:199
Shu FH, Lubow SH. 1981. *Annu. Rev. Astron. Astrophys.* 19:277
Siess L. 2007. *Astron. Astrophys.* 476:893
Siess L. 2009. *Astron. Astrophys.* 497:463
Siess L. 2010. *Astron. Astrophys.* 512:A10
Sills A, Adams T, Davies MB, Bate MR. 2002. *MNRAS* 332:49
Skumanich A. 1972. *Ap. J.* 171:565
Smartt SJ. 2009. *Annu. Rev. Astron. Astrophys.* 47:63
Smartt SJ, Eldridge JJ, Crockett RM, Maund JR. 2009. *MNRAS* 395:1409
Smith N, Chornock R, Silverman JM, Filippenko AV, Foley RJ. 2010. *Ap. J.* 709:856
Smith N, Hinkle KH, Ryde N. 2009. *Astron. J.* 137:3558
Smith N, Li W, Filippenko AV, Chornock R. 2011a. *MNRAS* 412:1522
Smith N, Li W, Foley RJ, Wheeler JC, Pooley D, et al. 2007. *Ap. J.* 666:1116

Smith N, Li W, Miller AA, Silverman JM, Filippenko AV, et al. 2011b. *Ap. J.* 732:63
Smith N, Owocki SP. 2006. *Ap. J. Lett.* 645:L45
Smith N, Vink JS, de Koter A. 2004. *Ap. J.* 615:475
Soderberg AM, Brunthaler A, Nakar E, Chevalier RA, Bietenholz MF. 2010. *Ap. J.* 725:922
Spruit HC. 1992. *Astron. Astrophys.* 253:131
Spruit HC. 2002. *Astron. Astrophys.* 381:923
Steidel CC, Adelberger KL, Giavalisco M, Dickinson M, Pettini M. 1999. *Ap. J.* 519:1–17
Stothers RB, Chin C-W. 1985. *Ap. J.* 292:222
Stothers RB, Chin C-W. 1991. *Ap. J.* 374:288
Stothers RB, Chin C-W. 1993. *Ap. J. Lett.* 408:L85
Stroud VE, Clark JS, Negueruela I, Roche P, Norton AJ, Vilardell F. 2010. *Astron. Astrophys.* 511:A84
Struve O. 1963. *Publ. Astron. Soc. Pac.* 75:207
Suda T, Hirschi R, Fujimoto MY. 2011. *Ap. J.* 741:61
Suijs MPL, Langer N, Poelarends A-J, Yoon S-C, Heger A, Herwig F. 2008. *Astron. Astrophys.* 481:L87
Sweet IPA, Roy AE. 1953. *MNRAS* 113:701–15
Taam RE, Sandquist EL. 2000. *Annu. Rev. Astron. Astrophys.* 38:113
Talon S, Charbonnel C. 2005. *Astron. Astrophys.* 482:597
Talon S, Charbonnel C. 2008. *Astron. Astrophys.* 440:981
Tanvir NR, Fox DB, Levan AJ, Berger E, Wiersema K, et al. 2009. *Nature* 461:1254–57
Tauris TM, Langer N, Kramer M. 2011. *MNRAS* 416:2130
Tauris TM, van den Heuvel EPJ. 2006. *Compact Stellar X-ray Sources*, ed. W Lewin, M van der Klis, pp. 623–65. Cambridge Astrophys. Ser., No. 39. Cambridge, UK: Cambridge Univ. Press
Taylor WD, Evans CJ, Sana H, Walborn NR, de Mink SE, et al. 2011. *Astron. Astrophys.* 530:L10
Thielemann F-K, Arnett WD. 1985. *Ap. J.* 295:604
Tiffany C, Humphreys RM, Jones TJ, Davidson K. 2010. *Astron. J.* 140:339
Toma K, Sakamoto T, Meszaros P. 2011. *Ap. J.* 731:127
Tout CA, Wickramasinghe DT, Lau HH-B, Pringle JE, Ferrario L. 2011. *MNRAS* 410:2458
Tout CA, Wickramasinghe DT, Liebert J, Ferrario L, Pringle JE. 2008. *MNRAS* 387:897
Townsend RHD, Owocki SP, Howarth ID. 2004. *MNRAS* 350:189
Tur C, Heger A, Austin SM. 2007. *Ap. J.* 671:821
Tur C, Heger A, Austin SM. 2010. *Ap. J.* 718:357
Tylenda R, Hajduk M, Kaminski T, Udalski A, Soszynski I, et al. 2011. *Astron. Astrophys.* 528:A114
ud-Doula A, Owocki SP, Townsend RHD. 2008. *MNRAS* 385:97
Ulmer A, Fitzpatrick EL. 1998. *Ap. J.* 504:200
Umeda H, Nomoto K. 2008. *Ap. J.* 673:1014
van Bever J, Vanbeveren D. 1998. *Astron. Astrophys.* 334:21
Vanbeveren D, De Donder E, van Bever J, Van Rensbergen W, De Loore C. 1998. *New Astron.* 3:443
Vanbeveren D, De Loore C. 1994. *Astron. Astrophys.* 290:129
Vanbeveren D, De Loore C, Van Rensbergen W. 1998. *Astron. Astrophys. Rev.* 9:63
van der Hucht KA. 2001. *New Astron. Rev.* 45:135
van Loon JTh, Cioni M-RL, Zijlstra AA, Loup C. 2005. *Astron. Astrophys.* 438:273
van Marle AJ, Owocki SP, Shaviv NJ. 2009. *MNRAS* 394:595
van Veelen B. 2010. *Supernovae interacting with their circumstellar media.* PhD thesis. Utrecht Univ., Utrecht, the Netherlands. 123 pp.
Venn KA, Brooks AM, Lambert DL, Lemke M, Langer N, et al. 2002. *Ap. J.* 565:571
Venn KA, Lambert DL, Lemke M. 1996. *Astron. Astrophys.* 307:849
Vink JS. 2009. In *Eta Carinae and the Supernova Imposters*, ed. K Davidson, RM Humphreys, pp. 221–47. New York: Springer (astro-ph/0905.3338)
Vink JS, Brott I, Gräfener G, Langer N, de Koter A, Lennon DJ. 2010. *Astron. Astrophys.* 512:L7
Vink JS, de Koter A. 2005. *Astron. Astrophys.* 442:587
Vink JS, de Koter A, Lamers HJGLM. 2001. *Astron. Astrophys.* 369:574
Vink JS, Muijres LE, Anthonisse B, de Koter A, Gräfener G, Langer N. 2011. *Astron. Astrophys.* 531:A132
von Zeipel H. 1924. *MNRAS* 84:665–701

Walborn NR. 2009. *Massive Stars: From Pop III and GRBs to the Milky Way*, ed. M Livio, E Villaven. STScI Symp. Ser. 20. Cambridge, UK: Cambridge Univ. Press (astro-ph/0701573)
Walborn NR, Howarth ID, Evans CJ, Crowther PA, Moffat AFJ, et al. 2010. *Astron. J.* 139:1283
Walborn NR, Maiz Apellaniz J, Sota A, Alfaro EJ, Morrell NI, et al. 2011. *Astron. J.* 142:150
Walborn NR, Morrell NI, Howarth ID, Crowther PA, Lennon DJ, et al. 2004. *Ap. J.* 608:1028
Waldman R. 2008. *Ap. J.* 685:1103
Wellstein S. 2001. *Präsupernovaentwicklung enger mussereicher DoppelsternSysteme.* PhD thesis. Potsdam Univ., Potsdam. 146 pp.
Wellstein S, Langer N. 1999. *Astron. Astrophys.* 350:148
Wellstein S, Langer N, Braun H. 2001. *Astron. Astrophys.* 369:939
Wheeler JC, Cowan JJ, Hillebrandt W. 1998. *Ap. J. Lett.* 493:101
Winget DE, Nather RE, Clemens JC. 1994. *Ap. J.* 430:839
Wolff SC, Strom SE, Cunha K, Daflon S, Olsen K, Dror D. 2008. *Astron. J.* 136:1049
Woosley SE. 1993. *Ap. J.* 405:273
Woosley SE, Blinnikov S, Heger A. 2007. *Nature* 450:390
Woosley SE, Bloom JS. 2006. *Annu. Rev. Astron. Astrophys.* 47:507
Woosley SE, Heger A. 2006. *Ap. J.* 637:914
Woosley SE, Heger A, Weaver TA. 2002. *Rev. Mod. Phys.* 74:1015
Woosley SE, Langer N, Weaver TA. 1993. *Ap. J.* 411:823
Woosley SE, Langer N, Weaver TA. 1995. *Ap. J.* 448:315
Yoon S-C, Dierks A, Langer N. 2012. *Astron. Astrophys.* 542:A113
Yoon S-C, Langer N. 2005. *Astron. Astrophys.* 443:643
Yoon S-C, Langer N, Norman C. 2006. *Astron. Astrophys.* 460:199
Yoon S-C, Woosley SE, Langer N. 2010. *Ap. J.* 725:940
Yorke HW. 1986. *Annu. Rev. Astron. Astrophys.* 24:49
Young TR. 2004. *Ap. J.* 617:1233
Zahn J-P, Brun AS, Mathis S. 2007. *Astron. Astrophys.* 474:145
Zaussinger F, Spruit HC. 2011. *Semiconvection* (astro-ph/1012.5851v2)
Zickgraf F-J, Kovacs J, Wolf B, Stahl O, Kaufer A, Appenzeller I. 1996. *Astron. Astrophys.* 309:505
Zinnecker H, Yorke HW. 2007. *Annu. Rev. Astron. Astrophys.* 45:481

Annual Review of Astronomy and Astrophysics

Volume 50, 2012

Contents

Indexes

Errata

An online log of corrections to *Annual Review of Astronomy and Astrophysics* articles may be found at http://astro.annualreviews.org/errata.shtml